NASA CONTRACTOR REPORT

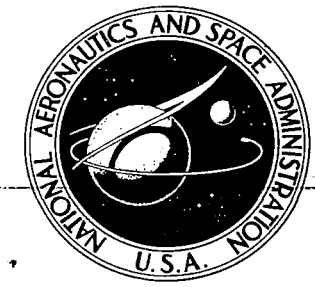

NASA CR-1212

SMALL PERTURBATION DYNAMICS OF THE NEUROMUSCULAR SYSTEM IN TRACKING TASKS

by Raymond E. Magdaleno, Duane T. McRuer, and George P. Moore

Prepared by
SYSTEMS TECHNOLOGY, INC.
Hawthorne, Calif.

for Ames Research Center

NATIONAL AERONAUTICS AND SPACE ADMINISTRATION • WASHINGTON, D. C. • DECEMBER 1968

NASA CR-1212

SMALL PERTURBATION DYNAMICS OF THE NEUROMUSCULAR SYSTEM IN TRACKING TASKS

By Raymond E. Magdaleno, Duane T. McRuer,
and George P. Moore

Issued by Originator as Technical Report No. 154-1

Prepared under Contract No. NAS 2-2824 by
SYSTEMS TECHNOLOGY, INC.
Hawthorne, Calif.

for Ames Research Center

NATIONAL AERONAUTICS AND SPACE ADMINISTRATION

For sale by the Clearinghouse for Federal Scientific and Technical Information
Springfield, Virginia 22151 – CFSTI price $3.00

FOREWORD

This report was prepared under Contract NAS2-2824 between Systems Technology, Inc., Hawthorne, California, and the NASA-Ames Research Center, Man/Machine Integration Branch. The NASA project monitor was Mr. C. B. Dolkas and the STI technical director was Mr. Duane T. McRuer, the project engineer was Mr. Raymond E. Magdaleno, and the consultant was Dr. George P. Moore of the University of Southern California (formerly with the University of California at Los Angeles).

ABSTRACT

Recently both high quality physiological data and human operator describing function data of low variability and large dynamic range have become available. The purpose of this report is to model the neuromuscular system aspects of these data using control engineering descriptions of the individual components as well as the system functioning of ensembles of these components. In particular we are interested in a neuromuscular system model which is compatible with the input/output data for the whole human in tracking situations.

The component data of interest include recent anatomical and physiological data for the muscle spindle and input/output studies of the muscle. These data indicate that quasi-linear models can describe the basic behavior of these two elements in tracking tasks. This report contains two key developments: (1) the variation in muscle system parameters as a function of average muscle tension or operating point, and (2) the role of the muscle spindle both as an adaptive equalization element and in its effect on setting muscle tone or average tension.

The pertinent whole human data include the covariation of high and low frequency describing function phase data and the variation of high frequency phase with set tension changes interpreted from force disturbance experiments. Further the force disturbance data as well as tremor frequency results for various spring and inertia restraints are also influenced by muscle tone. The phase data trends are used to illustrate the muscle spindle's adaptive characteristics — lead/lag series equalization and an actuation command input for the fine control of position. Finally the force disturbance and tremor frequency data are used to illustrate the effect of spindle location, i.e., the spindle feeds back an interior muscle length instead of total length. This produces constraints on the closed-loop system dynamics which serve to explain the changes in the force disturbance response and tremor frequency values as muscle tone and manipulator restraints are varied.

CONTENTS

FIGURES

SYMBOLS

b	Constant in empirical curves fitted to force/velocity data
$B(P_o)$	Equivalent damper for muscle system
C_f	Constant of proportionality for average motor nerve firing rate
C_{f_d}	Constant of proportionality in spindle model (under dynamic fiber control)
C_{f_s}	Constant of proportionality in spindle model (under static fiber control)
dB	Decibel, $20 \log_{10}( )$
$D(s)$	Denominator of the loop gain transfer function (p. 94)
D_s	Denominator of G_s
$\overline{e^2}$	Mean square error
f	Average nerve firing rate in pulses/second
f_f	Steady-state firing rate after a transient decay
f_{max}	Muscle firing rate producing tetanus
f_o	Operating point average firing rate
f_p	Peak firing rate at termination of stretching
Δf_α	Incremental alpha motor neuron firing rate
Δf_d	Dynamic fiber perturbation firing rate
Δf_s	Static fiber perturbation firing rate
F	Muscle output force; also disturbance force
F_s	Force on manipulator
$G_M(\gamma_o)$	Muscle and manipulator dynamics
G_s	Spindle describing function (see Eqs. 27 and 34)
h_m	Limb/manipulator response to pendulum impact
i	Summation index
I_a	Primary or annulospiral ending

I_m, I_{min}	Value of manipulator inertia
I_1	Value of manipulator inertia
I_p	Inertia of pilot's limb on pitch tracking
j	$\sqrt{-1}$
$j\omega$	Imaginary part of the complex variable, $s = \sigma \pm j\omega$
K_a	Specific value of controlled element gain
K_c	Controlled element gain
K_e	Series elastic component of muscle
K_F	Manipulator spring rate
K_h	Small signal equivalent spring (under static fiber control)
K_m	Equivalent spring gradient for muscle
K_n	Small signal equivalent spring (under dynamic fiber control)
K_p	Human pilot gain
K_r	Parallel combination of springs (see Eq. 27)
K_s	Small signal equivalent spring for the nuclear bag region of a muscle spindle
K_{sp}	Spindle describing function gain
L	Actual length of muscle
L_o	Operating point length of muscle
ΔL	Perturbation muscle length (positive for shortening)
m	Integer
ms	Millisecond
M	Limb plus manipulator inertia
N_M	Numerator of G_M (see Eq. 32)
N(s)	Numerator of the loop gain transfer function (p. 94)
N_s	Numerator of G_s
P	Tension

P_d	Force due to dynamic fiber stimulation (p. 90)
P_{d_o}	Operating point force for dynamic fiber portion of spindle model
P_o	Operating point tension
P_1, P_2	Particular operating point tensions
P_{s_o}	Operating point force for static fiber portion of spindle model
P_T	Tetanic tension
s	Complex variable, $s = \sigma \pm j\omega$; Laplace transform variable
t	Time
T_h	Muscle/manipulator system time constant for isometric restraint
T_I	General lag time constant of human pilot describing function
T_K, T'_K	Lead and lag time constants in precision model of human pilot describing function
$1/aT_K$	Open-loop spindle model pole
T_{lag_i}, T_{lead_i}	General lag and lead time constants
T_L	General lead time constant of human pilot describing function
T_N	First-order lag time constant approximation of the neuromuscular system
T_{N_1}	First-order lag time constant of the neuromuscular system
V	Velocity of muscle shortening
V_m	Maximum velocity of muscle shortening
V_o	Operating point velocity
ΔV	Differential velocity of contraction
x	Limb length
x_1	Internal muscle length
x_m	Spindle model length (p. 89)
x_n	Spindle model length (p. 89)
x_s	Length of nuclear bag region of muscle spindle model (p. 89)

$Y_c(j\omega)$	Controlled element (machine and display) transfer function
Y_p	Pilot describing function
α	Low frequency phase approximation parameter
α_c	Alpha motor neuron command
γ	Gamma command following gamma motor neuron delay (p. 100)
γ_b	Gamma bias input due to γ_d
γ_{b_o}	Steady-state value of γ_b
γ_c	Gamma command input due to γ_s
γ_{c_o}	Steady-state value of γ_c
γ_d	Gamma input due to dynamic gamma motor neuron
γ_o	Total gamma bias
γ_s	Gamma input due to static gamma motor neuron
Δ	Characteristic equation
Δ'	Closed-loop characteristic equation
ζ_N	Damping ratio of second-order term in pilot's describing function (p. 64)
λ	Controlled element unstable pole position
σ	Real axis of complex plane
σ_e	Root mean square error
σ_i	Root mean square input
τ	Pure time delay
τ_e	Effective time delay
τ_α	Net time delay in the alpha motor neuron pathway (p. 100)
τ_γ	Net time delay in the gamma motor neuron pathway (p. 100)
$\Delta\varphi_{low}$	Incremental low frequency phase angle
ω	Angular frequency, rad/sec
ω_i	Forcing function bandwidth

ω_M Undamped natural frequency of limb/manipulator system (p. 84)

ω_N Undamped natural frequency of second-order term in the pilot's describing function (p. 64)

$| \; |$ Magnitude

Σ Summation

$\uparrow$ Increase

$\downarrow$ Decrease

∂ Partial derivative

INTRODUCTION

The neuromuscular system referred to here is the output or actuation element of the human controller. It is a composite of neural and muscular components situated in the spinal cord and the periphery — typically a limb and its neural connections — operating on commands sent from higher centers. In recent years an ever more rapidly increasing amount of data on such systems has been generated by experimental psychologists, physiologists, neurologists, biomedical engineers, manual control engineers, etc. Some of these data are already in a form directly suitable for systems engineering interpretation; other data, while not in such form, are still sufficiently significant that they must be "explained" qualitatively as consistent with or derivable from any model advanced as a synthesis.

Besides providing data, almost all experimenters have also attempted an interpretation. These interpretations are usually confined to plausible explanations of their specific data. Unfortunately, such explanations for each of several related experiments involving various portions of the system do not sum to a plausible explanation of the whole. Thus the primary purpose of this report is to attempt a new synthesis of the extant data by providing models which are compatible with the over-all human operator's input/output characteristics as well as with the individual components of the neuromuscular system.

We are interested in engineering descriptions of neuromuscular systems in three respects:

Manual control engineering — The basic dynamics of the human operator and the precision of manual control are critically limited by the properties of the neuromuscular system. A basic understanding of this system will have important practical ramifications in better appreciating these limitations, as well as in determining the likely effects of control system nonlinearities (e.g., hysteresis, backlash, Coulomb friction, preload) on pilot/vehicle system stability and performance. This, in turn, should ultimately lead to a better understanding of some kinds of pilot-induced oscillations, and to the establishment of necessary or sufficient conditions for their elimination.

Control theoretic — The neuromuscular system is an archetypical adaptive actuation system which, if understood operationally, might serve as the inspiration for analogous inanimate systems with similarly useful properties.

Physiological system description — Systems engineering descriptions are a natural language for integrating the rapidly expanding knowledge of biological servomechanisms, and serve to implement the interpretation of physiological data, construct and validate models of basic physiological processes, and suggest further experimentation.

The next two sections contain summaries of the component and system data which must be "explained" by, or which provide a basic structure for, any valid neuromuscular system models. The section entitled "Physiology of the Neuromuscular System" describes the physiology of the neuromuscular system in some detail, thereby providing structural constraints for models, and also presents typical data on neuromuscular system components. The next section, "Human Operator Data Indicating Neuromuscular System Effects," is devoted primarily to a summary of some key human operator data which are especially indicative of neuromuscular system effects. This provides the over-all system data with which candidate neuromuscular system models should be compatible.

Building on this foundation, the sections entitled "Neuromuscular System Component Models for Small Perturbations" and "Closed-Loop Neuromuscular System Dynamics" are concerned with model development. To start, under "Neuromuscular System Component Models for Small Perturbations," simplified mathematical models for the neuromuscular system components are evolved. Then these components are connected into a system structure and its operations for typical control situations are explored. Finally, under "Closed-Loop Neuromuscular System Dynamics," the ability of the model to account for the experimental data is discussed.

PHYSIOLOGY OF THE NEUROMUSCULAR SYSTEM

This report is directed toward an understanding of certain basic data derived from studies of the human operator, and an attempt is made to interpret these data as consequences of the physiological and structural properties of those parts of the brain and musculoskeletal system whose features have been most intensively studied in the last decade. Although our knowledge of these systems is expanding quite rapidly, there are still such enormous gaps that any attempt at synthesis is necessarily incomplete and speculative. Nevertheless, we shall show that there is a substantial agreement and consistency in our present models of some physiological component processes and the over-all behavior of the human operator.

As a general scheme, we can view the human operator as a system operating on sensory input to produce a motor output (fig. 1). Abstractly, we can distinguish various sense modalities whose input is processed by higher regions of the brain, subjecting input information to various logical operations in addition to equalization functions. These in turn are used in the formulation of command signals to motor effector systems at more peripheral levels. It is this last segment with which we are primarily concerned in this report, and in this initial section we shall summarize the relevant physiological data from which we derive our basic block diagram and to which our neuromuscular system models are directed.

By "peripheral neuromuscular system" we mean the local organization of neurons, muscles, skeletal elements, and associated sense organs which are the basic functional blocks employed by the higher levels of the nervous system in the execution of motor acts directed by its command signals. For reasons which will become more clear later, we have shown in figure 1 two distinct classes of command signals (α_c and γ_c) arriving at the peripheral neuromuscular level. We shall not be primarily concerned with these signals, which are assumed to be appropriate to the sensory input and desired motor output (ref. 97); rather, we shall detail the components of the box labeled "peripheral neuromuscular system," which, as a protorype, we shall assume to operate from a restricted level of the spinal cord.

In the following subsection we discuss the muscle actuation system, starting with the properties of its basic component, the motor unit. This is followed by the basic physiology of the muscle. Finally, the operation of an open-loop

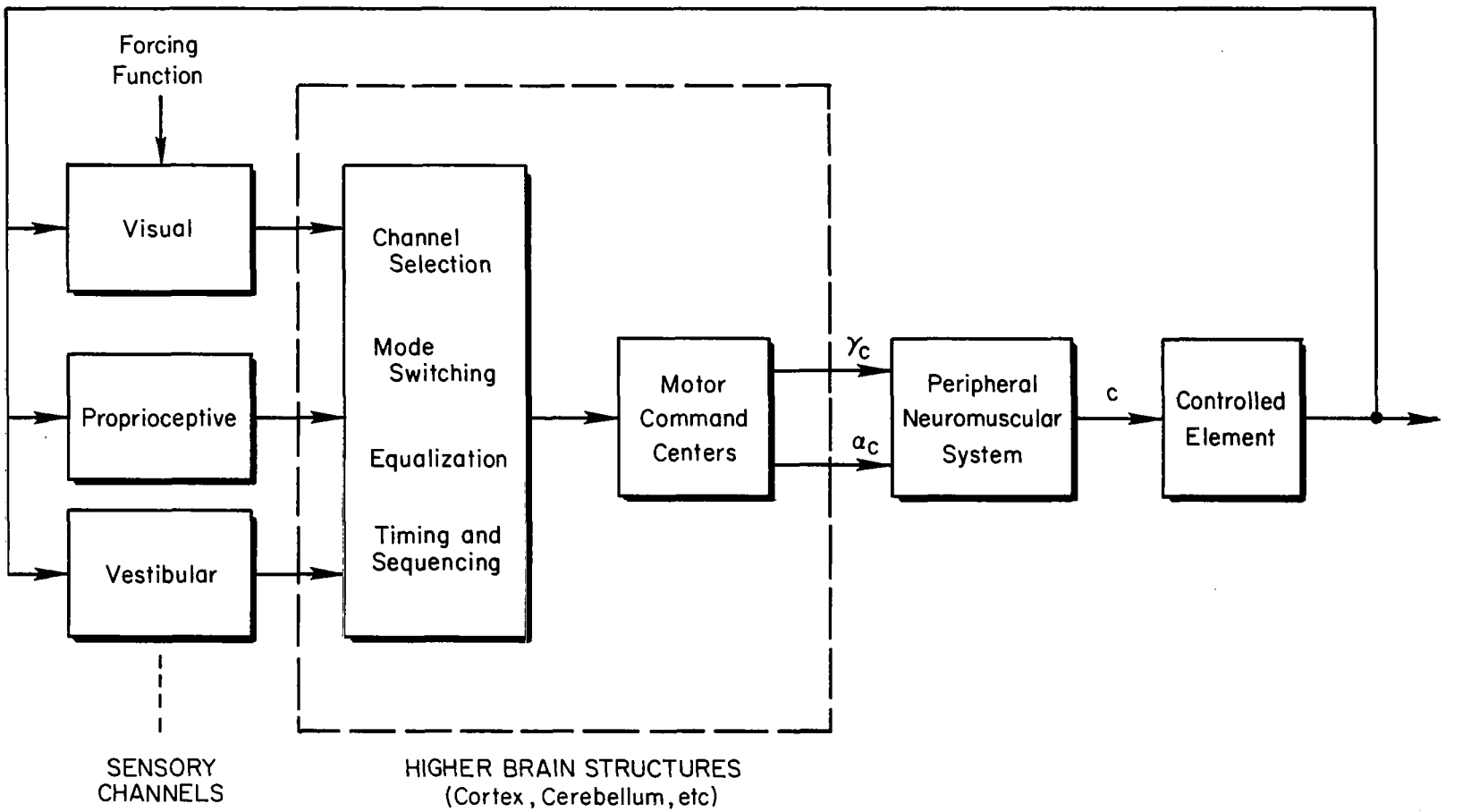

Figure 1. Generalized Man/Machine System

muscle control is described. In the next subsection, "Closed-Loop Neuromuscular Control Systems," we consider closed-loop neuromuscular control systems; specifically, the necessary muscle spindle and Golgi tendon organ feedbacks as well as the interconnections through the spinal cord. The stretch reflex illustrates the closed-loop functioning of the system. Finally, this subsection concludes with an example of the neuromuscular control of respiration which illustrates the coordinated functioning of all the elements. This leads to a typical manual control system block diagram for a hypothetical agonist/antagonist muscle pair.

Basic Anatomical and Functional Features of Muscle

Motor units. — The basic element for modification of skeletal muscle tension or length is the motor unit (fig. 2). This consists of a single motor neuron in the spinal cord, the axon through which it transmits impulses to the periphery, and all muscle fibers to which the axon is connected. As the motor axon reaches the muscle it innervates, it divides into multiple branches, or collaterals, each of which makes contact with a single muscle fiber; conversely, each muscle fiber is activated by only one input axon. The region at which the axon makes contact with the muscle fibers is called the "motor end-plate" or "neuromuscular junction" (fig. 3). This is a region of very small dimensions (a few square microns) where the membranes of the axon and the muscle come into very close contact.

Upon reaching the end-plate, a pulse traveling from the motor cell in the cord down the axon to the muscle triggers the release of a minute quantity of a chemical agent, stored at the end-plate, which diffuses across the junction to react with the muscle fiber membrane in such a way as to initiate a comparable pulse in the muscle. By a process that is not well understood, this electrical pulse, or sudden depolarization sweeping across the muscle membrane, triggers a set of energy-releasing chemical reactions in the muscle protein which cause contraction or development of tension. Thus, each unitary (pulse) event in the motor neuron elicits a unitary mechanical response in every muscle cell it reaches; the response is called the "muscle twitch." Like the electrical pulse, it is all-or-none, i.e., it is basically an invariant quantized event. Each muscle fiber contributes its individual twitch response to the summated over-all response of the motor unit.

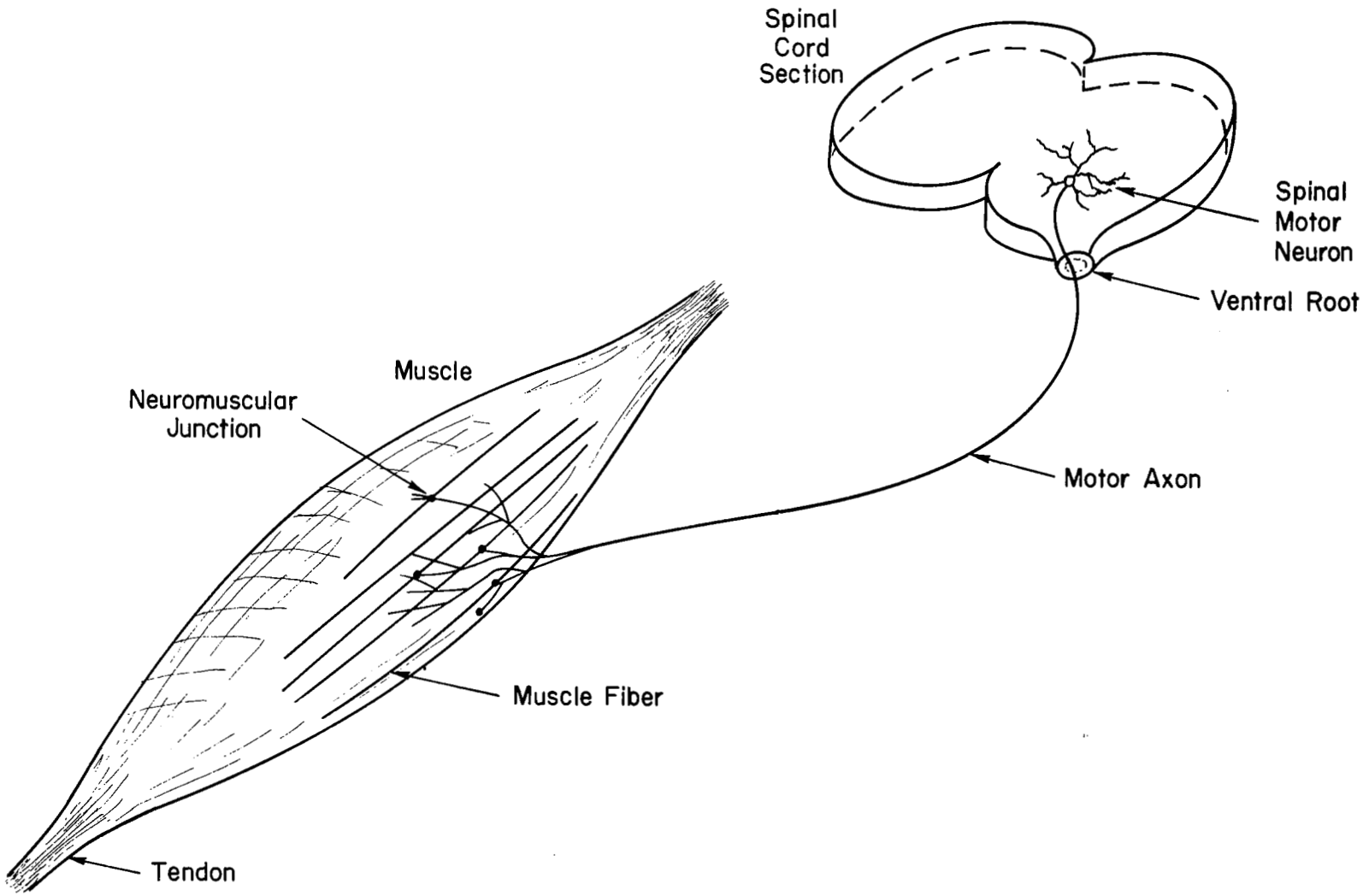

Figure 2. Motor Unit Components

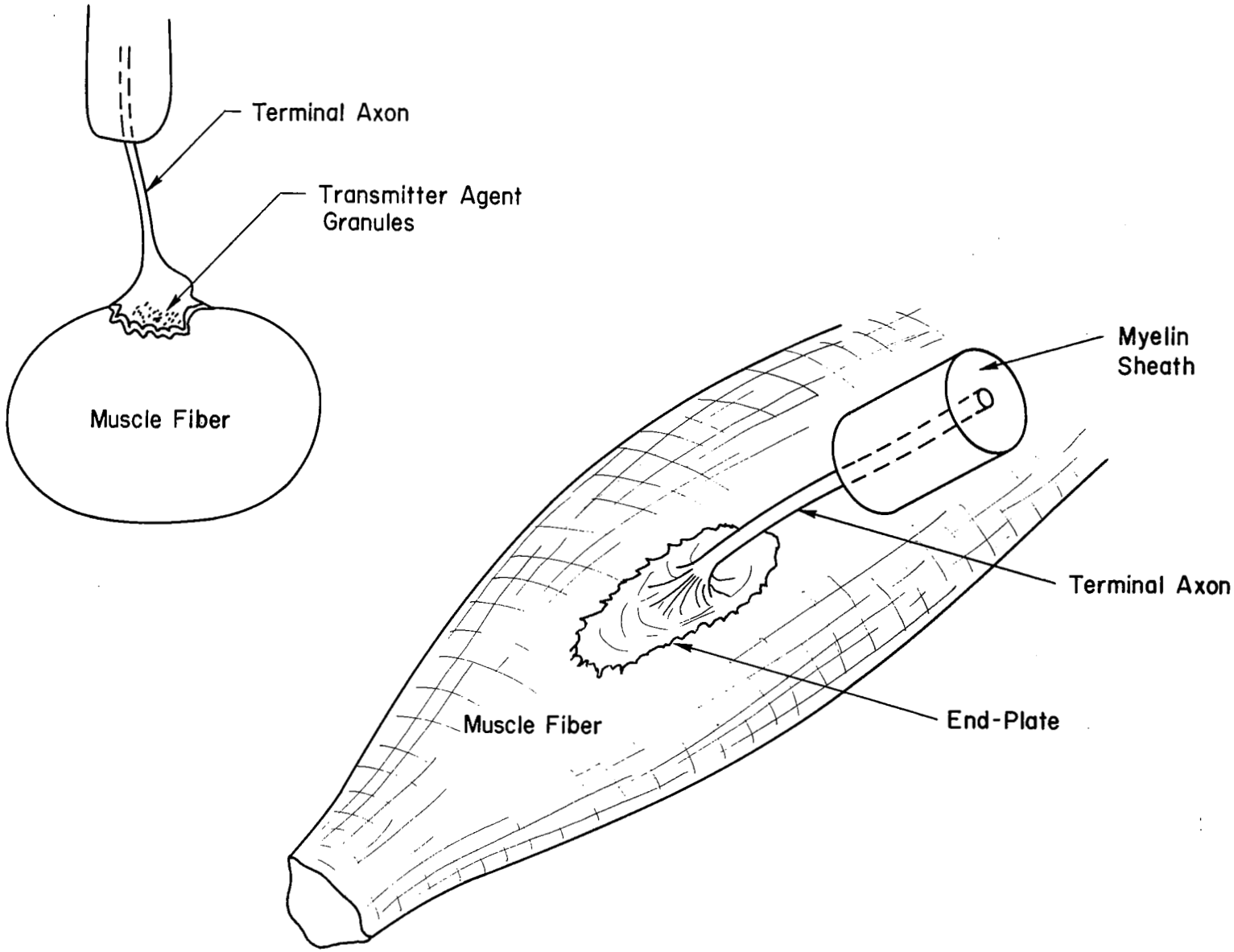

Figure 3. Detail of Neuromuscular Junction

A generalized tension time plot of a twitch response can be seen in figure 4, but considerable differences in its details will be manifested between different motor units. These arise because a motor neuron does not always innervate the same number of muscle fibers, nor do individual muscle fibers necessarily generate twitches with the same amplitude or time course. Indeed, it is this variability in the size of the motor unit and the details of its unitary events that contribute to the richness and complexity of neuromuscular control. This will be discussed in more detail later.

If a sequence of impulses reaches the muscle fiber each impulse will trigger a twitch response, and if the impulses are close enough together in time a summation of tensions will result. As can be seen from figure 4, the total tension developed will depend on the timing or frequency of the arriving nerve impulses, their time span, and the temporal characteristics of the muscle twitch. When the nerve impulse frequency is high enough, however, a saturation effect develops and the individual twitch responses fuse into a continuous maximum tension. This condition is called "tetanus." The neuron frequency necessary to produce this (the "tetanic fusion frequency") will of course depend on the twitch time of the muscle, which, as already pointed out, is variable from unit to unit.

A few general statements on the organization of neuromuscular elements should be made. First, it is important to note that all the muscle fibers in a motor unit lie within the same parent muscle; i.e., they are not distributed between various muscles. There may be anywhere from about 10—10,000 fibers in a unit, and from rather few to several million units within a muscle (ref 2). These show a characteristic distribution which will be discussed later. The fibers in a muscle are organized into a hierarchy of bundles called "fascicles," and these in turn are bound together to form the total muscle.

Motor neurons — The arrangement of motor neurons in the spinal cord is more complex. The motor neurons are always located in the ventral horn of the spinal gray matter, and their axons always leave the cord in an aggregated bundle known as the "ventral root" (fig. 2). They show a tendency to cluster together in functionally significant groups: sometimes the cluster consists of all motor cells whose axons reach the same muscle; sometimes the cluster, or nucleus, will innervate a group of muscles which functionally cooperate (i.e., muscles which are synergistic, such as those muscles which act to bend the arm at the elbow);

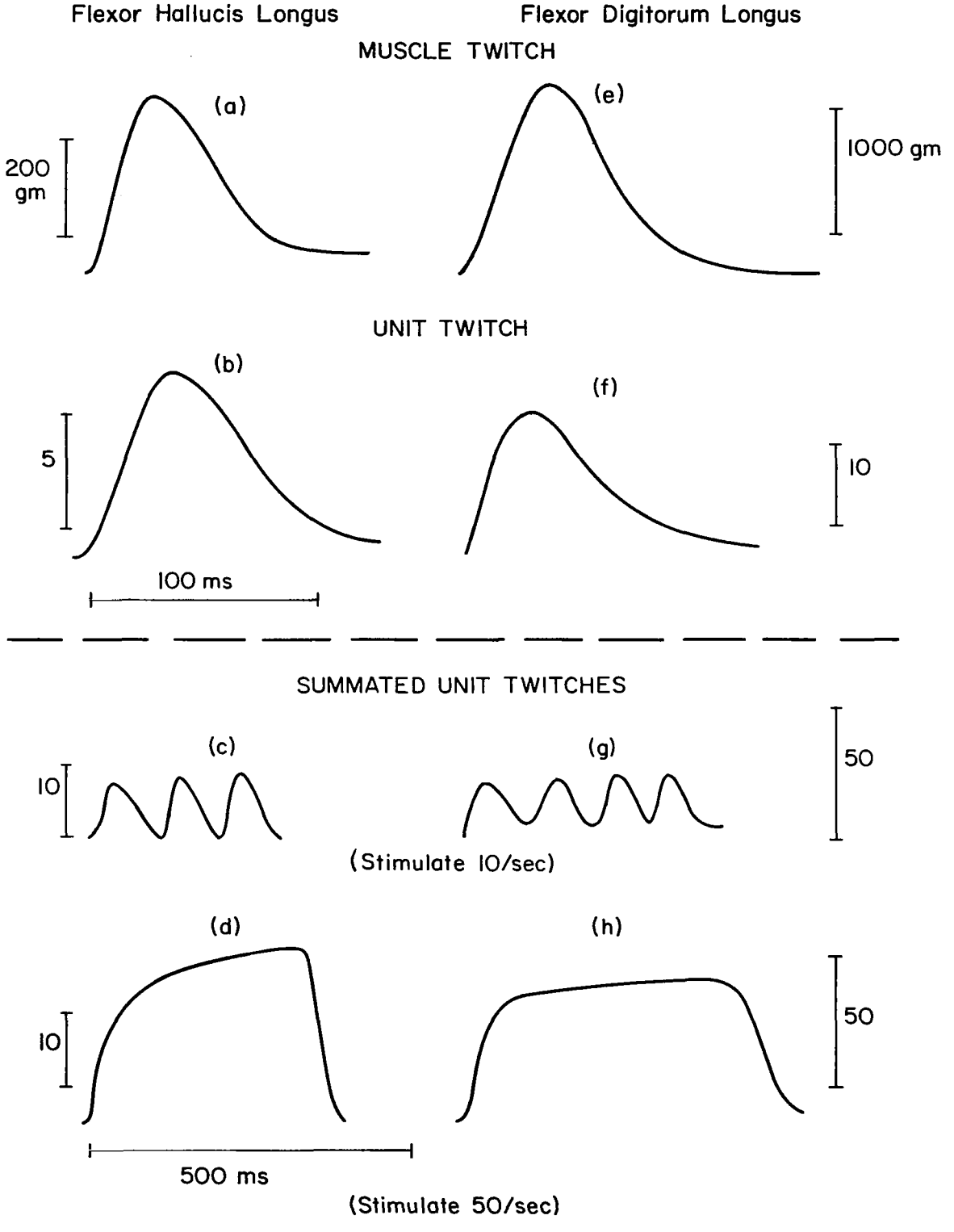

Figure 4. Plots of Tension Versus Time for Two Muscles

in other cases the nucleus is organized around an entire segment of a limb (ref. 3) as shown in figure 5.

This cellular proximity may be extremely important insofar as it may be necessary to the rapid integration of activity between these motor cells. Integration in motor neurons is one of the most intensively studied areas of modern neurophysiology and has led to so many important insights concerning the properties of neuron networks that a few generalizations important to our subsequent presentation will be made.

Synaptic input — It has already been mentioned that motor neurons communicate with muscle cells by means of pulse events which are transmitted along their axons. This is also a major means of communication between neurons, but there are important differences. When a pulse reaches the terminal region of an axon traveling to another neuron, it encounters a specialized ending of the axon (comparable to the neuromuscular junction) called a "synapse" (fig. 6). Here again the pulse releases a small quantity of chemical substance which diffuses to the postsynaptic neuron surface. Depending on the specific chemical structure of this agent (and there are only a few such agents employed by the nervous system), the permeability of the postsynaptic membrane to ions such as potassium, sodium, or chloride is momentarily altered. During this period, in which, effectively, an ion-selective impedance change occurs, currents flow into or out of the postsynaptic neuron, thereby altering the potential difference across its membrane. Normally situated at about 70 mV (negative inside with respect to outside), the potential shifts either in a more negative direction (hyperpolarization) or in a less negative direction (depolarization). The direction of change depends on the structure of the transmitter agent released by the presynaptic axon, but for any synapse this is always the same. Therefore, the postsynaptic response, i.e., the shift in potential, is basically invariant following each presynaptic impulse. Unlike the muscle fiber, however, the typical neuron receives input from many axons, and as many as 10,000 synapses have been counted on a motor neuron, distributed over the entire surface of the cell body, or "soma," and along its dendrites as well. These synapses represent the termination points of hundreds or thousands of other neurons which can contribute input to this single cell. Indeed, interest has been focused in recent years on the dendrites of motor cells because dendrites constitute as much as 80 percent of the motor neuron surface.

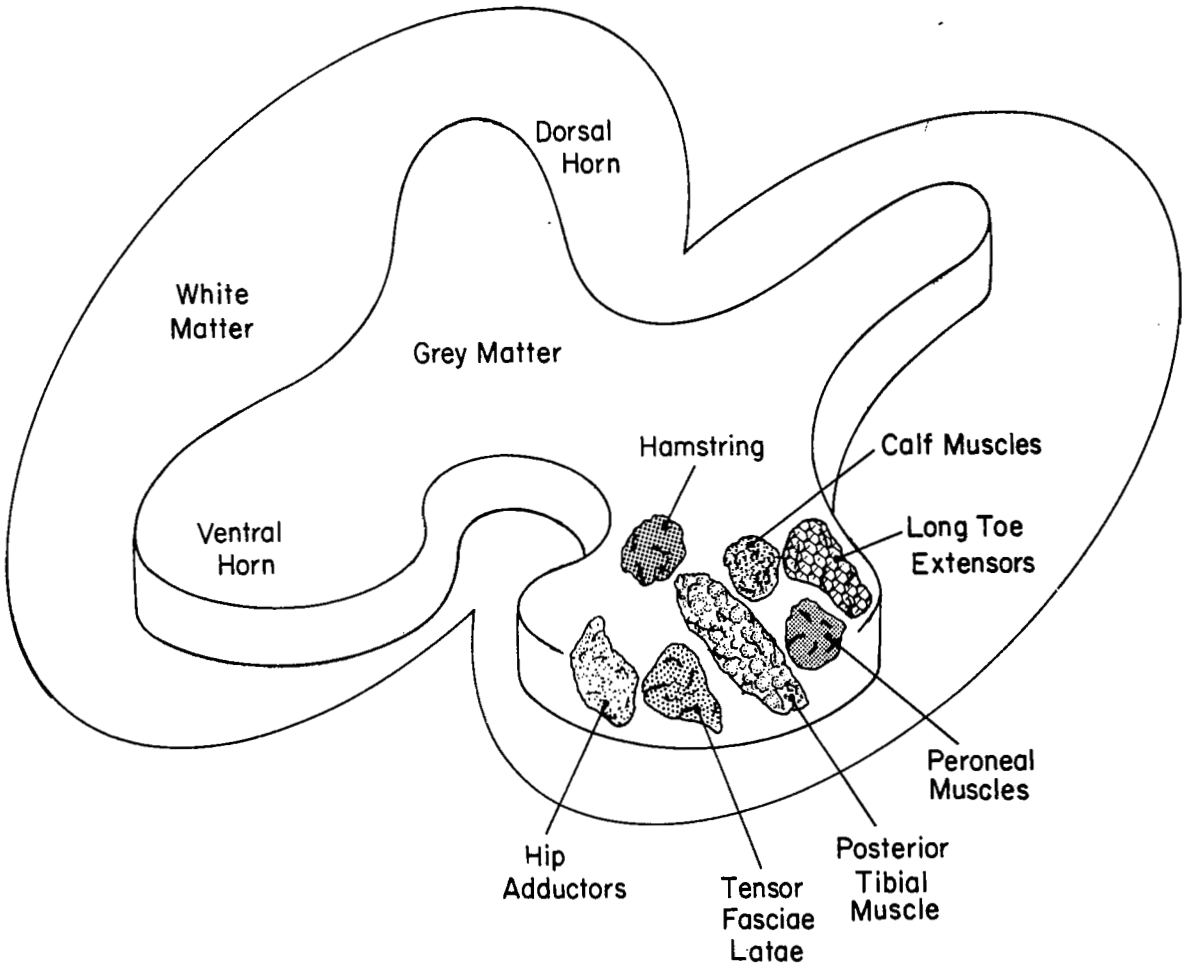

Figure 5. Schematic Representation of Spinal Cord Segment at Fifth Lumbar Level

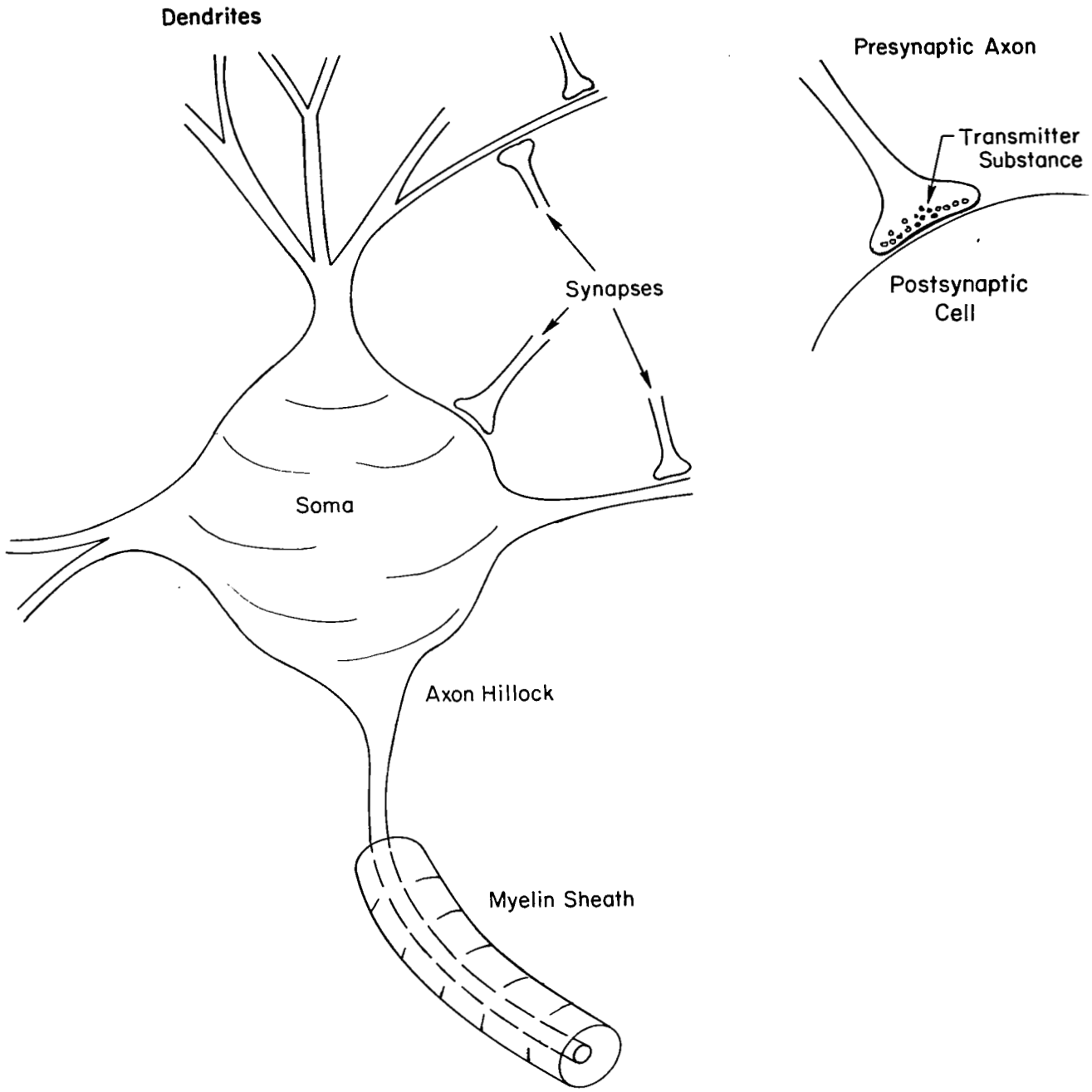

Figure 6. Neuron Schematic Diagram

The functional significance of the multitude of synaptic endings distributed over such a wide area of a neuron lies in the integration of their individual effects. An impulse at one synapse generates a typical change in potential in its localized area which, in an over-all sense, is summated with all the other minute changes generated by impulses arriving at other synapses. Some of these will tend to shift the over-all potential in a more negative direction, some in a less negative direction. In every neuron there is at least one specialized region at which, if the membrane potential falls to a low enough point (around −40 mV), the "threshold level," the cell generates a pulse which travels out along its axon. Until this point is reached, the cell is generating no output along the axon. After the pulse is generated, the membrane potential is reset to its original value (around 70 mV). Impulses which arrive at synapses which lower the postsynaptic membrane potential are termed "excitatory," while those which make the membrane more negative, or less likely to reach threshold, are called "inhibitory."

It has been fairly well established, at least for motor neurons, that the site at which this threshold/switching property is located is at the junction between the cell body and the axon, just prior to the point where an insulator-like substance surrounding the axon, the "myelin sheath," begins. This region is called the "axon hillock" and appears to be the point where the summated effect of all the minute synaptic potentials determines whether a pulse, or "spike," will be initiated and transmitted. For this reason it is important to note that synapses at the ends of the dendrites, because of their very remoteness, may have a much smaller effect than more proximate synapses. This has led to increased interest in determining regional differences in the termination of input sources from other neurons, and to some interesting speculation concerning the theoretical switching and computing properties of single neurons.

The very fact that dendrites receive such a high density of synaptic potential input, which leads to complex field patterns in the tissue spaces they occupy, has led to considerable interest concerning the possibility that neurons in close proximity can communicate with each other, i.e., influence each other, by means of the fields set up in their dendritic networks. Certainly, from a theoretical point of view it is clear that at certain moments the dendritic tree of a motor neuron can act as a spatially complex current sink, which, due to the overlap of

dendritic networks, could act as a powerfully excitatory agent to neighboring cells. This could be important in the generation of synchrony or antisynchrony in a pool of synergistic cells.

Axon transmission — In general, axons do not receive synaptic input but they do have membranes with the threshold property described earlier. They are specialized parts of the neuron insofar as they exhibit primarily transmission functions. Their transmitting ability arises from the fact that the existence of the nerve impulse at any region of the axon will always cause the potential to be lowered in an adjacent region to the point where threshold is reached, thereby exciting the adjacent region to generate a pulse. In normal use, the transmission is unidirectional because axon membrane is incapable of generating a new pulse for a millisecond or so (the "refractory period") after its last one; hence, the impulse can invade only sections of the axon which have not yet been activated. Indeed, the nerve pulse moves along the axon at just such a rate that it cannot "reach back" far enough to re-excite the region it has passed, now recovering from the refractory period. This rate is a function of the axon thickness and myelin thickness; for the largest axons (among them those belonging to motor neurons) the conduction velocity may be as much as 100 m/sec. For the smallest unmyelinated fibers, conduction velocities are only a few meters per second.

In the terminology developed here we can now say that the impulse conducted along a motor axon will always trigger a change in potential in the muscle fiber which exceeds threshold, i.e., the transmission is one-to-one.

Parameters of control for motor units — There are several motor system parameters which are relevant to the control of muscle tension at the peripheral level of the motor unit. The first important parameter is the size of the motor unit itself, i.e., the number of muscle fibers innervated by a single motor neuron. There is a large variation in the size of motor units, sometimes referred to as the "innervation ratio." For a large and powerful muscle such as the gastrocnemius as many as several thousand muscle fibers are directly innervated by a single neuron in the lumbar region of the cord; at the other extreme, a motor cell in the oculomotor nucleus in the brain stem may control as few as ten muscle fibers which serve to rotate the eyeball (table I).

A second obvious parameter is the total number of fibers available in the entire muscle. Again, a powerful muscle such as the gastrocnemius, as would be

TABLE I

NUMBER OF MUSCLE FIBERS AND MOTOR UNITS FOR VARIOUS MUSCLES

Muscle	Number of muscle fibers (In thousands)	Number of motor units	Size of motor unit (Innervation ratio)
Superior rectus of eye.....	42	2000	23
Lateral rectus of eye.....	22	1740	13
Biceps.....	580	3500	163
Sartorius.....	222	740	300
Cricoarytenoideus posterior.....	16	140	116
Rectus femoris.....	186	600	305
Gracilis.....	145	275	527
Semitendinosus.....	508	712	713
Gastrocnemius.....	1505	778	2037
Tensor tympani.....	11	55	20

expected, has a very large number (on the order of a million), while the smallest muscle, the tensor tympani (which controls the mechanical impedance of the series of ossicles in the middle ear), has only about 1000 fibers. Taken together, the innervation ratio and the total number of muscle fibers enables us to compute the total motor neuron pool size (i.e., the number of motor neurons) for each muscle (see table I).*

Assuming that all muscle fibers of comparable diameter have the capacity of generating the same amount of tension, it follows that the size of the motor unit determines the minimum quantum of tension or force which the muscle can "negotiate" in the control of movement. Thus, every firing of a biceps motor neuron generates the obligatory twitch contraction of about 1000 muscle fibers, and variations in biceps contractile force must be transacted at quantum levels of that magnitude, which for that muscle is approximately 10 grams, or some one hundred times the minimum quantal force for the extraocular muscles.

*These figures should be taken only as an indication of approximate quantities.

A third factor of extreme importance in the graduation of muscle tension is the firing frequency of the motor neuron. In general, tension in the motor unit is a monotonically increasing function of firing frequency. A typical plot can be seen in figure 7 in which tension (in a motor unit) is plotted against stimulation frequency; for comparison the strength of a maximum voluntary contraction is shown in a similar diagram of a whole muscle activated by electrical stimulation of its motor nerve. As the stimulation frequency is increased to the point where all individual twitch responses become fused (i.e., the muscle is "tetanized"), it can be seen that (1) there is a region of relatively rapid rise in tension as a function of frequency, (2) there is an asymptotic value of maximum tension which apparently can be achieved in maximum voluntary effort, and (3) the tetanus/twitch ratio of tension is, in the example shown, about six to one, and the range in general is usually given as a twofold or fourfold increase. Clearly, this ratio will also be important for the control of tension. Another variable, which appears to be intrinsic to the muscle fiber itself, is a characteristic properly known as the "twitch time" (the time required for a twitch to develop and subside), it being an important phenomenon that mammalian muscles are inherently either "fast" or "slow" (ref. 9). Generally, the "slow" fibers are tonically active postural-type muscles which maintain fixed tensions over relatively long time periods. "Fast" muscles are those related to phasic, i.e., short term kinetic movements. The twitch times for slow and fast muscles can be seen from the tension time curves of figure 8. Also shown is a twitch response curve of an extraocular muscle fiber which is noticeably faster than that for a fast muscle. Refractory periods and action potential durations for muscle also tend to parallel twitch times (ref.11), slow fibers having longer recovery times and action potentials (which is unimportant because their longer twitch times mask their inexcitability). The duration of the twitch will naturally influence the firing-frequency/tension relation. Thus, as one would expect, the tetanic fusion frequency of slow fibers is quite low, e.g., less than 20 impulses/sec, whereas the fusion frequency of the extremely fast extraocular muscles is around 200 impulses/sec (ref. 1). These fusion frequency differences also amount to differences in range of firing frequency.

We can integrate this entire presentation by pointing out that muscle properties seem to be optimized for control requirements. Thus, for the extraocular muscles, which have the tightest argument for fine control, it has already been pointed out that [1] the motor unit size (or innervation ratio) is smallest,

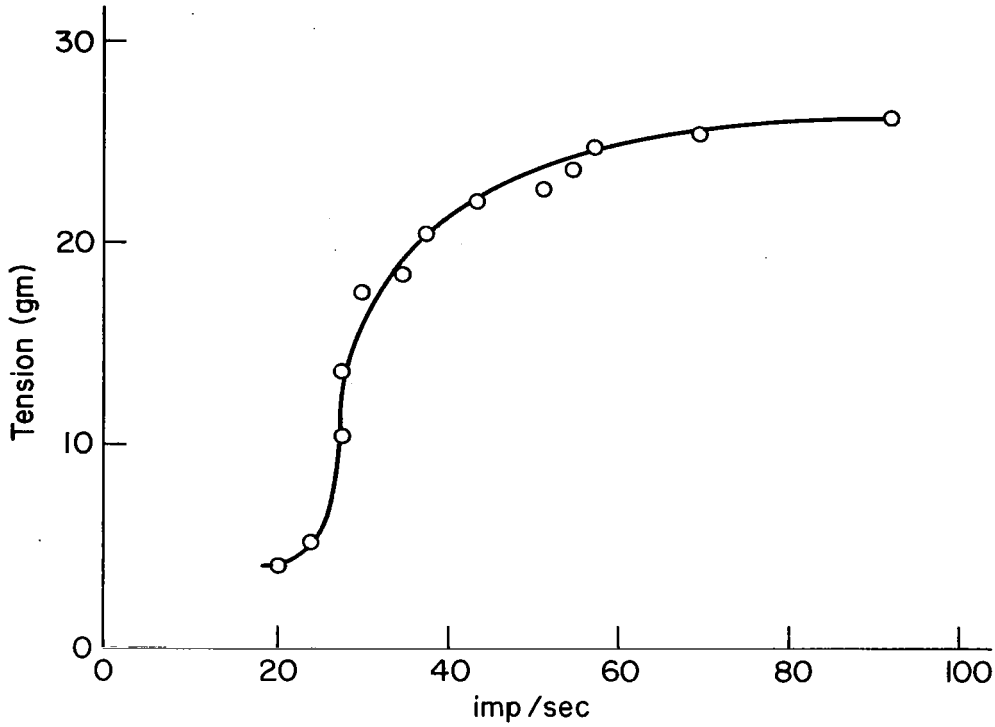

(a) Motor Unit (Gastrocnemius)

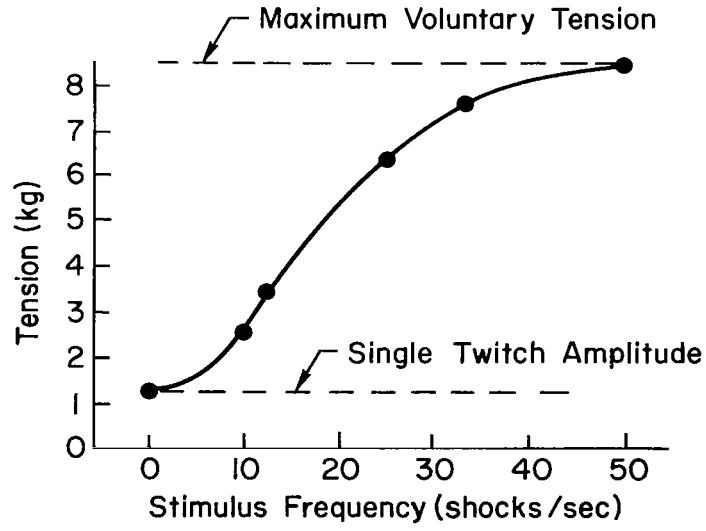

(b) Whole Muscle (Adductor Pollicis)

Figure 7. Tension Versus Stimulus Frequency

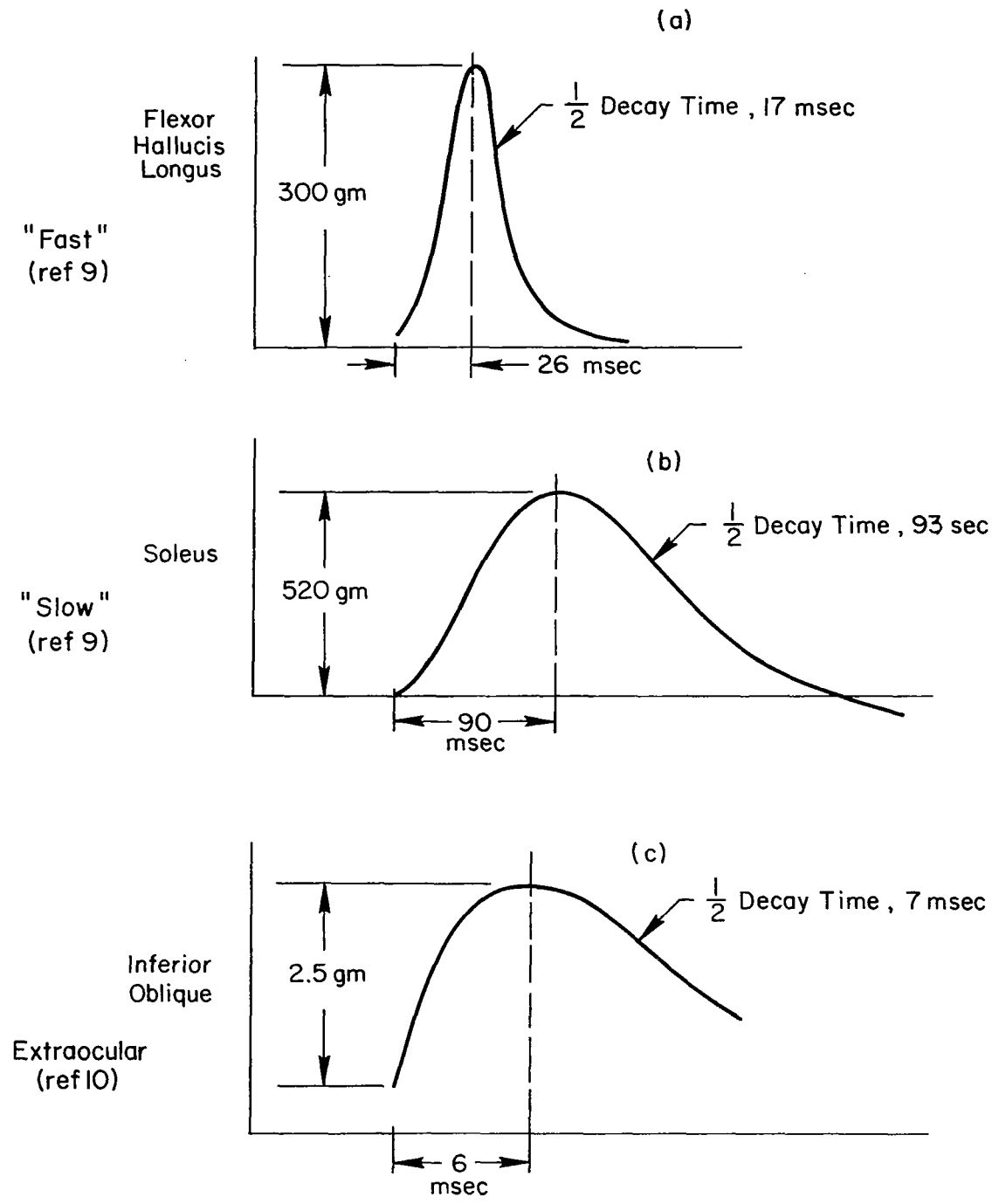

Figure 8. Twitch Responses

[2] the minimum negotiable force is smallest, [3] the size of the motor neuron population is largest (see table I), [4] the twitch time is shortest (and therefore the fusion frequency is highest), and [5] the maximum firing frequencies are greatest; moreover, [6] for these muscles the tetanus/twitch tension ratio is also greatest. Consequently, the control system can work with smaller quanta of tension, great numbers of motor units, faster responses, a wider range of controlling signal frequencies, and a greater dynamic range of forces in each unit.

Conversely, the slow acting muscles used in relatively inexacting maintenance tasks such as posture have parameters at the opposite extreme, and therefore enjoy a very reasonable and profitable economy in control and maintenance costs.

Utilization of motor units in voluntary activity —We know relatively little about the detailed way in which the nervous system utilizes these various parameters in the development, adjustment, and maintenance of muscle force under voluntary conditions. Apparently a subject provided with audio feedback from the electromyogram (EMG) can learn to control the discharge of any given motor unit within minutes (ref. 71). However, it has been demonstrated, at least in some muscles, that in the progressive development of tension from minimal strength to maximal voluntary force production each motor unit is recruited into the action at a rather precise and reproducible tension level; that, once brought into the effort, the motor unit frequency increases rapidly as over-all tension increases to a maximum firing rate for that neuron (ref. 12 and fig. 9a). The tension range for the muscle, when the unit first enters and when it reaches it maximum rate, is rather narrow. For example, in the gastrocnemius/soleus complex in man, which can develop 50–60 kg of tension, a typical motor unit may increase its rate of discharge from an initial rate of four times per second to a maximum of ten times per second over a range of 150 grams, i.e., less than one percent of the total tension range for the muscle (fig. 9b). Thus, in the production of variable tensions the nervous system <u>does not use all available motor units</u> first at low frequency and then at progressively higher frequencies, nor does it <u>rotate</u> the effort in any obvious way among motor units. Rather, it appears to bring in (or drop out) each unit at a stable threshold level of tension and to raise its frequency quickly to a maximum, bringing in other units as needed to increase tension.(fig. 9c). There is considerable variability in the size of motor units in a given muscle. As a result the maximum tension which a motor unit is capable of generating will vary from unit to

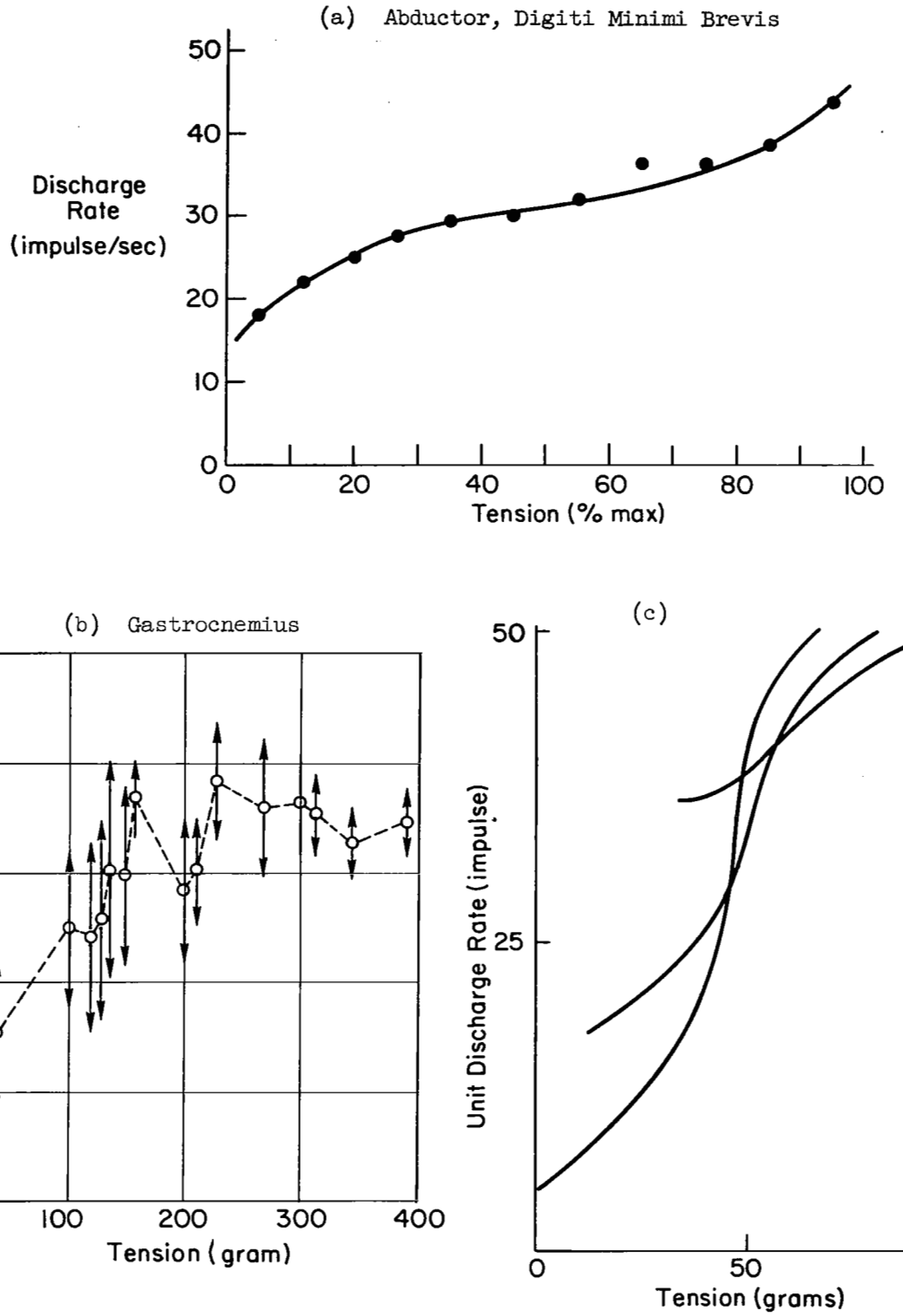

Figure 9. Voluntary Tension Versus Motor Unit Discharge

unit. Typical distributions of tetanic tension for a slow and a fast muscle are shown in figure 10.

It has recently been shown that the order in which motor units are recruited may depend on the size of the motor unit, smaller units being recruited first. This means that at low tensions the increments of tension are small, while at large tensions the increments are larger. Apparently, however, this arrangement lends itself to a nearly constant relative fineness of control (refs. 14, 15).

The most efficient way to use a muscle is to drive it so that twitches fuse, thus eliminating the necessity of repeatedly stretching the series elastic components in the fibers themselves. Consequently, one paradoxical feature of the central control of the motor unit is that while neurons which are recruited into a voluntary contraction do reach a firing frequency plateau, this rate of discharge is considerably below the tetanic frequency and indeed often is below the minimum frequency necessary for summation. It must be concluded that significant summation of twitches occurs only at maximal or nearly maximal voluntary tensions.

It has been shown that there is a progressive increase in the maximal normal firing frequency of a motor unit as one proceeds up the spinal cord from more posterior segments, innervating the hind limbs, toward the upper levels, innervating the arms (ref. 13). Since motor cells are capable of firing at frequencies at least ten times greater than those observed, it has been suggested that their firing frequencies are regulated by negative feedback loops in the spinal cord ("recurrent inhibition"). Thus, it is postulated that every outgoing impulse may also be relayed to an interneuron (the so-called Renshaw cell) which, in turn, feeds back to partially inhibit the motor cell (see p. 47, "General Features of Spinal Cord Organization").

Because the nervous system is incapable of increasing the number of its cells (neurons mature but do not divide after birth), it follows that increased strength in a muscle, as a result, say, of exercise, cannot be due to an increase in the number of motor units, nor does the innervation ratio change. Rather, the size of the muscle fibers themselves changes and, since the development of force in a muscle (extra fast or slow) is proportional to cross-sectional diameter (in tetanus a force of 2.4 kg/cm^2 is typically cited, i.e., ref. 16), the increase in fiber size is reflected in the increased tension which can be produced.

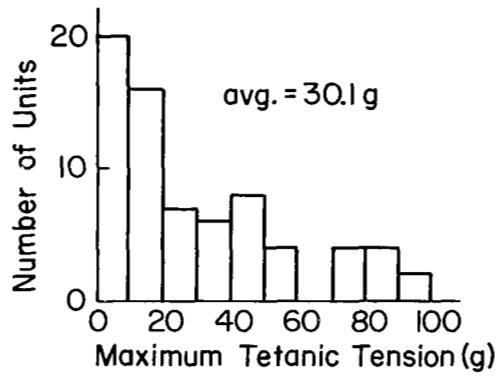

(a) *Gastrocnemius*

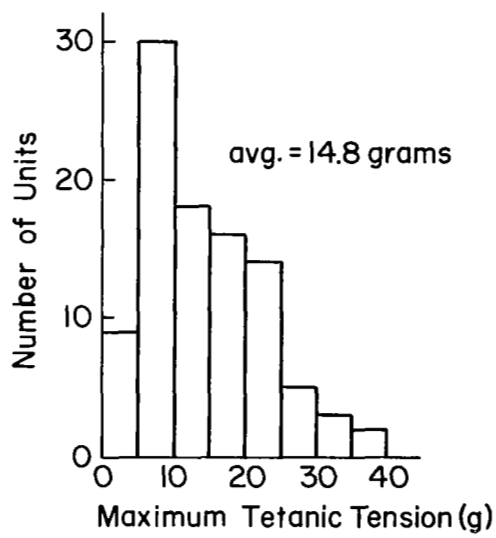

(b) *Soleus*

Figure 10. Distribution of Maximum Tetanic Tension

Basic physiological properties of muscle. — An understanding of the significance of particular patterns of impulse activity generated by motor neurons in the spinal cord depends on an understanding of the electromechanical properties of the muscle cells to which these impulses are directed. Some of these have been alluded to in our earlier discussion of twitch responses and tetanic contractions, and these properties will be elaborated in more detail here.

It is often convenient in studying the physiological properties of muscle to restrict attention to two extreme modes of muscle operation, namely, those cases in which, during contraction, the over-all length of the muscle remains constant (isometric contraction) and those in which the load on the muscle remains constant (isotonic contraction). Many natural movements, of course, are intermediate between these, but some simplifications in the treatment of experimental data are possible in these two restricted conditions.

From experiments using a combination of isometric, isotonic, and abrupt load reduction contractions it can be shown that muscle can be represented by a combination of a series elastic component plus a contractile component where only the latter is influenced by motor nerve stimulation. One can further distinguish the active from the passive properties of the contractile component — the latter consist of the mechanical properties of muscle which is not being stimulated, while the former are those which are observed during stimulation, to which the passive properties are usually added.

Length/tension relations — One very useful characterization of the muscle fiber is the length/tension curve shown in figure 11 which indicates the tension produced in an unstimulated fiber by stretching it beyond its natural* length. On a linear scale (fig. 12) this passive curve shows that the muscle properties deviate significantly from those of a purely elastic element, and, indeed, irreversible damage to the fiber usually results if the stretch exceeds about 100 percent of the resting length.

The passive length/tension curve can be compared on the same diagram with the corresponding active curves, the muscle being stimulated by shocks of varying

*A vague term usually taken to mean the resting length of the muscle in the body.

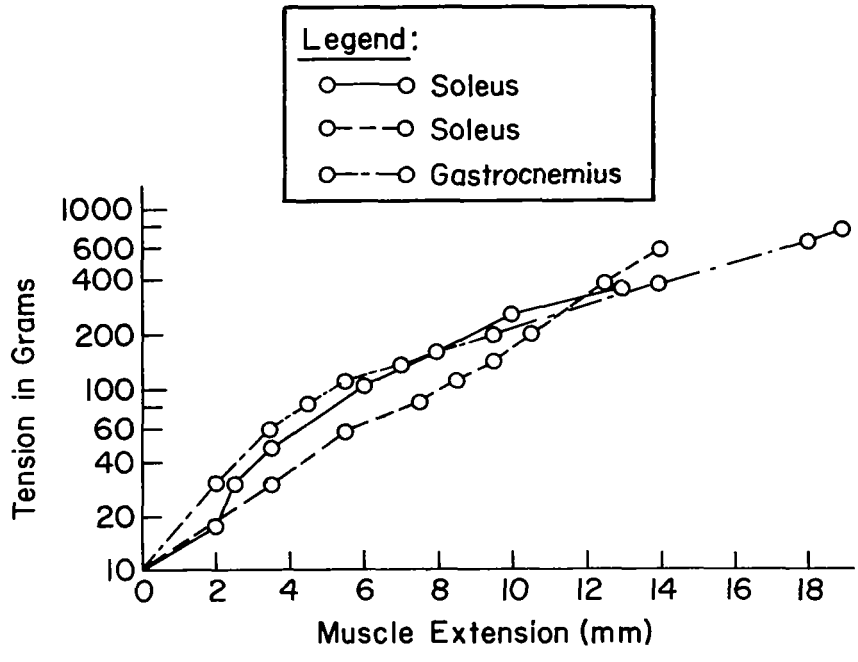

Figure 11. Passive Length/Tension Relations

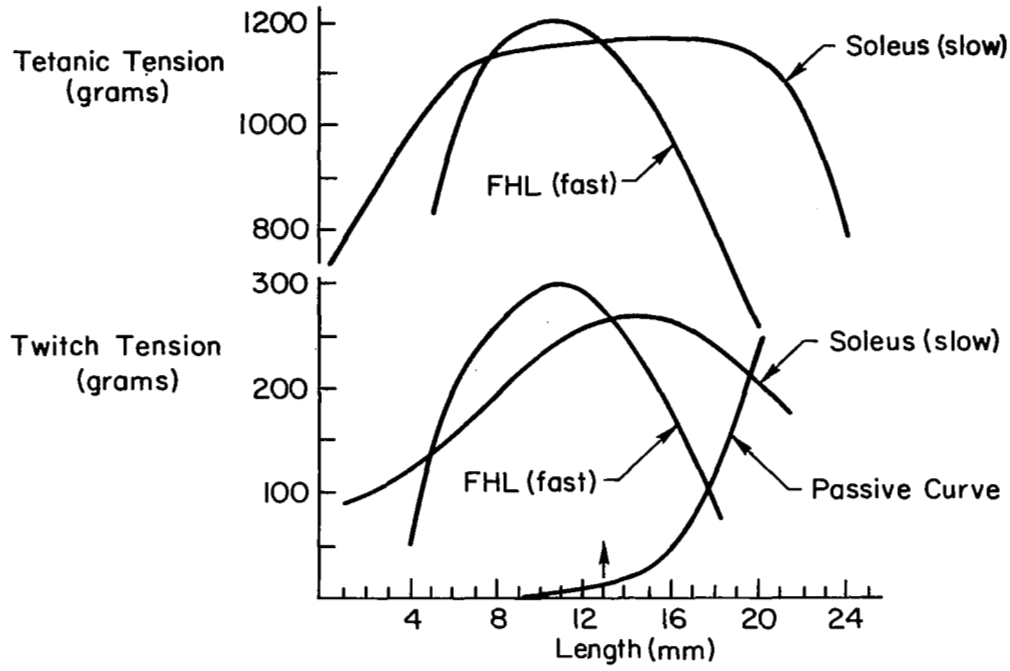

Arrow indicates muscle length for ankle at right angle

FHL - Flexor Hallucis Longus

(a) Whole Muscle

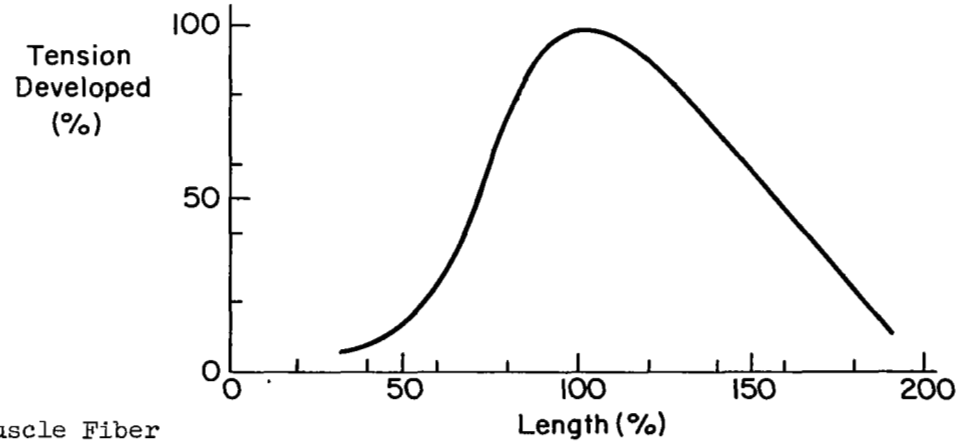

(b) Single Muscle Fiber

Figure 12. Length/Tension Curves for Whole Muscle and Single Muscle Fiber

frequency applied directly to the muscle or to its motor nerve. In figure 12a the active length/tension curves are shown for a whole muscle during single-twitch contractions and during tetanus. Corresponding curves for a single muscle fiber have also been measured, as shown in figure 12b. The tension is measured under isometric conditions, the length being held constant by a restraining device. Ideally, to generate the entire curve the muscle would be slowly stretched beyond its rest length (generating the passive curve), whereupon a stimulus of appropriate frequency would be applied and the muscle would be allowed to slowly contract, its length/tension parameters being plotted simultaneously. In general, the curve can be generated in the opposite direction with little evidence of hysteresis. In addition, intermediate curves corresponding to lower rates of stimulation can be derived. An example from extraocular muscle is shown in figure 13. As in figure 13, it is customary to subtract the passive tension corresponding to each length from the total measured tension to obtain the tension actively generated by a stimulus.

Although the curve in figure 13 is constructed under isometric conditions, considerable information about the isotonic behavior of the muscle can be obtained from the diagram. For example, if a muscle fiber initially at rest length is suddenly tetanized and allowed to contract against a constant load, then shortening will occur if the tetanic tension developed at this initial length exceeds the load. Since it is a general property of muscle that its peak active tension is generated at its natural length, then as the muscle shortens its developed tension is reduced, causing it to shorten to that length at which it generates a tension equal to the load. (If the load is greater than the total tetanic tension developed at the initial length, the muscle will be lengthened by the load until its increasing total tension becomes equal to the load or until it is fully extended.) Clearly, for every stimulus frequency there is a unique equilibrium length which will be achieved by the muscle when acting against a constant load, and this point on the length/tension curve is indifferent to the manner in which the movement of the muscle takes place. But while the final point is the same, the time course of tension, length, and velocity of shortening will be quite different.

Force/velocity relations —Another basic property of muscle is that the force which a muscle is capable of generating is a function of the velocity at which it is shortened (or lengthened). The relationship between these parameters is

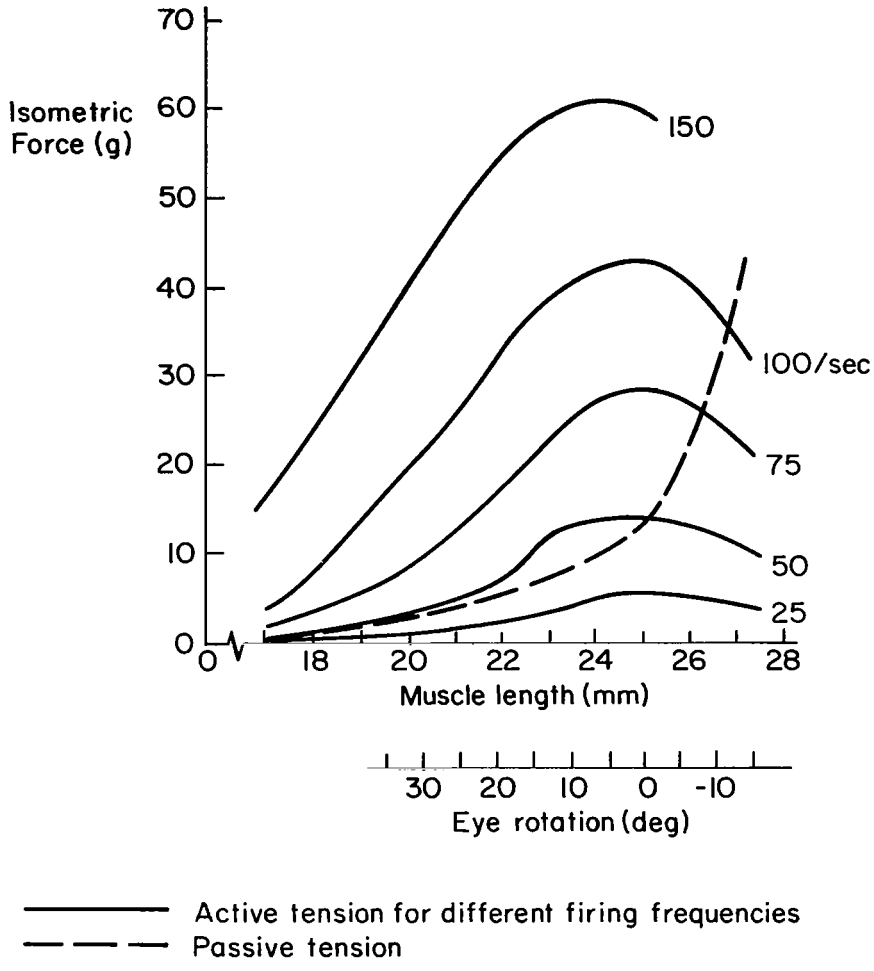

Figure 13. Length/Tension/Frequency Curves For Whole Muscle; Extraocular Muscle (from Ref. 33)

summarized by the force/velocity curve. Typical force/velocity curves for tetanized animal muscle are shown in figure 14a (ref. 24). A similar curve for human biceps muscle during a maximal contraction effort is shown in figure 14b (ref. 25). At intermediate levels of effort (as measured by EMG techniques) a family of curves, figure 14c, is generated (ref. 26).

These curves are obtained experimentally by first setting the muscle to a fixed length, and then exciting it and allowing it to develop tension. When the tension developed exceeds the weight of the load, the load (previously supported and not applied to the muscle) is lifted and the initial velocity of the contraction is measured. (If the load is greater than the maximum tension developed by the muscle, extension or "negative shortening" occurs, but the results for this type of motion do not lie along an extension of the force/velocity curves for shortening, see reference 70.) Thus the muscle exhibits viscous characteristics similar to those of a nonlinear damper.

Series elastic component —The series elastic component behaves like an inert nonlinear spring, whereas the contractile component's properties (length/tension and force/velocity relationships) depend on motor nerve firing frequency and muscle length (ref. 83). Typical curves are shown in figure 15 for two different muscles (ref. 24).

These curves are obtained experimentally by setting the muscle to a fixed length and tetanizing it. Then a latch is released so that the load on the muscle drops from its isometric value to something less. This abrupt load reduction causes the muscle to shorten a certain amount almost instantaneously, after which the contraction proceeds at constant velocity, as predicted by the force/velocity relationship. Thus, the ratio of the change in load to the abrupt change in initial length is attributed to the series elastic component because the viscous characteristics of the contractile component prevent its abrupt shortening. Additional evidence indicating the inert character of the series elastic component is given in reference 83; the measured results of abrupt load reductions from a number of different initial loads all gave the same curve.

Fast and slow skeletal muscle —Recent experiments on the force/velocity relations in muscles have confirmed the existence of a crucial difference in the properties of mammalian muscles which appear to fall into two distinct classes. On the basis of many such observations, muscle fibers are classified as either

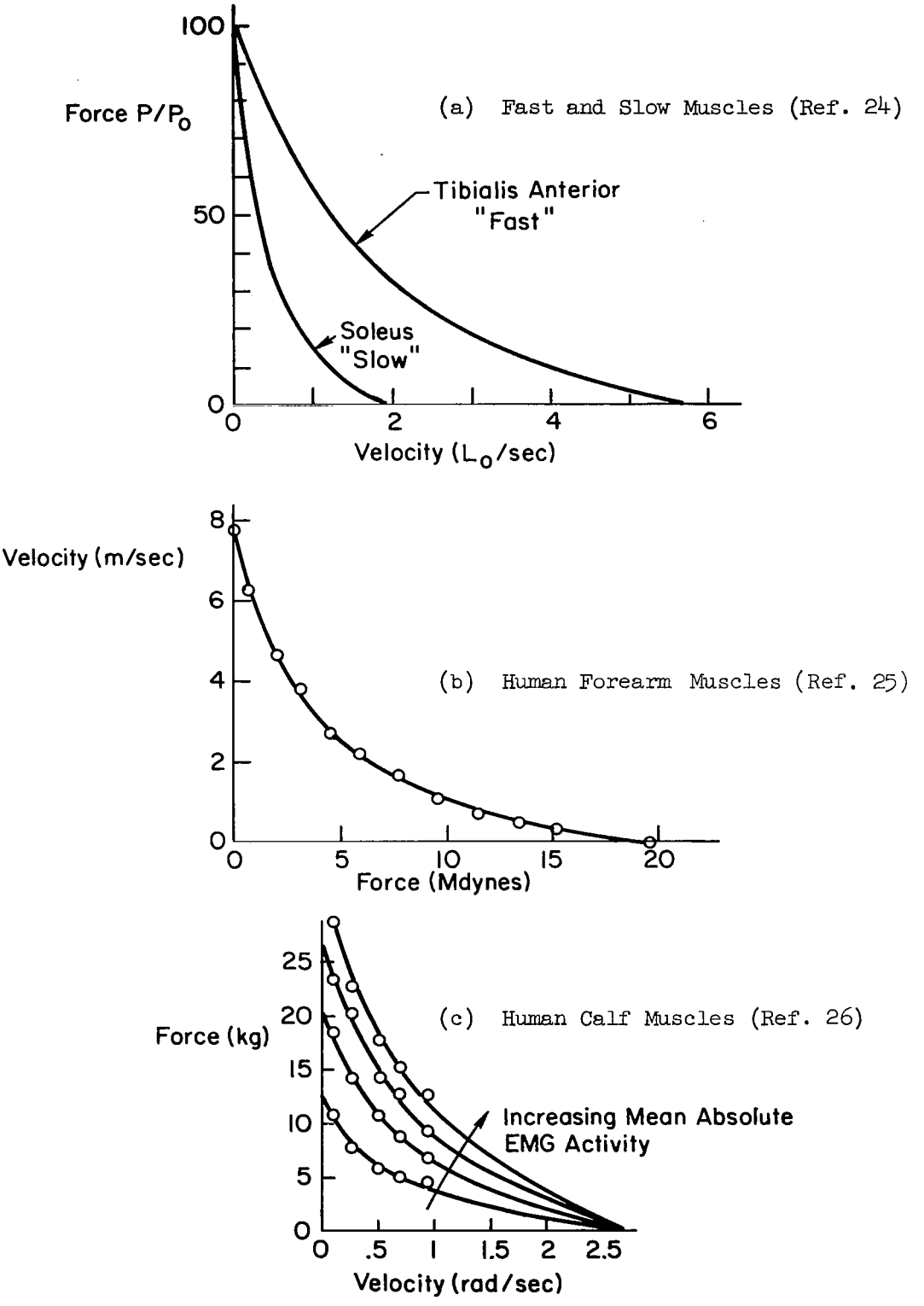

Figure 14. Force/Velocity Curves

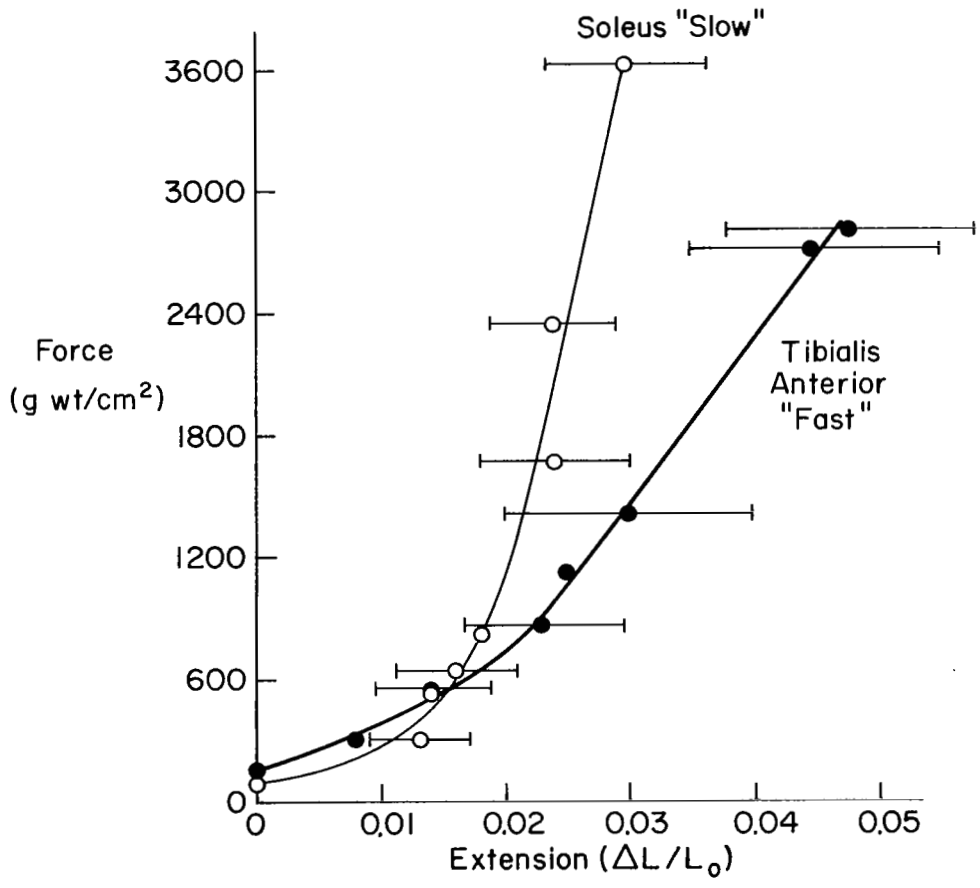

Figure 15. Series Elastic Component (from Ref. 24)

"fast" or "slow," a distinction which seems to apply to the speed as opposed to the strength of the contractile processes of muscle* (refs. 9, 16, 17, 18, 24, 99, 100).

The difference between fast and slow muscles can be seen from figure 14a in which the force/velocity relations for a typical slow and fast muscle are shown. Another expression of this difference can be seen from the tension/time relations of the twitch response of slow and fast motor units.

A similar relationship is seen in figure 12, which shows the twitch responses of single motor units and whole muscles of two muscles consisting apparently of purely slow and fast fibers, respectively. Several other variables related to speed of contraction are also correlated with this basic property. For example, the tetanic fusion frequency for slow muscles is much lower, as would be expected (e.g., 16 times per second in soleus versus 64 times per second in gastrocnemius), but this is also associated with a slower firing frequency of the innervating motor cell whose afterpotentials are much longer (refs. 11, 21), and the connecting axon whose conduction velocity is lower (refs. 1, 22). Finally, as shown in figure 15, the series elastic component for slow and fast muscles is significantly different.

The significance of the fast/slow distinction, however, extends far beyond the simple aspect of velocity because a number of other extremely important physiological features are correlated with the velocity property. Indeed, it has been shown by cross-innervation studies that the muscle fiber derives its properties in some mysterious way from the axon which innervates it.

Since there are, as already indicated, muscles which consist almost entirely of purely slow or fast muscle fibers, considerable interest has been shown in the different ways these muscles are used. For example, the soleus (a slow muscle) and the gastrocnemius (a fast muscle) both have the same functional effect, i.e., ankle extension, yet they have utterly different physiological properties. It has been hypothesized that the slower muscle, which requires much lower neuronal discharge for control over its tension range, is used for ankle extension functions which are slow and tonically maintained (such as standing), whereas the faster muscle is used for brief, phasic, rapid movements (such as running).

Most muscles are mixtures of motor units with fast or slow properties, and it has been assumed that this corresponds to a functional differentiation in

*Intermediate types of motor units have also been reported, but appear to be relatively few in number (ref. 99).

that muscle between tonic, postural, maintained use and phasic rapid use. Even within the extraocular muscles which are inherently faster than other skeletal muscles, there appears to be a natural grouping of fast and slow fibers with correspondingly different sizes of innervating axons. Again, there appears to be a functional distinction in their use, the fast fibers becoming activated during rapid eye movements, the slower fibers being active during maintained eye fixation (ref. 10).

Open-loop muscle control. — The significance of the length/tension/frequency family of curves for muscle becomes clear when we consider the action of a pair of comparable muscles in the positioning of a limb or in fixing the direction of gaze of the eye. This latter problem has been considered by Robinson (ref. 23), who has made careful measurements of the forces developed by the extraocular muscles of the eye as a function of length and stimulus frequency.

The eye is normally rotated or held in position by the concerted action of three pairs of muscles. In the present discussion we will restrict our attention by considering only the two muscles which serve to rotate the eye in a horizontal plane, the horizontal recti (fig. 16a). If we assume that the two muscles (the medial and lateral recti) are identical in their mechanical properties, we can use the data obtained by Robinson to plot the activity of these muscles which would be required to fixate the eye in a given direction.

The length/tension curves for various frequencies of stimulation are given in figure 13, which shows the passive and actively generated tensions in each muscle. If we assume that the length/tension/frequency curves for each antagonist muscle are identical, and assume also that the total tension in each muscle will be the sum of the active and passive tensions (shown in fig. 13), then the resultant tension/length/frequency family is that shown in figure 16b. We assume further that the frequencies of stimulation referred to are sufficiently accurate measures of over-all motor unit firing rates so that the numbers associated with each curve are reasonable representations of ensemble activity in the motor unit pool. Assuming initially that the eye is directed straight ahead and each muscle is being stimulated 50 times per second by its nerve supply, each is exerting about 30 grams of force. The eye position is in fact stabilized because any momentary increase in force generated by one muscle will serve to stretch the antagonist

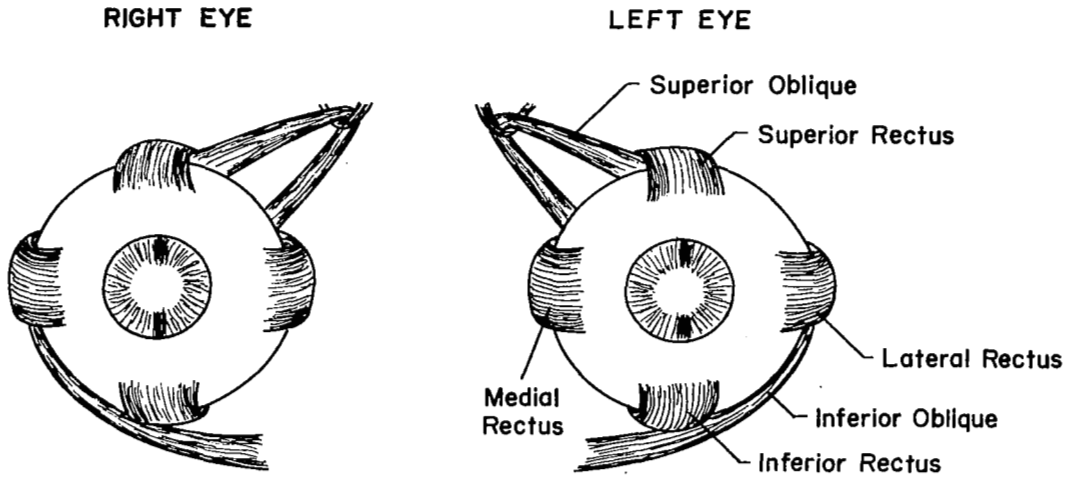

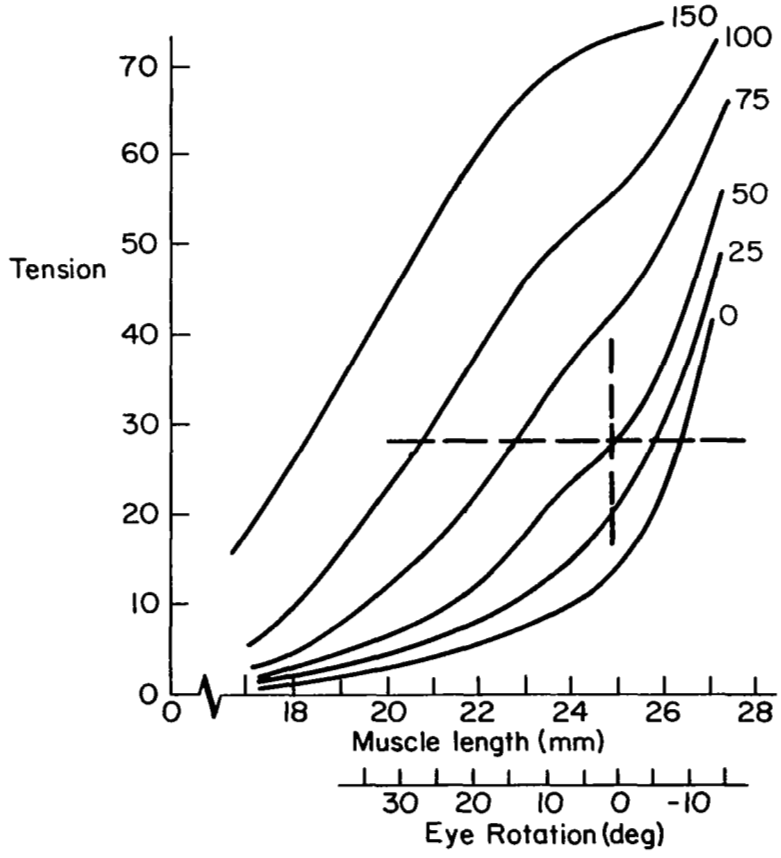

Figure 16. Effect of Stimulus Rate on Length Versus Total Tension Curves (from Ref. 23)

muscle, an effect which can be seen to increase its resistance at constant stimulus frequency.

Now, suppose that the stimulus frequency to the muscle which rotates the eye to the right is increased to 75 pulses/sec and the stimulus to the antagonist is decreased to 25 pulses/sec. The former muscle is initially capable of developing at least 40 grams of tension, while the latter can develop only about 17 grams, at least at the starting lengths corresponding to 0^{o} rotation. This imbalance of tensions will result in a rotatory movement to the right, the agonist contracting, the antagonist extending. But as the antagonist is lengthened, its total tension (active plus passive tension) increases, the relationship being that given by the curve at 25 pulses/sec stimulation. Conversely, the muscle at 75 pulses/sec shortens along the 75 pulses/sec curve and its tension drops. It follows that there must be some length increase in the antagonist at which its total tension is equal to that of the agonist which has shortened by the same amount. Inspection of figure 16b indicates that this point lies between 6^{o} and 14^{o}.

We can generalize on this calculation by pointing out that it is always possible in this situation to calculate the stimulus frequencies necessary to generate muscle forces corresponding to a given position of the eye. The solution is derived from the full family of curves, subject to the constraint that an equal change in length (but of opposite sign) of agonist and antagonist must occur, and each amount corresponds to a final angular position. The final angular position determines the location of the two vertical lines which intersect the length/tension family for each muscle. From this we can see that the solution is underdetermined and a unique solution depends on our choosing either the final tension or one of the final firing frequencies. In other words, the solution to the general problem of eye position and controlling signal requires specification of at least two of the three parameters —final position, final tension, and final firing frequency. The fact that many final tensions or frequencies of stimulation will leave the eye in the same position suggests that the solution, in practice, is optimized against some other criterion. But it is likely that in most eye movements requiring fixation at a given point there is a fairly constant and reproducible firing rate achieved by the driving motor neurons. The most important aspect of the situation is that, since the eye is a fixed load whose dynamics and inertial properties are independent of position, there is the rather unique possibility in this system for open-loop control.

Closed-Loop Neuromuscular Control Systems

In practice, very few muscle systems enjoy the property of the extraocular muscles which actuate a constant load. Most muscles exert their effect on skeletal elements, carrying varying loads with complex dynamics and moving in complex ways. In such instances, when it is not possible to predetermine the requisite motor command signal pattern, e.g., when we attempt to lift an unknown load, it is clear that some form of feedback and control is required. Certain elements of the neuromuscular system which are critical to the execution of skilled motor acts are discussed in the following subsections. The discussion begins with the critical sensory element of muscles, the muscle spindle, and its feedback relations with the motor units in the spinal cord, a relationship which alters the effective characteristics of the muscles themselves, and concludes with the Golgi tendon organs.

Muscle spindles and other peripheral neuromuscular sensory elements. — Muscle spindles constitute the most important and most numerous sensory organs of vertebrate muscle (refs. 7, 27, 33). There may be, typically, from 50 to 100 such organs in a single mammalian muscle, and each may have a quite complex organization in terms of its motor and sensory innervation.

A spindle has a length of several millimeters and is known to consist of several distinct and specialized regions. Within the fluid-filled capsule enclosing the organ are two distinct types of special muscle fibers, the thicker bag fibers, in which there is an enlarged nuclear region, and the thinner, simpler, but more numerous chain fibers.

A highly simplified diagrammatic view of a muscle spindle is shown in figure 17. This shows the central axis of the spindle which consists of a globular nuclear bag region connected to either pole of the spindle by means of a pair of nuclear bag fibers which are themselves typical striated muscle fibers (approximately 25 μm in diameter). These nuclear bag fibers are known as "intrafusal fibers," and do not contribute significantly to the development of tension in the muscle.* Rather, they appear to be motor fibers related solely to control within the spindle itself. From their microscopic appearance the bag fibers appear to be normal striated muscle fibers, and hence would be expected to have dynamic and mechanical properties similar to those of the extrafusal fibers discussed in the previous section. Chain fibers lack the nuclear bag region. They have smaller diameters

*Intrafusal fibers may generate only a few milligrams of tension even when stimulated tetanically (ref. 98).

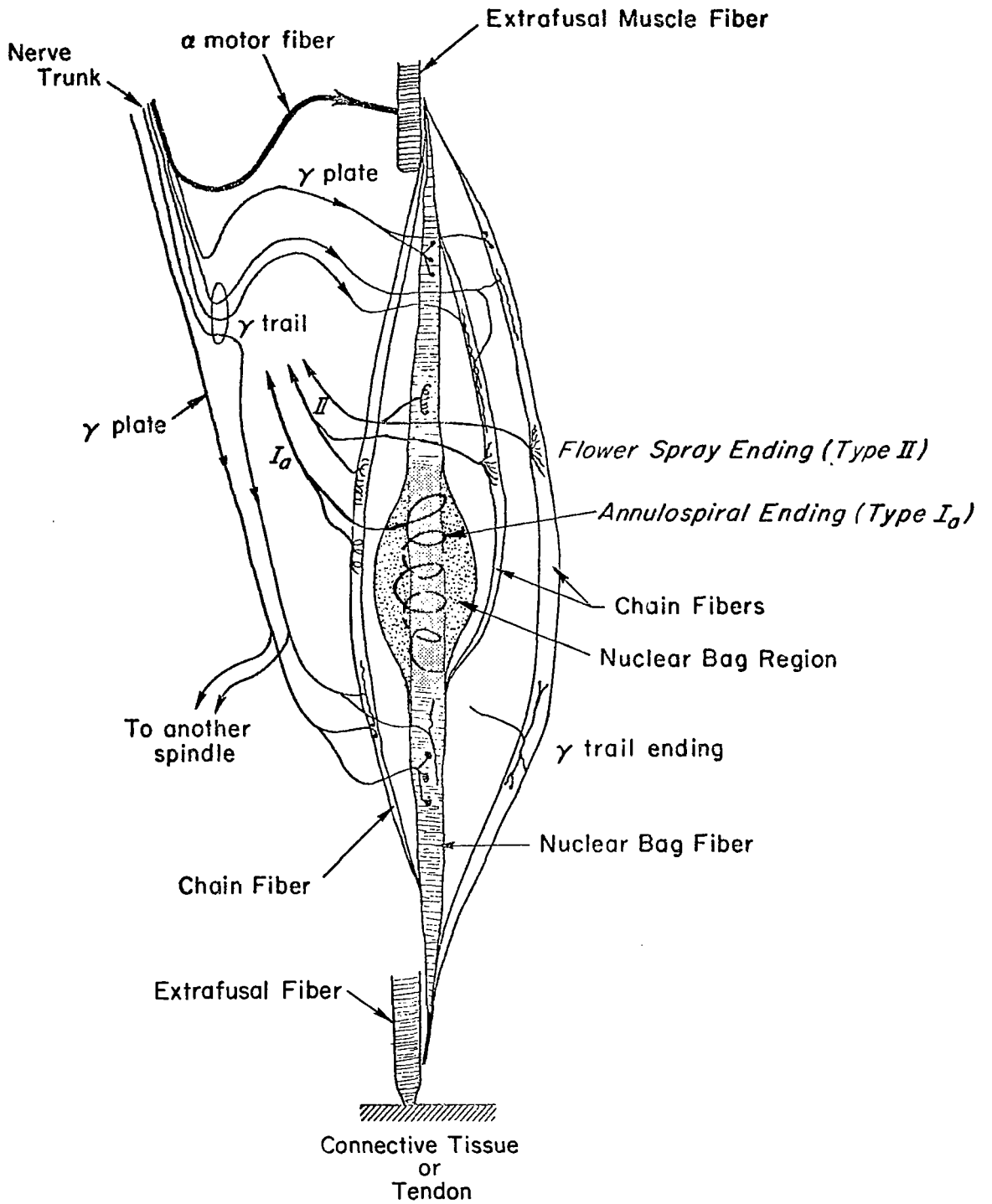

Figure 17. Generalized Muscle Spindle Anatomy

and are connected in series and in parallel with the nuclear bag fibers. All spindles have at least one nuclear bag fiber, but may not have any chain fibers. In this report we discuss only the nuclear bag fibers.

The motor nerves supplying the intrafusal fibers have their cell bodies situated in the spinal chord. Their axons have a diameter somewhat smaller than that of the axons of the nerve supply to the extrafusal muscle fibers. To distinguish these two classes of motor cells, axons, and muscle fibers, the terms "gamma" (referring to the spindle motor system) and "alpha" (referring to the main muscle motor system) are used.

The motor and sensory fibers supplying muscle spindles can be summarized as follows:

Sensory innervation — Two distinctly different sensory fibers arise from the muscle spindle; the larger of these, the primary ending (also referred to as the "annulospiral ending" or Type Ia afferent), apparently can have multiple origins in the spindle, i.e., can have its endings imbedded in both the nuclear region of the bag fiber and the chain fibers. Each spindle usually has a single primary ending, and this afferent innervates but a single spindle. The secondary endings (also called "flower-spray" or Type II afferents) arise from the nuclear chain fibers, with occasional branches to the bag fibers, but these never terminate at the bag region. Secondary fibers may be traced back to more than one spindle. The axons arising from secondary endings are smaller in diameter than those from primary endings.

Motor innervation — Considerable disagreement and confusion have arisen concerning the motor innervation of the spindle, but there is now a general consensus that there are four distinctly different fiber types:

- "Gamma-plate" fibers, which are gamma size motor fibers which terminate in the polar regions of the bag fibers with platelike endings, and may also terminate with plates on the chain fibers.
- "Gamma-trail" fibers, which terminate more centrally, principally on the chain fibers with diffuse endings, but possibly also have similar endings on bag fibers in the equatorial regions.
- "Beta" fibers, which end in the extreme polar regions of the bag fibers and are believed to be collaterals of alpha motor cell axons going to extrafusal fibers (ref. 58).

- The gamma-plate and gamma-trail endings are now held to be large gamma size fibers, but there is in addition a smaller gamma size motor supply whose function is not understood.

In this report we discuss only the behavior of the larger diameter primary endings — how they respond to changes in muscle length and gamma activity.

Before summarizing the physiological behavior of the primary ending, we must first indicate something about the relation between mechanical events at the nuclear bag region and the electrical events in the sensory annulospiral nerve endings. Much evidence has been accumulated which indicates that mechanical deformations of sensory terminals lead to the development of electrical potential fields at the terminals which are directly proportional to the strength of the deformation (ref. 28). These generator potentials are in fact very accurate mappings of the forces operating on the terminals and can follow rather high frequencies of change in the deforming stimulus. The fields are an inherent property of the receptor membrane itself, and the fields are utilized by the sensory axon in the production of nerve impulses in specialized triggering regions near the receptor endings. Nerve impulses, in fact, are generated at a rate directly proportional to the magnitude of the generator potential; hence, there is a continuous transmission of impulses at a frequency which is a linear function of that potential and hence of the strength of the deformation. The system exhibits a high degree of sensitivity to length changes; a significant shift in firing frequency can result from length changes of only a few microns (ref. 29). We can use this relationship to reconstruct the time course of tension changes at the nuclear bag region from observed trains of nerve impulses.

Response properties of the primary ending — In this section we will briefly consider some of the data concerned with input/output relations in the primary (annulospiral) ending of the spindle. First we will consider the steady-state relations between the firing frequency in the spindle Type Ia axon as a function of muscle length, and how this is influenced by gamma activity. Next we will present data regarding the response of the primary ending to transient changes in muscle length, and how such responses are modified by gamma activity. Finally, we will consider the response of the primary ending to sinusoidal stretching in the presence of gamma stimulation.

The primary ending of a spindle usually shows some spontaneous discharge even when the extrafusal muscle fibers are at their normal resting body length. This is presumably due to a small amount of residual tension in the spindle. Even in the absence of any motor signals from the cord, this spontaneous rate of firing in the spindle will increase monotonically as a function of increasing muscle length (from a few pulses per second to a hundred or more pulses per second). This arises because the disposition of the spindle within the muscle serves to transmit length changes in the muscle to the bag region where the change is reflected as an increase in bag tension. Conversely, shortening of the muscle (either passively or in response to an alpha motor command signal) will reduce the tension on the bag and hence reduce the spindle Type Ia sensory fiber firing frequency.

Control of spindle response by gamma motor fibers — As discussed earlier in this section, a number of gamma fiber types have been observed histologically, although there is some controversy over their roles and interconnections. Our interest here centers on the two gamma fiber types identified and studied in references 32 and 67. There, these two fiber types (called "dynamic" and "static" fusimotor fibers*) were differentiated by their effect on the response of the primary ending to step velocity changes in the muscle length. However, static or dynamic fiber stimulation had similar effects on the steady-state sensitivity, i.e., relation between primary ending firing rate and muscle length. Stimulation of either kind of gamma fiber usually displaced the frequency/extension curves upward without appreciably altering their slope. A typical example is shown in figure 18.

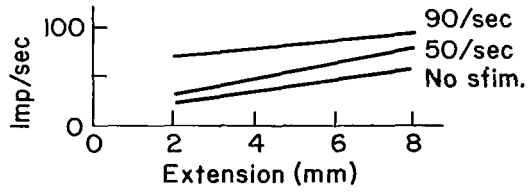

Figure 18. Frequency/Extension Curve for Primary Ending (Adapted from ref. 32)

*Unfortunately, we are not justified as yet in uniquely identifying the physiologically identified dynamic or static gamma fibers with the plate and trail endings defined anatomically.

To illustrate the differentiation of static and dynamic gamma fibers, first consider the primary ending response to a step velocity input in the absence of gamma fiber stimulation. The form of the transient response of the primary ending firing rate is shown in figure 19, where instantaneous firing frequency* is plotted versus time. The input is a step velocity which lasts until the muscle has been stretched 5 mm and is then terminated. Prior to stretching the spontaneous firing rate is f_o. Then there is a transient response to the step velocity input. Soon the firing rate reaches a steady rate of increase during the stretching velocity. At the termination of stretching the peak firing rate is f_p. After a transient decay the new steady-state firing rate is f_f. A measure of the velocity sensitivity is given by $f_p - f_f$ (called the "dynamic index"), whereas a measure of steady-state sensitivity is given by $f_f - f_o$ (plotted in fig. 19).

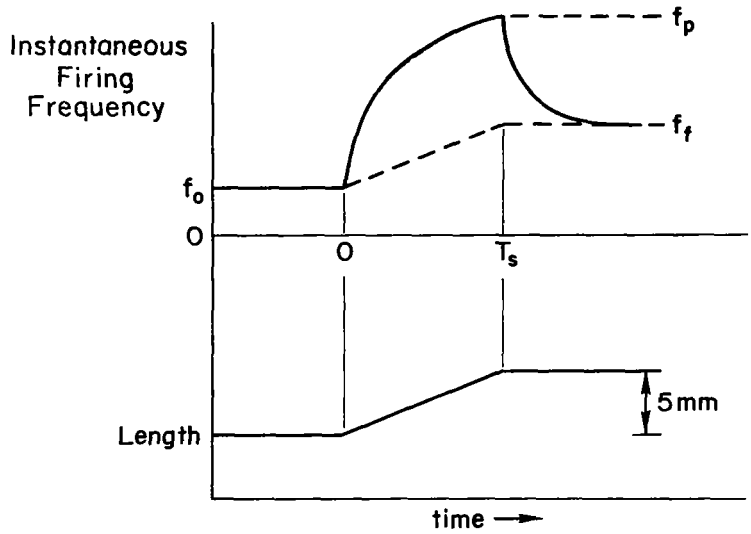

Figure 19. Response of the Primary Ending to a Step Velocity Input to Muscle

Stimulation of a dynamic gamma fiber has a much larger effect on the dynamic index than does static fiber stimulation, as shown in figure 20. The data have been plotted as the dynamic index versus fiber stimulation frequency for various

*Defined as the reciprocal of the time interval since the immediately preceding spike potential.

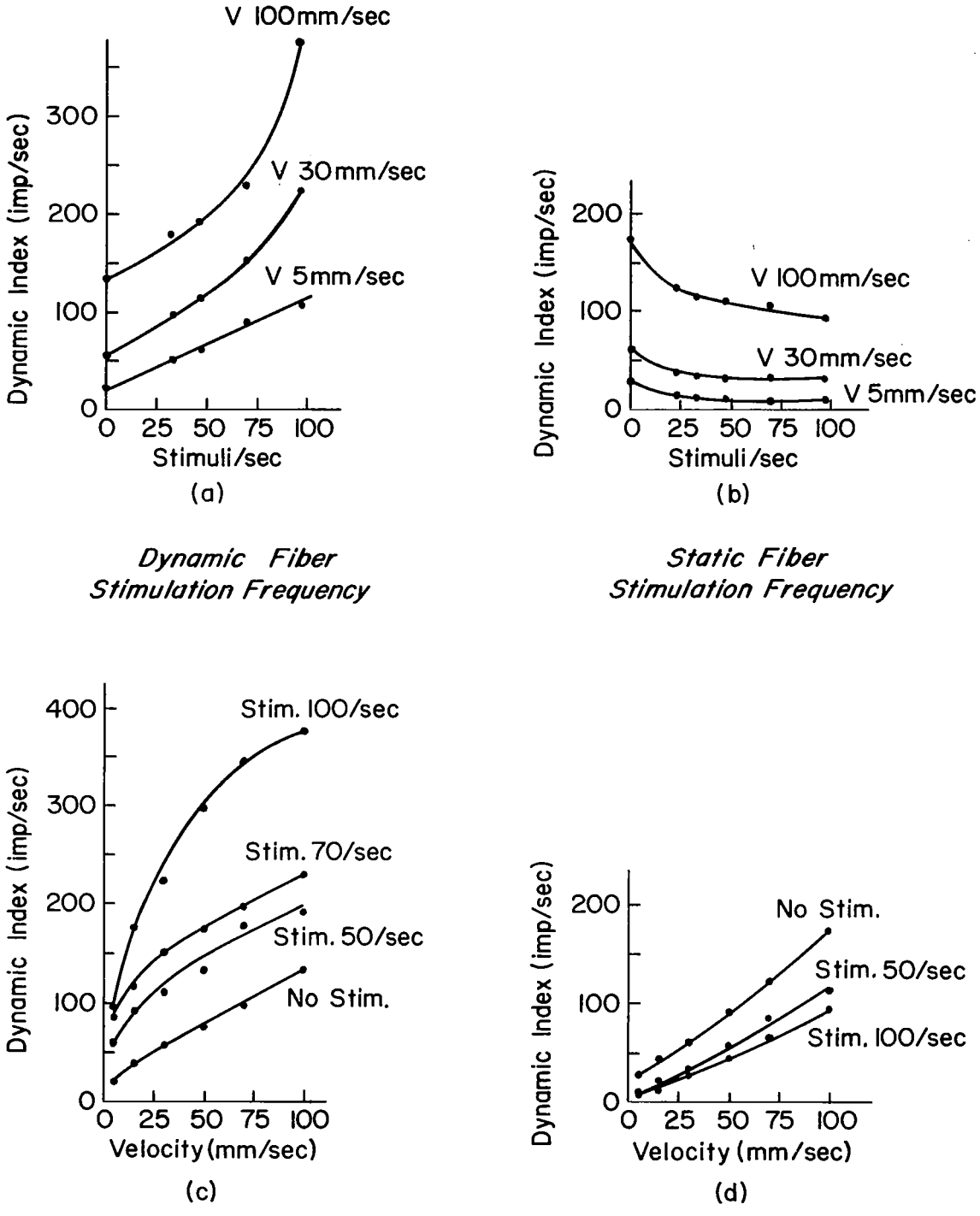

Figure 20. Effects of Dynamic or Static Fiber Stimulation on the Dynamic Index for Various Stretching Velocities

velocities in figures 20a and 20b. At any constant velocity, dynamic fiber stimulation produces a linear increase in the dynamic index or velocity sensitivity. However, static fiber stimulation has essentially no effect on the dynamic index other than to cause it to decline slightly.

In figures 20c and 20d the dynamic index is plotted versus velocity for various stimulation frequencies. For a constant dynamic fiber stimulation frequency, the dynamic index is a function of velocity. At the lower velocities, the slope of this function increases as dynamic fiber stimulation rate increases. At higher frequencies these curves have essentially the same slope. (In the discussion of models in subsequent sections we will be more interested in the small signal behavior, i.e., low velocities.) Note that static fiber stimulation produces a slight decline in the dynamic index. Thus the dynamic fiber has a strong effect on the dynamic index, whereas the static fiber has essentially no effect at the higher stimulation frequencies.

Some limited results for the response of the primary ending to small amplitude sinusoidal muscle stretching in the presence of dynamic fiber stimulation are given in reference 67. These results are shown in figure 21 for a 0.1 mm peak-to-peak sinusoidal stretching. In the absence of any stimulation, the primary ending responds in a sinusoidal fashion, but only to lengthening, i.e., it becomes silent for shortening. However, with dynamic fiber stimulation the sinusoidal primary ending response is biased upward about a state-state level (reflecting the fig. 19 results). The phase of the response is about 40° to 60° and appears to be independent of dynamic fiber stimulation frequency. Other results discussed in ref. 67 indicate that the phase angle is not appreciably changed by different dynamic fiber stimulation frequencies.

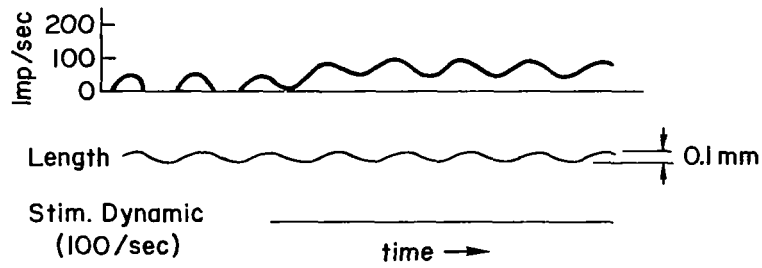

Figure 21. Response of the Primary Ending to Small Amplitude Sinusoidal Stretching at 2 Hz

Note that for the particular frequency (2 Hz) and stretching amplitude (0.1 mm peak-to-peak) used in figure 21, the instantaneous peak stretching velocity is about 0.63 mm/sec. A movement of this size represents a small signal perturbation when compared with the movements in figure 19 and the data in figure 20 where the final length corresponds approximately to the maximum muscle length in situ. Thus the lower velocity portions of the data in figure 20 are closer to a small signal analysis than are the large velocity portions. Conceivably, the nearly equal slopes of the curves in figure 20c at high velocity may reflect nonlinearities.

Spindle interconnections —The sensory fibers leaving the muscle spindle enter the spinal cord and form direct synaptic connections with the motor neurons supplying the muscle in which the spindle is imbedded (fig. 22). The nature of this monosynaptic coupling is such that increases in spindle firing frequency generate increases in the corresponding motor neuron firing frequency, and hence produce increasing motor unit contractile forces or resistance to stretch. The spindle axon also makes more complex connections which effectively inhibit the antagonist pool of motor neurons. This reveals the underlying importance of the spindle/motor-neuron feedback loop in stabilizing the length of the muscle. Influences tending, for example, to increase the length of the muscle, such as sudden increases in load, augment spindle activity which reflexively generates motor command signals tending to resist changes in length.

The Golgi tendon organs —Almost as numerous as the spindle receptor organs in a muscle are the Golgi tendon organs. From a few to as many as a thousand, they are localized in the muscle at the tendon insertions. Like the spindle receptors, they are deformation-sensitive. About 0.5 mm in length and 0.1 mm in thickness, they are structurally quite different from the spindles, consisting mainly of nerve terminals reaching the tendon fascicles which are surrounded by a sheath. As yet there is no clear-cut evidence that the afferents arising from these receptors form distinct classes; therefore, the discussion that follows will refer to only one single class of afferent fibers, the Type Ib axons.

The Type Ib axons are large (8 μm to 12 μm) myelinated fibers having conduction velocities of 75 −120 m/sec. The receptors are activated by stretch or tension on the tendon, and are presumed to have properties of impulse generation via generator potentials similar to those described for spindles. Under steady applications of tension, the Golgi organs continue to fire impulses indefinitely without

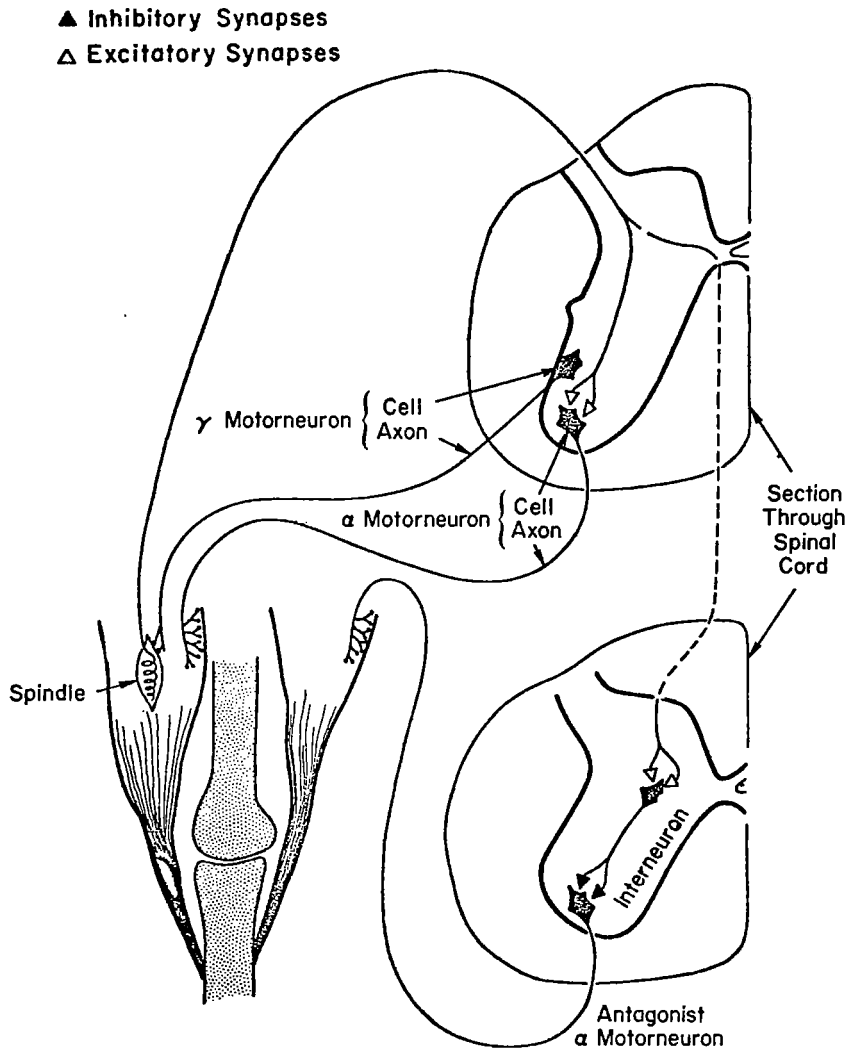

Figure 22. Reflex Arcs of Muscle Spindle

appreciable adaptation (refs. 34, 35). Further, their response to muscle length changes has rate-sensitive as well as steady-state components.

The differences between Golgi organs and spindles are quite remarkable. There is no evidence, for example, of any efferent motor control of Golgi sensitivity comparable to the gamma innervation of spindles. A major difference lies in the differential sensitivity of the Golgi organ to passive as opposed to active tension in the muscle. Many Golgi organs remain inactive when the muscle is passively stretched, even at full physiological extension of the muscle, at which time the equivalent of several hundred grams of tension are developed. Thus, the threshold to passive activation may be quite high. In contrast, the reaction to motor stimulation of the muscle shows that Golgi organs will be activated at much smaller over-all tensions of the whole muscle. For example, a tendon organ which is silent during passive extension of the muscle which generates 600 grams of tension will respond to a motor-nerve-evoked twitch in the muscle whose peak tension is less than 100 grams. Indeed, it has been shown that the tendon organ can respond to tensions actively generated by one or two muscle fibers or a single motor unit in series with it (ref. 35). In part, this is due to the rate-sensitive effect of the twitch, but even when rate is not a factor, as when the muscle is tetanically stimulated to a constant tension, the Golgi organ is characteristically activated by less than 200 grams of tension (refs. 34, 35).

This striking difference in response to passive versus actively maintained tensions is in a sense an artifact of the measurement process, since the measurements in an experiment are made at the bony insertion of the muscle. There the net forces acting along the main axis of the muscle are usually not in the direction of the main axis of the muscle fibers. The passive versus active tension difference, then, is due primarily to the difference in the distribution of forces acting on the tendon organ when the tension is induced by different means. Motor stimulation produces forces along the muscle fibers which act in a line with the tendon, but may be only partially represented in the bony insertions.

If the muscle tension (measured at the insertion) is plotted against the firing frequency of the Type Ib afferent, then for both actively and passively produced tension the relationship is linear, as can be seen from figure 23. The active tension curve usually has a slope essentially the same as that of the passive curve, but it is shifted to the left, which is equivalent to having a

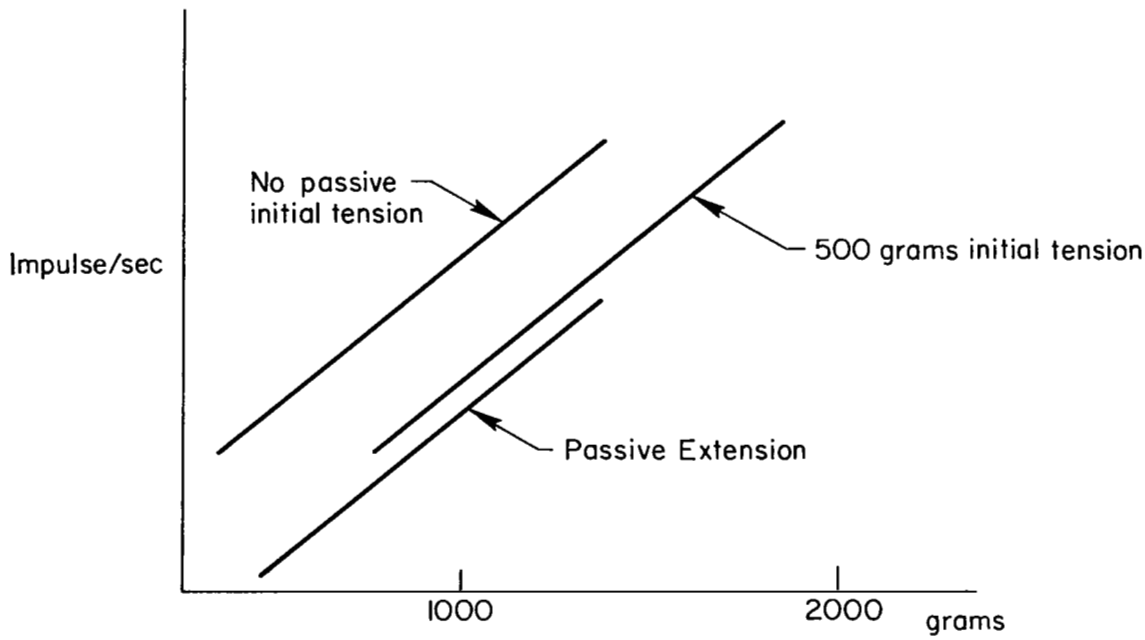

Figure 23. Steady-State Firing Frequencies of Golgi Organ as a Function of Tension

lower threshold. If an initial tension is placed on the muscle by passive extension, then the plot of total tension versus firing frequency is shifted to the right with the same slope, and the magnitude of the shift is such that, again, in the steady-state the generally observed response is essentially a measure of active tension, although in some receptors it could be more accurately described as total tension.

Like spindle afferents, Golgi organ afferents can fire at quite high rates (several hundred pulses per second), and their dynamic responses have also been quantified (refs. 35, 101). Centrally, the Type Ib axons make polysynaptic connections and, at least in the case of extensor muscles, the central connections are inhibitory to the motor neurons supplying the muscle in which the tendon organ is located. Thus, in the active generation of tension in a muscle, a closed-loop negative feedback loop is activated which tends to limit the total tension production in the muscle. At present the physiological significance of this loop is speculative, but it may be that, in addition to its regulatory contributions (see quantitative models in refs. 103 and 104), this negative feedback, or "autogenetic inhibition" as it is sometimes called, may serve to protect the muscle from a tension overload which could tear the tendon.

It should be recalled that unless the gamma output of the spinal cord increases during alpha activity, spindle discharge will decrease (e.g., the "silent period" of the spindle during a twitch contraction) when the muscle contracts. Conversely, the tendon organ discharge increases during a twitch, and this difference is a useful identifying characteristic of the two types of receptors. Both tend to increase their discharge during lengthening of the muscle.

Between them, the spindle and tendon organs generate a continuous stream of length and tension information to the spinal cord and higher centers.

General features of spinal cord organization.—The central nervous system consists of the brain and the spinal cord which is attached to it in the region of the medulla. The spinal cord, throughout its length, is surrounded by the bony vertebral column, a union of separate bones which effectively define a sequence of spinal cord segments. At the side of each vertebra there are two openings through which all the sensory nerves enter and all the motor nerves leave that section of the cord. The sections of the chord thus consist of 8 cervical, 12 thoracic, 8 lumbar, and 5 sacral segments. The

cord is considerably enlarged at the cervical and lumbar levels, at which point the respective nerves supplying the muscles of the arms and legs are located. A cross section through the cord shows the internal pattern to consist of butterfly-shaped gray matter surrounded by white matter. The gray matter is made up of dense collections of cell bodies, while the white matter consists of axon tracts traveling up and down the cord, the myelin of each axon contributing to the white appearance. Incoming sensory axons arrive via the dorsal root, while outgoing motor fibers leave via the ventral root. It has already been pointed out that the motor neurons of the gray matter tend to aggregate in groups, or nuclei, that have functional significance. These cells are easily recognized under a microscope, as they are by far the largest cells visible in the cord.

Organization of the gray matter —A number of schemes are in existence which divide the spinal gray and white matter into geographical regions on the basis of the morphology of the neurons involved (refs. 36, 37). An example of one of the most useful schemes in mammalian research is shown in figure 24. Region IX in this figure corresponds to the region of large motor neuron cells; each of the other regions of the gray is earmarked by some pertinent structural features of the cells involved.

This type of anatomical subdivision can be contrasted with physiological or functional subdivisions of the cord in which regions of the cord are delineated on the basis of functional similarity. As might be expected, there is often considerable correspondence between these two techniques.

In the dorsal horn of the gray matter (e.g., Zones I—IV of fig. 24) are cells primarily concerned with or under the domination of sensory input pathways from the dorsal root fibers.* From some of these cells arise axons which pass into the white matter, aggregating to form pathways connecting local spinal regions (propriospinal pathways) or pathways relaying information to higher centers.

At more intermediate regions of the gray matter are located interneurons, cells lying in the integrative pathways between sensory input and motor output. They may receive input from the periphery (for example, from skin receptors, joint position receptors, or muscle receptors), as well as from the sensory

*The cell bodies of all incoming sensory axons are actually outside the CNS, strung along the vertebrae in swellings, or ganglia, at each spinal level.

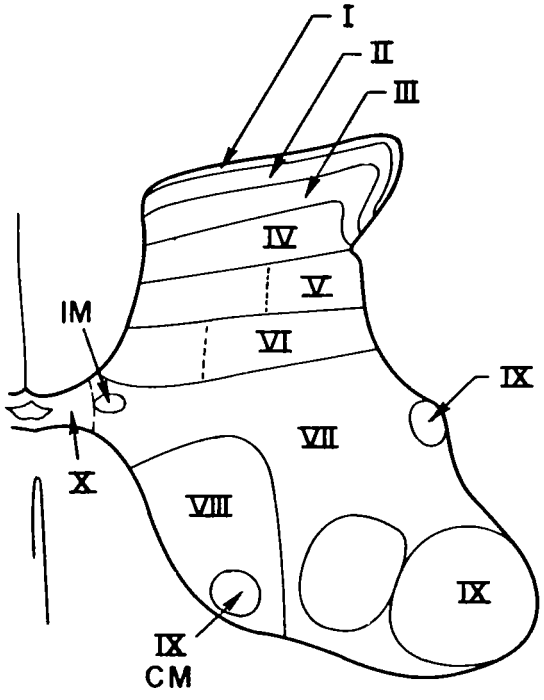

Figure 24. Regional Division of Spinal Gray Matter at the Sixth Lumbar Level (After Ref. 36)

centers in the midbrain (e.g., the vestibular system), the higher integrative centers (e.g., the cerebellum), or the cerebral cortex.

Certain specific regions (for example, Area VIII in fig. 24) may abound in cells specializing in communication with the other side of the spinal cord, both receiving axons from and sending axons to the opposite side.

The gamma motor neurons discussed in the preceding subsection are located in the same region as the corresponding alpha motor neurons, but no obvious pattern of distribution has been observed.

Organization of the white matter —In addition to propriospinal pathways located in the white matter (refs. 4, 68), a number of very important long pathways, both ascending and descending, occupy standard locations in the chord. They are the "dorsal column" pathways which carry touch, pressure, and joint position information to cortical levels; the "spinocerebellar" pathways which carry a variety of proprioceptive information (including that from spindles) to the cortex of the cerebellum; and the "spinothalamic" pathways which carry touch, pressure, pain, and temperature information to the midbrain, the thalamus, and, ultimately, the cerebral cortex.

There are a considerable number of descending pathways whose functions are not clearly understood (refs. 4, 69). The most important of these are the "vestibulospinal" path through which, apparently, spinal motor systems are enabled to compensate for motions of the body in space; the "cerebellospinal" paths which therefore provide a closed spinocerebellar loop; the "rubrospinal" paths from the red nucleus in the midbrain, an area implicated in the control of gamma activity; the "reticulospinal" paths from the midbrain and medullary reticular formation, a complex integrating center also concerned with gamma control; and the "corticospinal" paths arising from the sensory and motor cortices and concerned with control of sensory and motor functions at the spinal level.

Functional patterns of activity in the spinal cord —In view of the elaborate connections which the spinal cord makes with higher centers, it is somewhat surprising that the spinal cord itself, when artificially isolated in experimental procedures, is capable of exhibiting a wide variety of complex and autonomous activity (refs. 52, 54). For example, in experimental animals such as the dog appropriate stimulation of the foot pads will elicit coordinated walking movements

of the four legs; tickling of the flank will provoke scratching movements of an appropriate limb directed at the source of irritation. These observations of isolated spinal cord reflexes suggest that complex integrated motor patterns involving large sections of the chord, and high level pattern-recognition ability, are already incorporated into this level of organization. Indeed, it appears that much of the intrinsic organization of the isolated cord is based on a hierarchy of functionally significant reflexes.

The most elementary of these reflexes, in terms of its minimum organization, has already been referred to in our discussion of spindle activity. This is the monosynaptic or stretch reflex (also called the "myotatic reflex"), so called because anatomically it is a closed arc involving a single synapse (that between the annulospiral afferent and the motor neuron back to the muscle) and it is excited by stretching the muscle. Because the connection is excitatory, increasing tension on the muscle, which tends to increase its length, is met by an increasing active contractile resistance. The stretch reflex is commonly tested clinically by such maneuvers as tapping the tendon at the kneecap, which provides sudden excitation to the extensor muscles of the leg and causes the familiar knee-jerk response.

A concomitant of this monosynaptic reflex is a simultaneous multisynaptic reflex which inhibits the antagonist muscles.

A striking phenomenon to be observed in spinal animals showing active stretch reflexes is the so-called clasp-knife reflex (or "inverse myotatic reflex"). This occurs when the stretch to a muscle exceeds a critical value, at which point the muscle ceases its resistance to stretch and passively relaxes and extends. This is due to a multisynaptic arc which inhibits the motor neurons innervating the stretched muscle, and which is driven by activity in the Golgi tendon organs which are also stimulated by stretching of the muscle. The functional significance of this reflex is not entirely clear, but it is argued by some that this reflex serves a protective function of preventing overload of tension which might tear the muscle.

Another reflex of protective significance is the "flexor reflex," and it is encountered in all situations where a limb is subjected to painful stimulation. Such stimuli evoke activity in smaller diameter fibers which make contact with interneurons of the cord. The interneurons in turn radiate their output to all

flexor muscles of the limb in question, producing a withdrawal from the threatening stimulus.

Just as the inverse myotatic reflex can override the myotatic reflex, the flexor reflex represents the highest priority reflex in the cord and will override any other reflex responses in progress. It also stands farther up in the heirarchy of spinal reflexes insofar as it coordinates activity in a widespread group of muscles with common functional (i.e., flexor) properties. It also lacks the specificity of the two previous reflexes because any noxious stimulus to any part of the limb will elicit the response. An interesting adjunct of this reflex also reflects its more general character. As might be imagined, when the foot of an animal encounters a painful object and reacts with a protective flexor response, the weight of the animal's body is suddenly thrown on the remaining feet and considerable restabilization is necessary. The "crossed-extensor" reflex, which accompanies the flexor reflex, appears to provide this compensation by increasing the extensor tone of limb muscles on the opposite side of the body.

Properties of spinal networks —Recent careful study of these reflexes in their relation to activity occurring in single neurons of the spinal cord reveals some general themes in the structure of small groups of neurons which are adapted to the information-processing activities of the cord which shape the final motor output. First, we note the widespread occurrence of "reciprocal innervation," i.e., the concomitant excitation of an agonist group of muscles together with inhibition of antagonists, and vice versa, e.g., in the stretch reflexes (ref. 55). Second, we see commonly the anatomical substrate of recurrent collateral loops, leading either to the pattern of "recurrent inhibition" (ref. 56), i.e., the inhibition of synergist motor cells of the same pool, apparently through an intermediate neuron, or to "recurrent facilitation" (ref. 57), in which synergists or antagonists are excited by returning collateral loops.

Another basic pattern is referred to as "presynaptic inhibition," in which a neuron, often a small cell in the spinal gray, will be able to raise the effective threshold at selected excitatory synapses, thereby reducing their excitatory capacity. Conversely, other synapses may have their thresholds lowered by a process of "presynaptic facilitation" (ref. 54). Viewed over a large number of cells, these changes amount to a decrease or increase in gain. Such mechanisms appear to be commonly employed in mode-switching of sensory cells of the chord

by higher sensory control centers. Interneurons in the cord capable of responding to multiple types of sensory stimuli can have the gain of each mode changed by presynaptic inhibition or facilitation to emphasize transmission of certain types of stimuli (ref. 38).

The stretch reflex and closed-loop properties of muscle.— In a previous article great stress was pus on the basic length/tension relations for skeletal muscle. It was pointed out that this relationship is strongly dependent on the state of the muscle, and that it undergoes considerable transformation as the muscle is progressively subjected to increasing frequencies of stimulation. The family of curves so obtained, however, is applicable only to the isolated nerve/muscle preparation, and in this subsection we shall examine the changes in the length/tension relation which arise when the muscle is active under its normally innervated conditions, for under these circumstances the length changes imposed on the muscle will generate associated changes in afferent spindle discharge which will, in turn, reflexly evoke compensatory changes in alpha neuron discharge frequencies. In other words, we now examine the length/tension relations for muscle under closed-loop conditions in which the stretch reflex phenomenon, which is a feature of closed-loop behavior, is the governing relation.

Static closed-loop length/tension relations —It is now clear from a number of independent studies that the normally innervated muscle displays length/tension characteristics which are not only qualitatively different, but also are surprisingly simpler than those associated with isolated muscle.

An unusually beautiful example of this relation can be seen in figure 25, indicating that in a muscle being lengthened by applied tension the relation between length and active tension* is linear.

From available data it appears that this linear relation is generally valid; the slope of the length/tension curve, however, which has been termed the "myotatic loop gain" in ref. 40, shows considerable variation from muscle to

*"Active tension" in this example means that the passive contributions to tension at each length have been subtracted from the total measured tension. Such a manipulation of the data includes the implicit assumption that the "passive" components of tension are unchanged when the muscle is active.

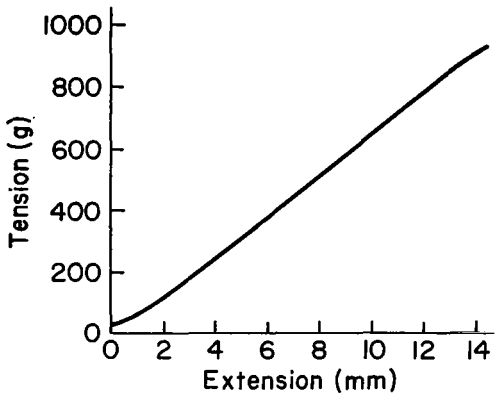

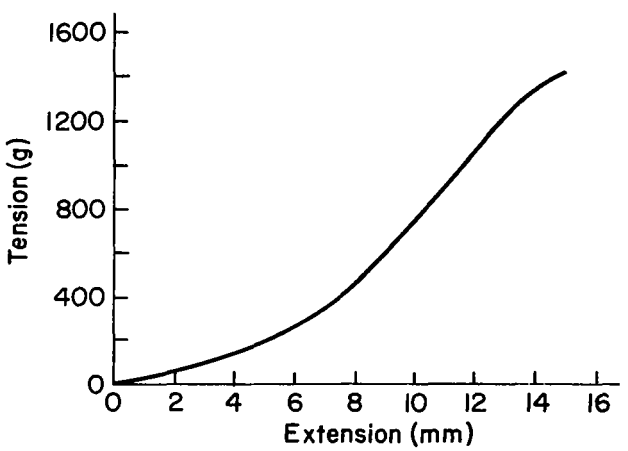

Figure 25. Closed-Loop Length/Tension Diagrams for Soleus Muscle (from Ref. 39)

muscle, the values ranging from 20 to 150 grams of reflex tension per millimeter of extension. This variation is very likely due to differences in gamma bias present during the experiment, since one would expect that the slope of these curves would be strongly influenced by gamma activity.

At first, the simplicity of this relation may seem surprising. However, an important consequence of feedback is to make closed-loop system characteristics more linear than the open-loop characteristics. Also, at a crude level of analysis there is, from the data we have already examined, reason to suspect that this linear relation would arise. It has been noted earlier, for example, that there is often a nearly linear relation between static muscle length and afferent spindle discharge frequency. Furthermore, we have previously seen data indicative of a linear relation between motor nerve discharge frequency and resulting muscle tensions. When we note that there is a highly linear relation between monosynaptic Type Ia afferent frequency and motor neuron output frequency, it is clear that, within a certain range, a linear static closed-loop relation might exist. This is confirmed by other data available which indicate that each of these relations is also linear under closed-loop conditions.

Dynamic properties of the closed-loop neuromuscular system — It has been shown that while the length/tension relation under closed-loop condition is not greatly altered by changing the velocity of lengthening of the muscle, there is a marked change when the muscle is allowed to shorten at any velocity (ref. 39). The hysteretic directional effect of changing muscle length on the tension developed in soleus muscle is shown in figure 26. Apparently the release curve is also fairly insensitive to rate of shortening. The cause of this phenomenon is

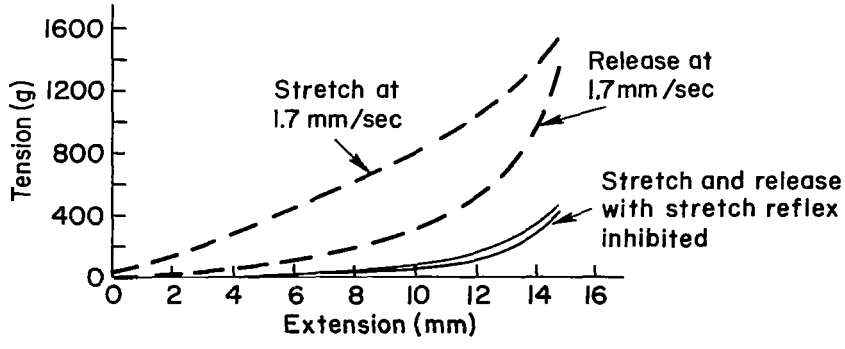

Figure 26. Closed- and Open-Loop Dynamic Length/Tension Diagram for Soleus Muscle (from Ref. 39)

not entirely clear, but probably involves at least two factors. First, for a given muscle length the spindle afferents will show considerably less activity during shortening than during lengthening. Second, the force which a muscle can develop depends on its velocity and direction.

Preliminary studies of the closed-loop behavior of the stretch reflex using sinusoidal changes in length or tension of the muscle and recording length and tension (refs. 60–62, 65), EMG activity (refs. 61–64), and spindle discharge patterns (refs. 65–67) have recently appeared and should eventually prove useful in deriving improved models for this system.

Command signals in the closed-loop control of movement.—Having considered the special sensory and motor components present at the spinal level for closed-loop control of muscle, and how the presence of these elements changes the effective properties of skeletal muscle by virtue of their central connections, we now consider how these elements can be utilized for effective control considered earlier for eye movement, there may be changes in load or in the operating characteristics of the neuromuscular elements themselves.

Because of inherent experimental limitations in present-day neurophysiological techniques, it has not yet been possible to obtain significant amounts of information about the closed-loop behavior of neuromuscular and sensory elements in humans performing skilled movements. However, some recent studies of the respiratory motor system in experimental animals have furnished data of undoubted significance to the understanding of human voluntary motor control.

The advantages of studying the respiratory motor system are that the important elements can essentially be observed simultaneously, and that the basically automatic features of this system, the periodic inflation and deflation of the lungs, are not appreciably perturbed by experimental procedures. Because this system involves loops not found, for example, in manual tracking, we shall outline first some of its organizational features.

Many muscles are involved in respiratory activity, but we will consider here only the intercostal muscles which effect an increase or decrease in the volume of the chest by moving the ribs, and the diaphragm muscles which push down on the viscera during inspiration.

The function of the respiratory control centers in the brain is to regulate the level of oxygen and carbon dioxide in the blood, and this is achieved by changing the ventilation rate of the lungs by varying the rate and/or the depth of respiration. In quiet respiration only the muscles of inspiration are used, and expiration occurs passively due to elastic recoil once the action of the inspiratory muscles has ceased. In heavier respiration the muscles of expiration become active.

One of the most potent stimuli to increase respiration is an elevated level of carbon dioxide, which apparently stimulates chemosensitive neuronal elements in the brain stem directly, and also stimulates a network of chemosensitive cells located in the walls of several major blood vessels, whose output also reaches the brain stem. These are connected to brain stem networks of neurons which are intrinsically organized to produce alternating bursts of impulses which are transmitted to motor neurons in the spinal cord. The organizational details of these brain stem netowrks are not well understood, but experiments suggest the existence of two mutually inhibitory pools of neurons which are active primarily during inspiration and expiration, respectively.

The control of respiratory volume is effected by several different means (fig. 27). First, an increase in blood CO_2 can cause an increase in frequency of firing of an individual cell during the inspiratory cycle. Second, the respiratory rate may be increased by altering the duration of the burst and the interburst period. Third, the antagonistic action of expiratory cells may be reduced during the inspiratory phase but may be accelerated during the expiratory phase. Fourth, there are apparently a large number of normally inactive neurons in the brain stem which can be recruited into an increased respiratory effort, thereby increasing the total drive to the spinal cord.

From a number of studies we find that for every state of blood gas level there is a corresponding output pattern from the brain stem which effectively commands the spinal neuromuscular apparatus to effect a maneuver adequate for maintaining a desired blood gas level or for offsetting any deviations from the optimum level which may have arisen (ref. 41). These commands are equivalent to a volume of air to be moved in and out of the lungs. But even though the parameters of the output are variable, the output is always patterned in a stereotyped way, with periods of approximately constant frequency nerve impulse bursts alternating with silence.

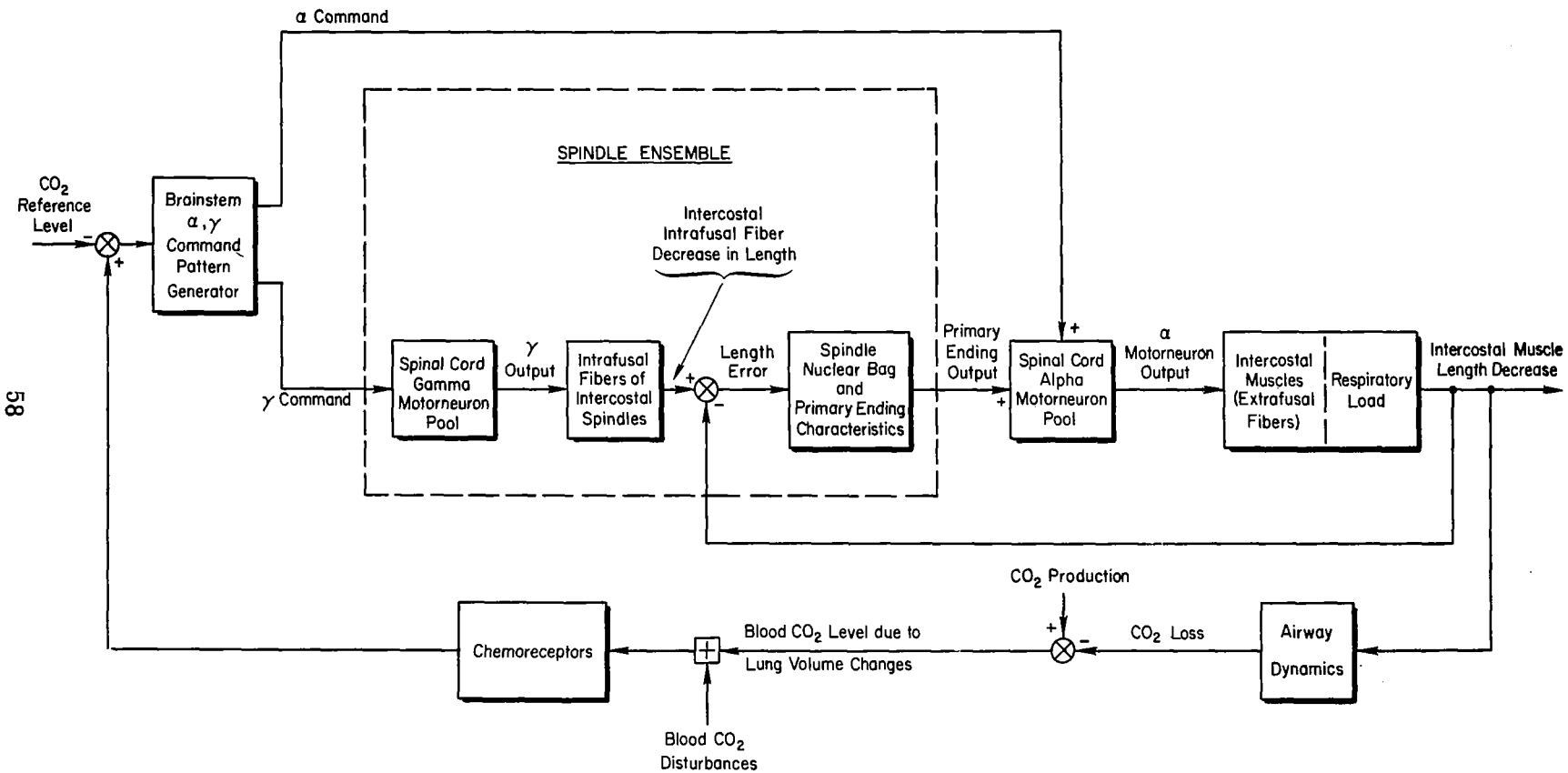

Figure 27. Neuromuscular Control System for Blood CO_2 Regulation

The firing patterns of motor neurons in the spinal cord look similar in many respects to those in the brain stem, and electrical recordings from individual motor neurons supplying the external intercostal muscles (which are inspiratory) and the internal intercostals (expiratory) show again the alternating burst/silence pattern of activity. Indeed, the phasing of firing of these two groups of motor cells with inspiratory and expiratory activity extends also to the gamma motor neurons in these pools. In fact, it has been shown that the pattern of firing of the gamma cells is closely related to the carbon dioxide level of the blood, suggesting that the command signal from the brain is relayed in parallel to both the alpha and the gamma system (refs. 42–48).

From these studies there is now considerable evidence that gamma activity slightly leads alpha activity in respiratory neurons. The evidence for this comes from direct simultaneous observation of several neurons, but is further strengthened by the finding that when the dorsal roots are cut (thereby interrupting the spindle flow to the alpha motor cells) the alpha cells may actually fail to fire during the normal phase of respiration, while the gamma cells continue to fire.* This suggests that alpha discharge may actually be dependent on a considerable amount of gamma-produced spindle support. In addition, observation of spindle discharge during contraction of respiratory muscles shows that, in contrast to what might be expected during inspiration, spindle discharge increases; we conclude, therefore, that increased gamma bias offsets the unloading effect of contraction. These observations apply to both inspiratory and respiratory intercostal muscles.

This parallel transmission of a command signal from the brain stem insures that adequate ventilation will occur in spite of changes in muscle power, airway resistance, or driving pressures; during the execution of the command signal, any mismatch between the required contraction (signaled via the gamma system) and the actual contraction will be signaled by the spindle afferent (which measures the difference between "required" muscle length and actual muscle length). If the shortening of the muscle is too small, for example, as a result of increased airway resistance, this will immediately cause a burst of impulses from the spindle to increase the level of excitation to the

*In humans, dorsal root section here leads to a paralysis of these respiratory muscles of which the subject is unaware.

corresponding alpha motor neuron. This hypothesis has, in fact, been tested in experiments in which the airway resistance was suddenly altered just prior to a respiratory cycle (refs. 48–50). The effect on alpha motor neuron discharge is immediate (i.e., much too fast to have arisen by CO_2 stimulation of the brain stem), suggesting that the gamma spindle loop can indeed be used to drive the neuromuscular system as a "follow-up servo."

Further investigation of the gamma fiber input to the intercostal muscles has revealed, in addition to the intermittent discharge phase-locked with respiration, a tonic gamma activity (ref. 51). This activity can be influenced by cerebellar stimulation and tilting of the head. In the case of the intercostal muscles, this is correlated with the fact that these muscles have a dual function — that of respiration on the one hand and postural control on the other. Thus, two independent routes of gamma excitation impinge on common spindles, one from the respiratory system and, simultaneously, one from the tonic postural or position-determining system. As a result the tension of intercostal muscles periodically fluctuates at an amplitude determined by the phasic gamma system. The fluctuation occurs about an average tension determined by postural demands via the tonic gamma system.* We know that intercostal motor units are of both the "fast" and "slow" types, and it is possible that the two systems of gamma input have their final expression selectively through fast or slow fiber systems.

Finally, we note that an extremely important aspect of reciprocal inhibition is exhibited by this system, for during inspiration it has been observed that expiratory spinal motor neurons are actively inhibited by supraspinal centers (ref. 43). This is an important finding, because if these antagonistic muscles were simply not excited during inspiration we would expect that the act of inspiration would initiate a stretch reflex response which would oppose inspiration.

Despite the superficial differences in the organization of this system when compared to those discussed earlier, we can generalize the conclusions drawn from these experiments when developing the over-all model of motor control which

*It is possible that some of the tonic gamma activity is also related to respiration and determines the midthoracic position around which the respiratory excursions are superimposed.

will be summarized in the section entitled "Neuromuscular System Component Models for Small Perturbations."

The preceding discussions of the basic functional elements utilized in the control of motor activity at the spinal level, and their interconnections, can be summarized and generalized to a typical manual control situation as shown in figure 28, where the relationship of motor and sensory elements for a hypothetical agonist/antagonist pair of muscles is presented. Supraspinal command signals are assumed to operate in parallel command pathways, a generalization of the experimental results presented under "Command Signals in the Closed-Loop Control of Movement," page 56, and are shown to the left in figure 28 feeding directly to gamma and alpha motor neuron pools. The internal organizational features of the spinal cord, discussed on pages 47–53, are omitted for clarity. This basic block diagram is the basis for our interpretation of human operator data to be presented under "Neuromuscular System Component Models for Small Perturbations" and "Closed-Loop Nuromuscular System Dynamics."

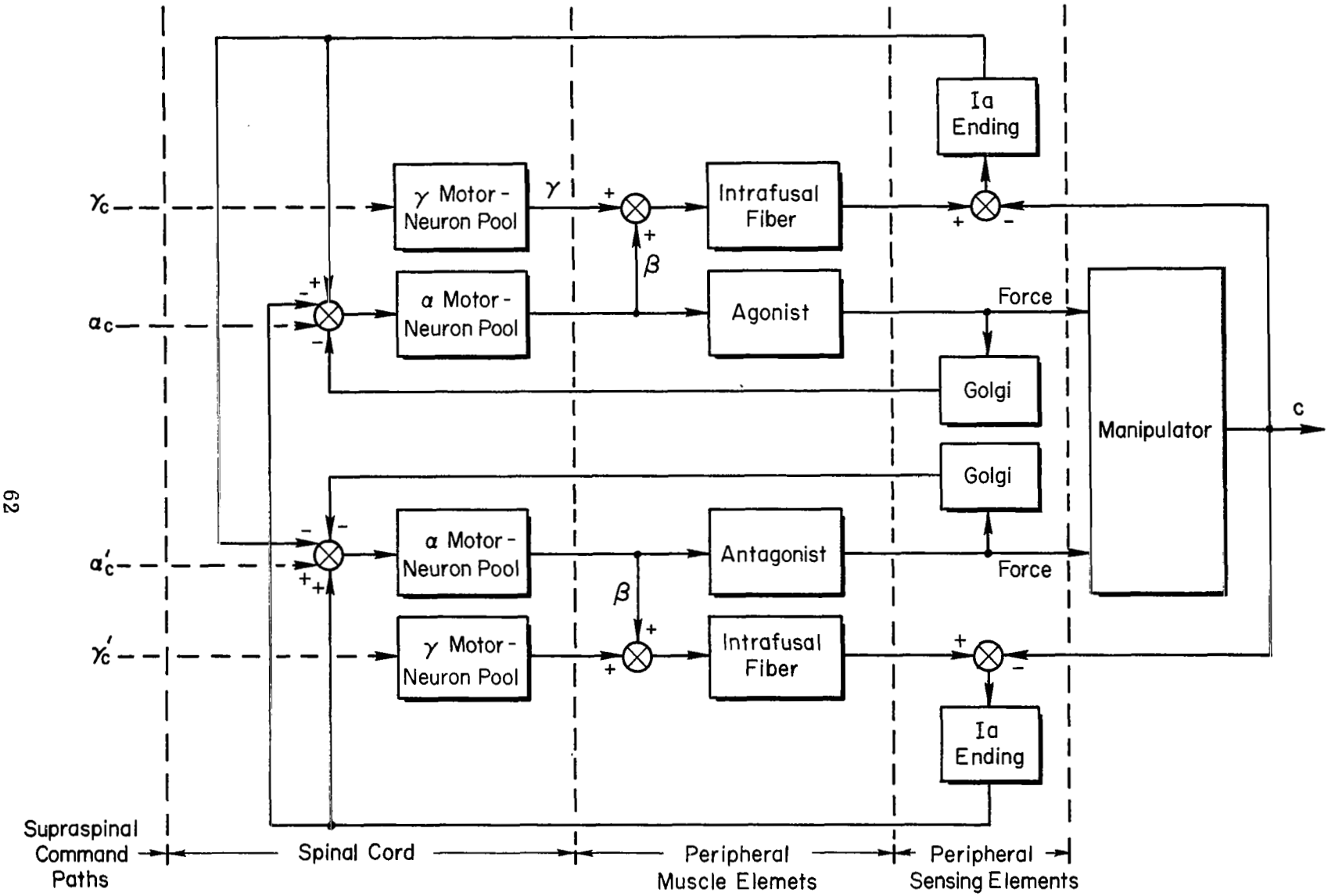

Figure 28. Agonist/Antagonist Neuromuscular Systems

HUMAN OPERATOR DATA INDICATING NEUROMUSCULAR SYSTEM EFFECTS

In this section we are interested in measurements of the human operator's input/output characteristics that reflect neuromuscular system effects. Data for the whole human have been taken with a variety of forcing functions, viz.,

- Single step and ramp inputs
- Step-ramp inputs
- Single sinusoids
- Square waves
- Random amplitude step sequences
- Force disturbance impulses
- Quasi-random inputs (sums of sinusoids)
- Random inputs (shaped Gaussian noise)

The form of the forcing function has a considerable effect on the response behavior (reference 94) and a single model for the human as a controller has not yet been evolved. Such a model, however, must ultimately account for the different responses measured for discontinuous and continuous predictable inputs and random-appearing inputs. In this report we will concentrate on the random-appearing and force disturbance forcing function cases. For these forcing function types the extant data has been carefully surveyed to distill out those data which are crucial to key neuromuscular system features. From a very large body of describing function data available for the overall human operator we can abstract a very few which are sufficiently precise and wide-band to permit their decomposition into components tentatively identifiable with neuromuscular system characteristics. Some of these are especially useful to provide connections between average muscle tension, or tone, and the neuromuscular system dynamics — and these connections will be the major thrust of the data described below. We shall consider the relationships between tension and, in order: high and low frequency phase covariation; some first-order effects of changes in manipulator dynamics on the high-frequency neuromuscular system dynamics; disturbance regulation and high-frequency dynamics; and tremor.

High and Low Frequency Phase Covariation

Spring-restrained low-inertia manipulator. — In this section we are interested in data that relate the effects of average muscle tension or tone on the neuromuscular system describing function data. These effects occur at very high and very low frequencies, so with measurements limited to mid-frequencies they show up primarily in the phase data.

To describe these data, several levels of approximation have been used to characterize the describing functions (refs. 72–74). Two of these are:

Precision Model

$$Y_p = \underbrace{K_p\left(\frac{T_L j\omega + 1}{T_I j\omega + 1}\right)e^{-j\omega\tau}}_{\text{Equalization and Gain}} \underbrace{\left\{\underbrace{\left(\frac{T_K j\omega + 1}{T'_K j\omega + 1}\right)}_{e^{-j\alpha/\omega}} \underbrace{\frac{1}{(T_{N_1} j\omega + 1)\left[\left(\frac{j\omega}{\omega_N}\right)^2 + \frac{2\zeta_N j\omega}{\omega_N} + 1\right]}}_{(T_N j\omega + 1)^{-1} \text{ or } e^{-j\omega T_N}}\right\}}_{\text{Neuromuscular System}} \quad (1)$$

Basic Delays

where

$$\alpha \doteq \frac{1}{T'_K} \pm \frac{1}{T_K}$$

where

$$T_N \doteq T_{N_1} + \frac{2\zeta_N}{\omega_N}$$

Approximate Model

$$Y_p = K_p\left(\frac{T_L j\omega + 1}{T_I j\omega + 1}\right)e^{-j\omega\tau}\,\frac{e^{-j\alpha/\omega}}{T_N j\omega + 1} \quad (2)$$

$$\doteq K_p\left(\frac{T_L j\omega + 1}{T_I j\omega + 1}\right)e^{-j\left[\omega(\tau + T_N) + (\alpha/\omega)\right]} \quad ; \quad \tau_e = \tau + T_N$$

The so-called Precision Model is a minimum form compatible with all the fine detail, low variability data for random-appearing forcing functions and also compatible with such things as the dynamics of the movement component in step

responses. The Approximate Model is a much simpler form in which the number of parameters is reduced without too serious a degradation in the analytical description of the data for mid-frequencies. Both models exhibit the same gain, equalization, and basic delay elements. They differ in their neuromuscular system aspects. For these the high frequency terms are third-order in the Precision Model. In the Approximate Model, the mid-frequency effects of these third-order terms are approximated by either a first-order lag (so-called neuromuscular lag) or a pure time delay. The latter can be summed with the basic latencies to give an overall time delay, τ_e.

The very low frequency characteristics appear in the data primarily as a phase lag. In the Precision Model these characteristics are represented by the lead/lag, $(T_K j\omega + 1)/(T'_K j\omega + 1)$, which is a minimum form suitable to characterize both amplitude ratio and phase data completely for the limited data of extremely high precision [i.e., those data for controlled element forms K_c, K_c/s, and $K_c/(s-\lambda)$]. For many other systems these low frequency effects are not so precise, and should be further approximated. If the low frequency effects are modeled by transfer characteristics containing m lags and leads, then the incremental phase shift due to these will be

$$\Delta\varphi_{low} = \sum_{i=1}^{m} \tan^{-1}\left(\omega T_{lead_i}\right) - \sum_{i=1}^{m} \tan^{-1}\left(\omega T_{lag_i}\right) \tag{3}$$

At frequencies well above the break frequencies of these lags and lead, i.e., $\omega > 1/T_{lead_i}, 1/T_{lag_i}$, this can be approximated by

$$\Delta\varphi_{low} = \sum_{i=1}^{m} \left(\frac{\pi}{2} - \frac{i}{\omega T_{lead}}\right)_i - \sum_{i=1}^{m} \left(\frac{\pi}{2} - \frac{1}{\omega T_{lag}}\right)_i \tag{4}$$

$$\doteq -\frac{1}{\omega} \underbrace{\sum_{i=1}^{m} \left(\frac{1}{T_{lead}} - \frac{1}{T_{lag}}\right)_i}_{\alpha}$$

This $e^{-j\alpha/\omega}$ phase characteristic is convenient to approximate the effects at mid-frequencies of very low frequency leads and lags. Our emphasis here will be on the α and equivalent time delay quantities contained in the Approximate Models exponential phase descriptor term, $e^{-j(\omega\tau_e + \alpha/\omega)}$.

Figure 29 illustrates the nature of typical pilot describing function data and the application of the previously given Precision and Approximate Model forms as descriptors of these data. The typical data shown are from a so-called subcritical task involving the control of a first-order divergence controlled element. The α and τ_e aspects do not affect the amplitude ratio at all, although they are clearly shown in the phase. The $\omega\tau_e$ phase due to time delay dominates the high frequencies, whereas the α/ω phase lag is the major low frequency effect. Their joint action tends to make the approximate phase look like an umbrella, with α controlling the left side and τ_e the right side, i.e., changes in τ_e shift the right side of the umbrella, while changes in α shift the left. Simultaneous increases in both α and $1/\tau_e$ shift the umbrella to the right, whereas decreases shift it to the left.

Some idea of the variation of α and τ_e and their connections is provided in reference 73. Figure 30, which is taken from reference 73, indicates that α and $1/\tau_e$ vary together for the experiments considered there. In terms of the describing function phase curve shown in figure 29, both ends of the umbrella are shifted together in an adaptive response to changes in forcing function bandwidth, ω_i $\left[\text{for } Y_c = K_c/(s)^2\right]$, or to changes in controlled element unstable pole, λ $\left[\text{for } Y_c = K_c/s(s-\lambda)\right]$.

Large inertia manipulator. — Reference 82 presents describing functions and performance measures taken for a very wide range of spring and inertia restraints as well as two controlled elements, $Y_c = K_c$ and K_c/s^2. The largest differences occurred for the latter. Figure 31 illustrates the effect of inertia on the pilot's describing function (the inertias are in units of ft-lb-sec^2/rad, $I_m = 0.0048$, $I_1 = 0.29$, and the pilot's limb contribution was $I_p \doteq 0.015$). With no spring restraint, increasing the inertia above that contributed by the pilot's limb degrades average performance ($\overline{e^2}$) reduces amplitude ratio and crossover frequency and causes a severe increase in phase lag, thereby constricting the available stability region. Some of the neuromuscular system dynamics can be seen at the higher frequencies for the larger inertias

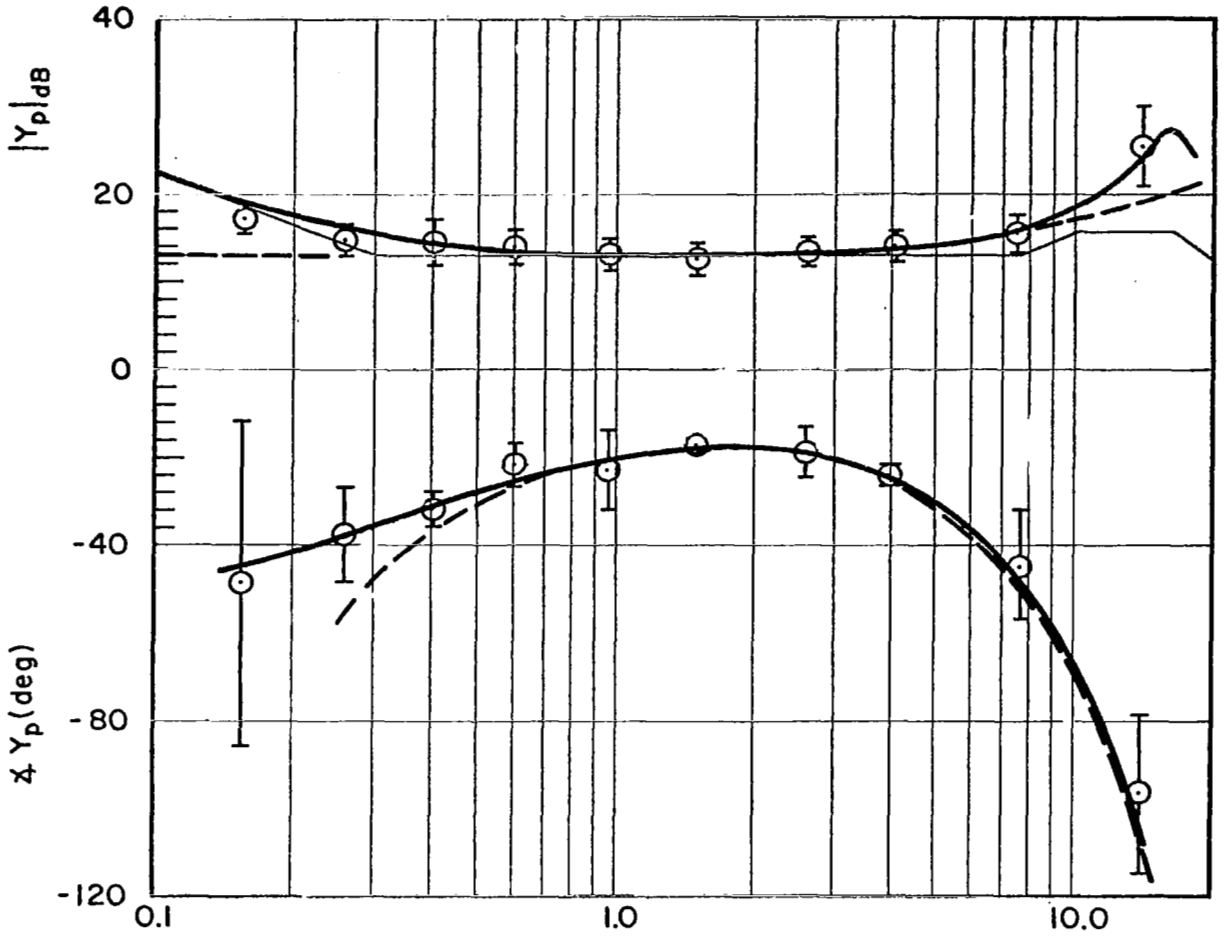

Precision Model (———)

$$Y_p = (25.1)\left(\frac{j\omega}{7.8} + 1\right)e^{-0.09\,j\omega}\left\{\left(\frac{\frac{j\omega}{0.3} + 1}{\frac{j\omega}{0.05} + 1}\right)\frac{1}{\left(\frac{j\omega}{10} + 1\right)\left[\left(\frac{j\omega}{16.5}\right)^2 + \frac{2(0.12)}{16.5}\,j\omega + 1\right]}\right\}$$

Approximate Model (— — —)

$$Y_p = (4.2)\left(\frac{j\omega}{7.8} + 1\right)e^{-j[0.21\,\omega + (0.25/\omega)]}$$

Figure 29. Typical Pilot Describing Function Data and Models ($Y_c = K_c/(s - 2)$; $\omega_i = 4.0$ rad/sec) (Ref. 2)

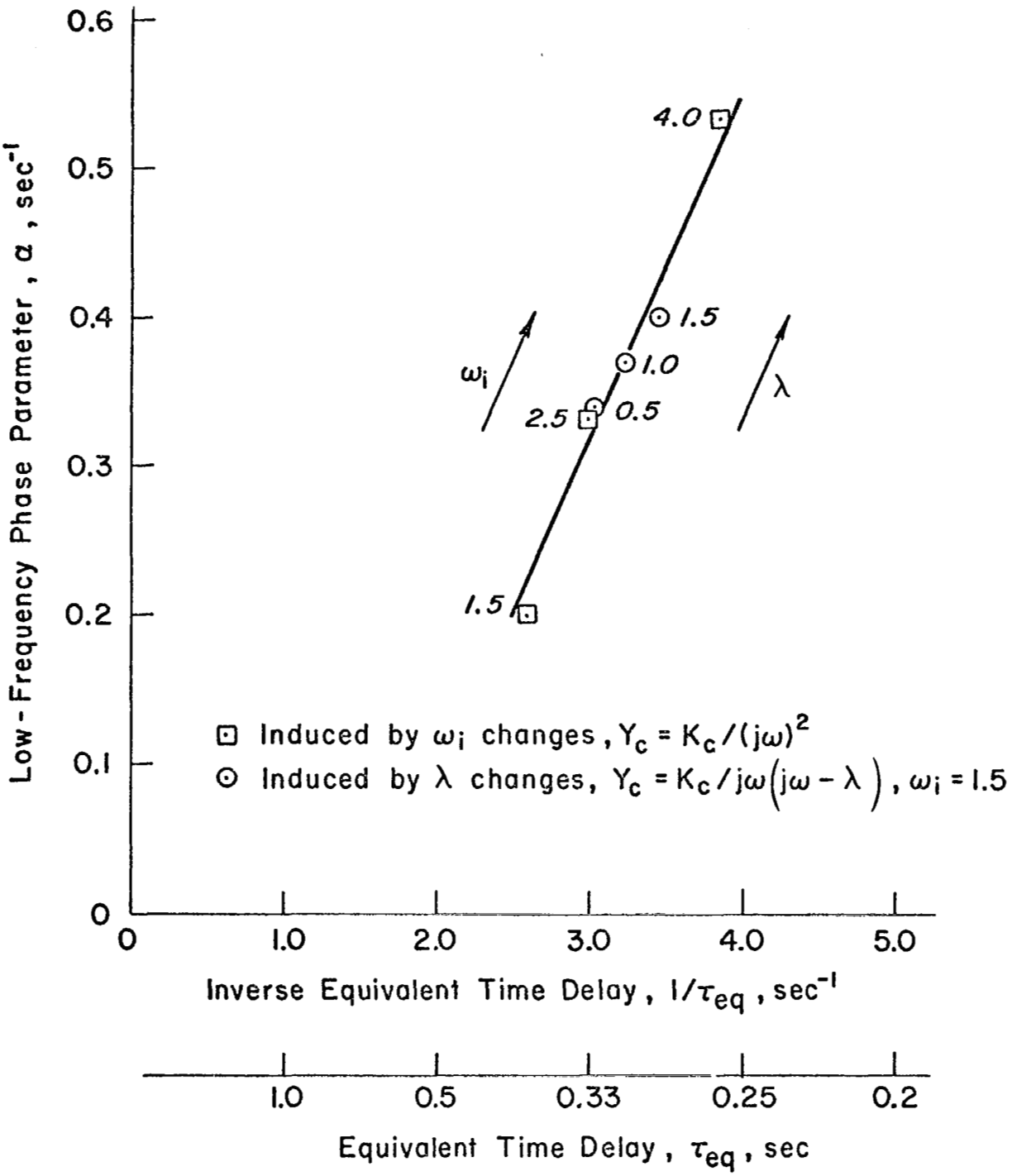

Figure 30. Connection Between Equivalent Time Delay and Low-Frequency Phase Lag

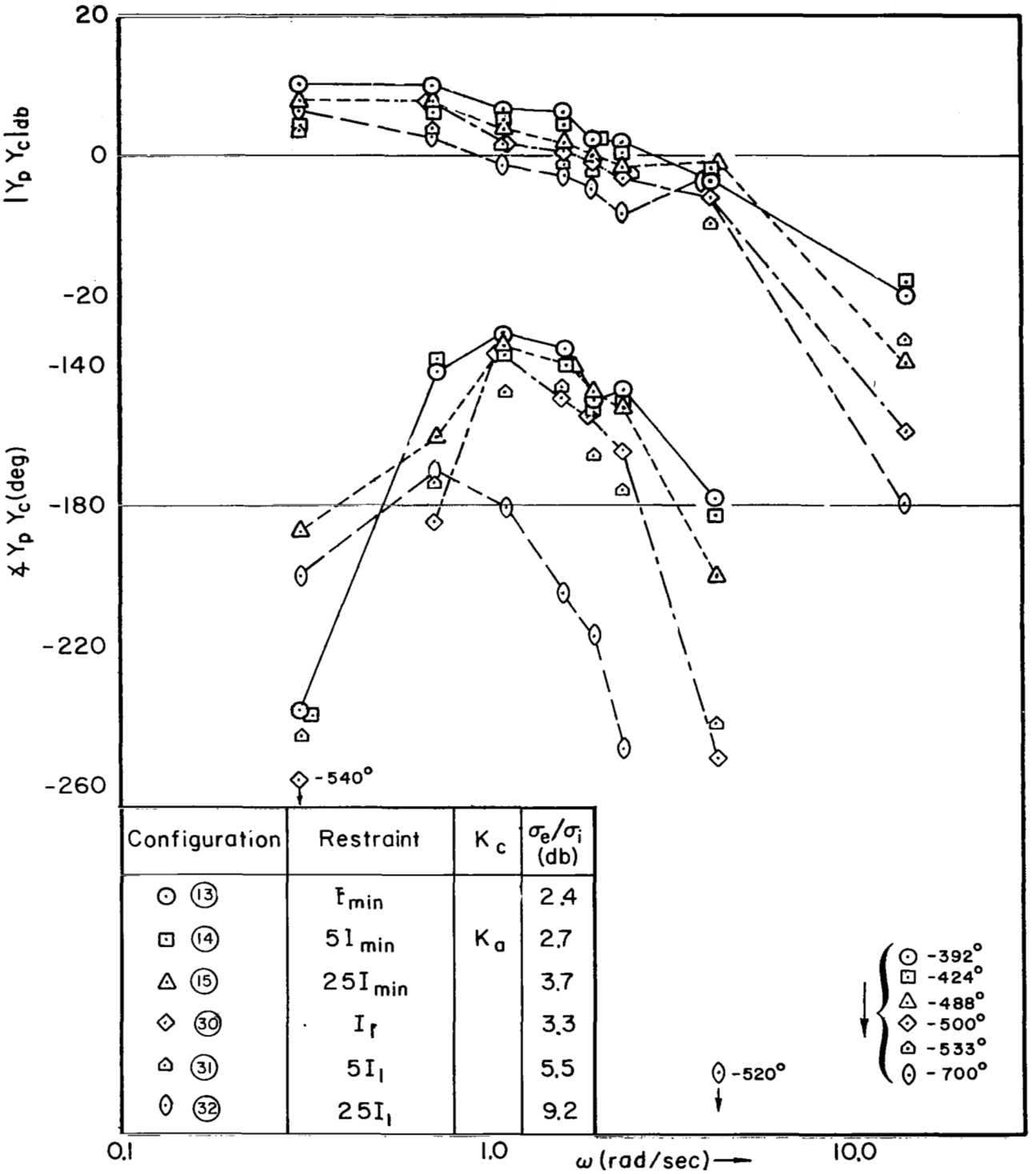

Figure 31. Averaged Open-Loop Describing Functions for $Y_c = K_c/s^2$ for Various Inertias

(resonance near 5 rad/sec). The exact nature of these dynamics is not clearly revealed in figure 31 because data at forcing function frequencies at 6.3 and 10 rad/sec were distorted in the data reduction process. Consequently, the major effect of inertia can only be assessed in terms of a τ_e increase as inertia increases.

Torque Disturbance Regulation

The effect of average voluntary muscle tension on the wrist twisting (supination-pronation) response to torque disturbance inputs has been investigated in references 75–78. (The ref. 76 work is reviewed in ref. 105.)

In reference 76 the relative amount of muscle tension was inferred from a sphygmomanometer cuff attached around the forearm. This was displayed to the subject who then could readily set the reading to any one of five levels. These experiments were carried out using irregularly spaced mechanical impulses delivered, without warning, by a pendulum. The manipulator restraint consisted of an inertia several times larger than that of the arm, and the subject was asked to resist the perturbing influence of the pendulum-produced disturbance on the load.

The transient response resembled that of a dominant second-order system with light damping (fig. 32a). Figure 32b shows similar results from reference 78 where the disturbance torque was delivered by a motor attached to the shaft of the handle which the subject grasped. A transducer sensed the grip force which is assumed to be indicative of muscle tone in the participating muscles.

Figure 33, adapted from reference 76, shows the general location of the upper pole position of a damped second order fitted to the transient response for five tension values. In general, increasing mean tension increases the natural frequency of these roots but leaves the damping ratio relatively unchanged. We are also interested in the effect of this trend on the high frequency phase which can be found by noting that, as for equations 1 and 2,

$$\frac{1}{1 + \left(\frac{2\zeta_N}{\omega_N}\right)j\omega + \left(\frac{j\omega}{\omega_N}\right)^2} \doteq e^{-(2\zeta_N/\omega_N)j\omega} ; \quad \omega < \omega_N \qquad (5)$$

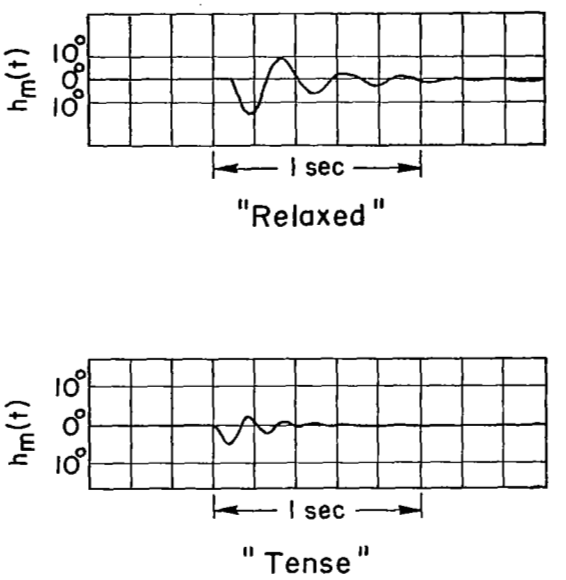

(a) Response to Pendulum Input (Adapted from ref. 76)

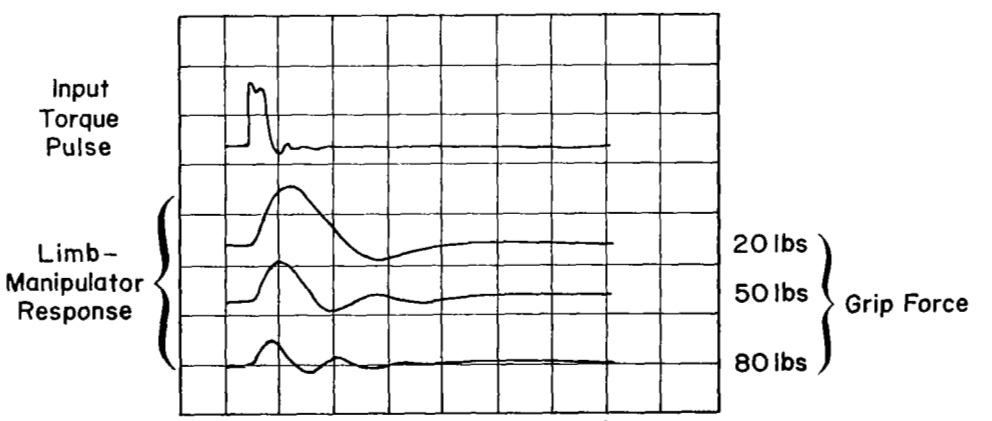

(b) Response to a Torque Motor Input (Adapted from ref. 78)

Figure 32. Responses to a Torque Disturbance for Various Tension Levels

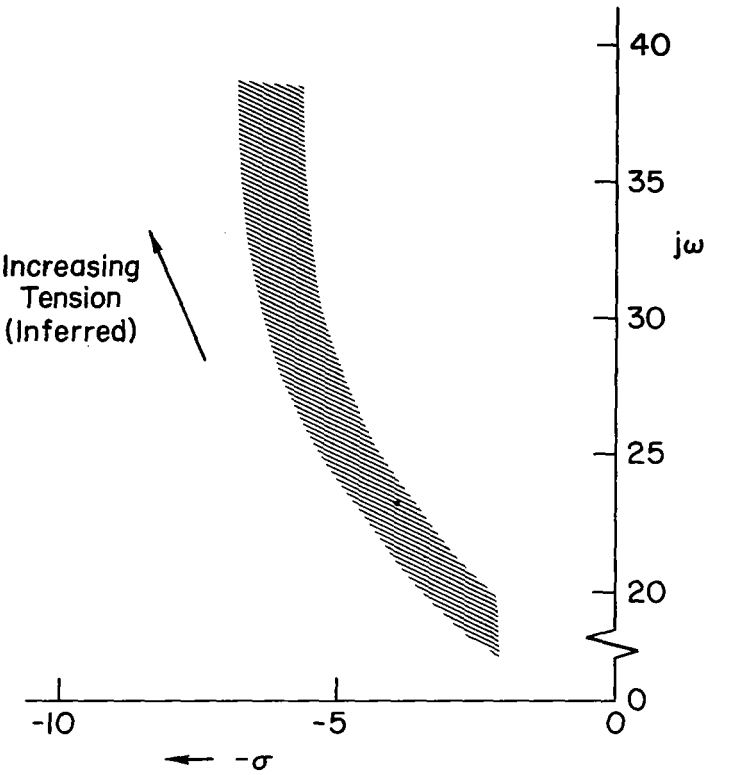

Figure 33. Upper Root Location of a Complex Pair Fitted to Some Reference 76 Transient Responses

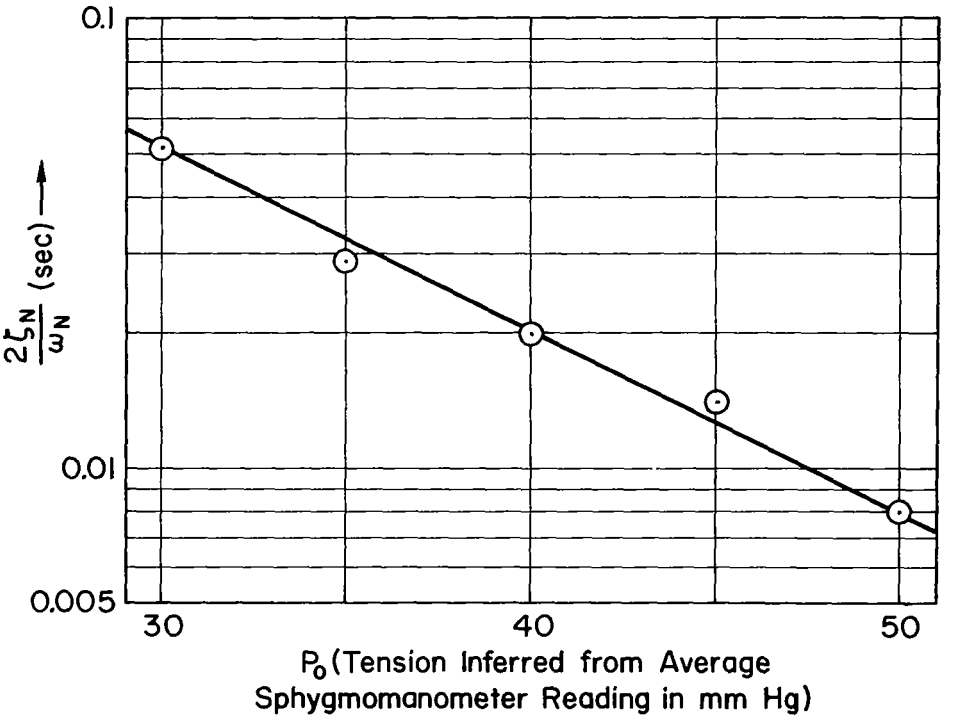

Figure 34. Effective Time Constant as a Function of Inferred Tension

for frequencies below ω_N. All of the ω_N's in figure 33 are at the extreme upper end of the measurement bandwidth of interest (see fig. 29). Thus the approximate phase of these complex roots behaves as an effective time delay given by $2\zeta_N/\omega_N$. Reference 76 also contained averaged data for three subjects which we can use to calculate the effective time delay for the five tension values (see fig. 34). The decrease in time delay as tension increases will move the high frequency portion of the phase to the right (see fig. 29).

Effects of Muscle Tension and Manipulator Restraints on Limb Tremor

Limb tremor has been observed in a variety of situations. It typically appears in the time history as an oscillation or in the power spectral density as a significant peak at high frequency. Tremor frequencies are often in the range of 6–10 Hz as in the analysis of finger velocity with different load masses (ref. 79). Generally, muscle tremor frequencies depend on both the manipulator restraint and muscle tension (refs. 80, 81, and 102). In figure 35 forearm flexor tremor frequency is plotted as a function of the mean tension at the wrist (ref. 80). This tension was exerted against a spring (attached to the wrist) which was oriented parallel to the upper arm. For each spring, increasing the tension causes a slight increase in tremor frequency except at the higher tensions where the data level off. However, an increase in spring rate produces an incremental increase in tremor frequency which is essentially independent of tension. Reference 102 had results similar to those in figure 35 except that only one spring rate was used.

In reference 81 the task was to track a ramp input (pursuit display). The subject gripped a handle in his fist and using wrist rotation about the forearm axis was able to generate his response. Four different load inertias were used. In addition muscle tension was inferred from handle grip tension as sensed from a rubber pneumatic balloon and pressure-voltage transducer. The dependence of tremor frequency on inertia and inferred muscle tone is given in figure 36. For each inertia there is an increase in frequency as tone increases whereas for constant tone an increase in inertia causes a decrease in frequency.

Additional results in reference 81 indicate that the tremor frequency of one hand is independent of the other. Specifically if one hand is controlling

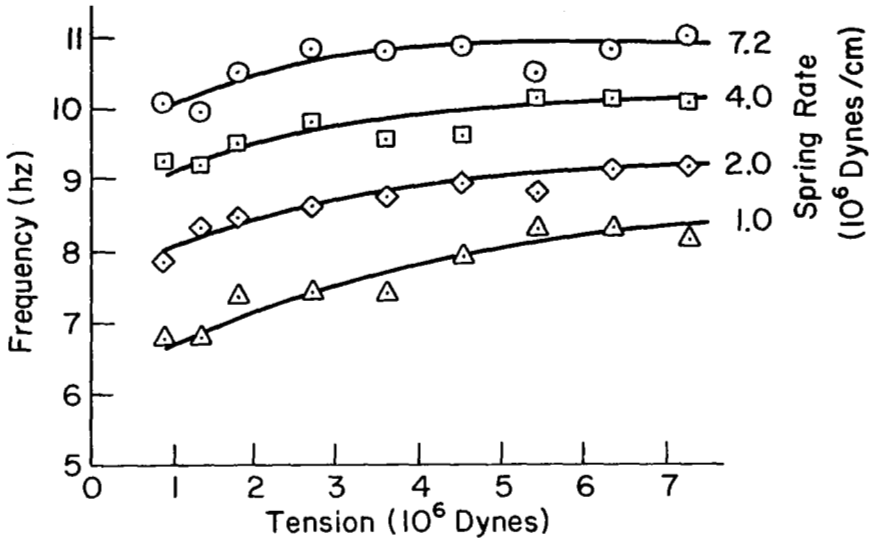

Figure 35. Effects of Muscle Tension and Spring Rate on Forearm Flexor Tremor (Adapted from ref. 80)

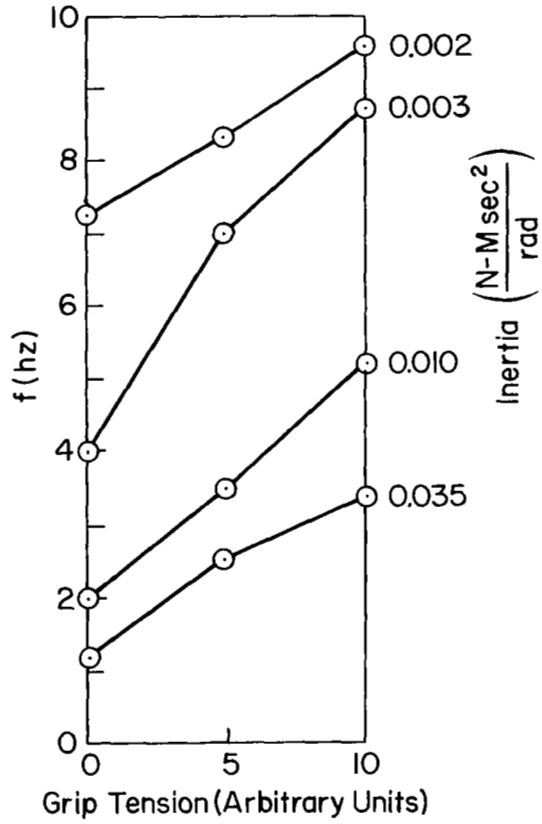

Figure 36. Effects of Inertia and Grip Tension on Limb Tremor During Constant Velocity Wrist Rotation

a large inertia without pressure, then its tremor frequency can be much less than that of the other hand if it is controlling a small inertia with great pressure. This suggests that the oscillation conditions are strongly dependent on the load and further that each neuromuscular system is independent of the other.

NEUROMUSCULAR SYSTEM COMPONENT MODELS FOR SMALL PERTURBATIONS

The effective connections or block diagram topography of the neuromuscular system in figure 28 are highly adaptive, i.e., the system can have many organizations (ref. 75), each peculiar to a specific control situation. The control situation of most interest in this report involves neuromuscular system operations in which the command inputs at the spinal level are the consequences of random-appearing visual inputs or random force disturbances on the manipulator, and the outputs are small motions of the hand exerted against a spring- and/or inertia-restrained manipulator. For these situations an appropriate neuromuscular system model can be made up by connecting ensembles of sensory and equalization components with associated ensembles of muscle and manipulator elements into an equivalent single-loop feedback system. The purpose of this section is to develop the component models; the next section will accomplish their combination into a system. The dynamics of the muscle/manipulator combination shall be discussed first, emphasizing the dependence of these dynamics on the operating point muscle tension. Then the muscle spindle's feedback, equalization, and actuation capabilities shall be described.

Muscle Model

We are interested in a simple muscle model appropriate for a tracking task involving relatively small movements. Involved here will be an agonist/antagonist muscle pair where each has an average tension, P_o (which does not appear across the load). Figure 37 shows such a pair for a simple system similar to the Biceps/Triceps System. For motion to occur, one muscle must relax while the other contracts, and thus the tension levels must seesaw about the average. The relationship between tension and length in response to motor nerve commands can be found from the muscles' isometric tension-length, force-velocity curves, and series elastic component, all described in the section entitled "Physiology of the Neuromuscular System," i.e., the muscle can be modeled by a series connection of a series elastic component and a contractile component (where the latter is described by the length-tension and force-velocity curves).

Figure 38 shows our interpretation of the isometric length-tension curves for a family of motor nerve firing frequencies, f. Here P is the tension in

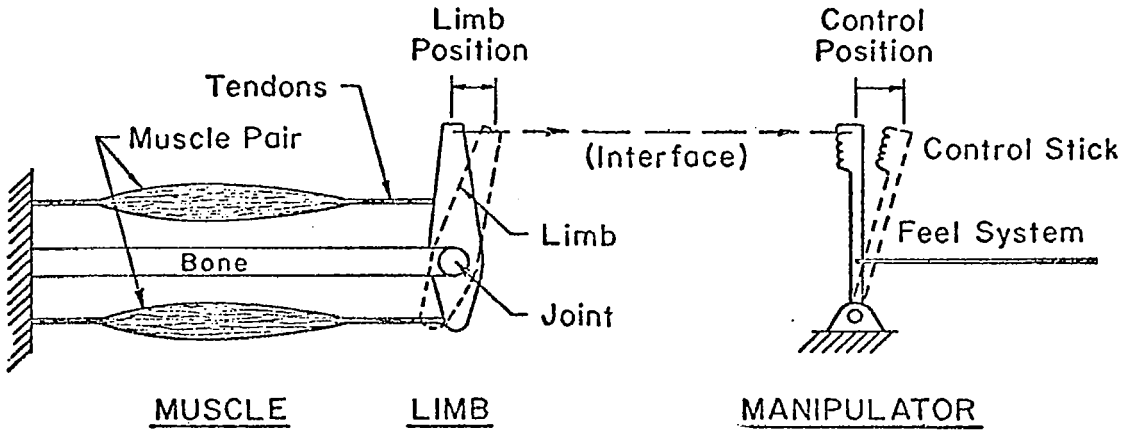

Figure 37. Agonist/Antagonist Muscle Pair

the muscle when it is set to a particular length, L, and stimulated at a motor nerve firing frequency, f. The solid curves (maximum and minimum stimulation frequencies) are typical of skeletal muscle (ref. 83). The dashed curves reflect test results (fig. 6b of ref. 84) for isolated muscles where, at a given length, the slope of the curves increases as firing frequency increases. The

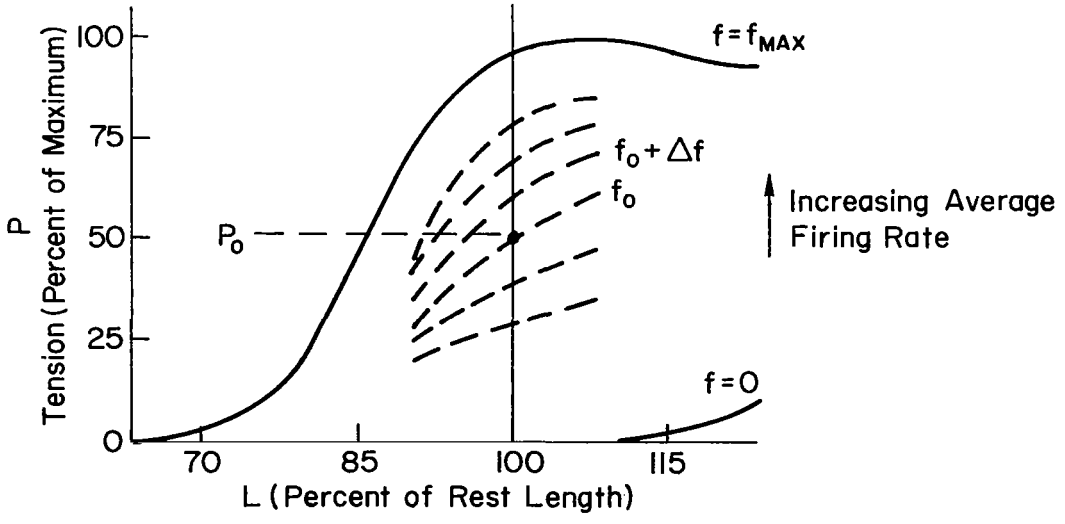

Figure 38. Isometric Length-Tension Curve

dashed curves also reflect the in vivo behavior if the family parameter is the average firing frequency as detected from surface electrodes (ref. 85).

The isometric tension changes due to small perturbations about the operating point, L_o, f_o, can be described by the first-order terms in a Taylor series expansion as

$$P = P(L, f) \doteq P_o(L_o, f_o) + \frac{\partial P}{\partial L}(L - L_o) + \frac{\partial P}{\partial f}(f - f_o) \qquad (6)$$

$$P = P_o + C_f \Delta f_\alpha - K_m \Delta L$$

where P_o = isometric tension at the operating point

Δf_α is the change in average firing rate of the motor neuron (or average electrical activity)

ΔL is the change in muscle length (chosen positive in the direction of muscle shortening)

K_m is the slope of the length-tension curve for constant f

C_f is the slope of the length-tension curves for constant length

Note that the partial derivatives C_f and K_m are evaluated at the operating point defined by f_o and L_o.

The in vivo human calf muscle force-velocity data and curve fits given in figure 13 are redrawn in figure 39 to reflect our interpretation for both shortening and lengthening velocities. Here F is the force exerted on the load by muscle during a shortening contraction at a steady velocity, V. (At V = 0 then F = P, the isometric tension for a particular situation.) For a series of values of average muscle electrical activity as measured by the electromyogram from surface electrodes, the load velocity increases as the load force decreases. The shape of the curves is typical of that obtained in isolated muscle under maximum stimulation frequency, figure 13. An exception is that the relationship for lengthening muscle (V negative) is somewhat steeper than an extrapolation of the shortening curves would predict (refs. 26 and 70). This results in a change in slope in the region of most interest (small positive and negative velocities). However, in the context of an agonist/antagonist muscle pair, one

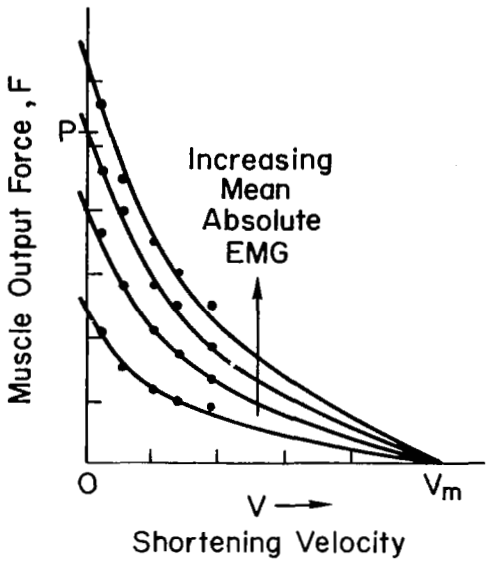

Figure 39. Force-Velocity Curves at Various Mean Absolute EMG Levels

muscle will be lengthening while the other is shortening, resulting in a continuous overall force-velocity relationship. Further, reference 86 didn't find a discontinuity in the tension response to a sine wave position input for a tetanized muscle. Thus we shall use continuous curves through V = 0.

Each of the force-velocity curves in figure 39 can be identified by the EMG activity level, or alternatively, by their intersection with the zero velocity line, since there the load that can just be supported is equal to the isometric tension. Empirical curves can be fitted to the data (ref. 26) described by

$$F = \frac{P(1 - V/V_m)}{(1 + V/b)} \qquad (7)$$

where V_m = the maximum velocity of shortening

b = a constant

P = the isometric tension pertinent to the operating point length and muscle activity

F = the muscle output force

V = velocity of shortening

This relationship is directly analogous to the force/speed characteristic of an actuator. Again a Taylor's series can be used to describe the small perturbation motions. To first-order terms

$$F = F(P, V) \doteq F_o + \frac{\partial F}{\partial P}(P - P_o) + \frac{\partial F}{\partial V}(V - V_o) \qquad (8)$$

Either actual data or equations fitted to the actual data can be used to evaluate the partials. In this case the second possibility is far more convenient, since equation 7 is directly pertinent. The partials, evaluated at P_o, V_o, are:

$$\frac{\partial F}{\partial P} = \frac{(1 - V_o/V_m)}{(1 + V_o/b)}$$

$$\frac{\partial F}{\partial V} = -\frac{P_o(1/b + 1/V_m)}{(1 + V_o/b)^2} \tag{9}$$

For steady-state tracking the operating point of interest is $V_o = 0$. Thus equation 8 becomes

$$F \doteq P_o + P - P_o - P_o\left(\frac{1}{b} + \frac{1}{V_m}\right)\Delta V \tag{10}$$

$$= P - B_m\Delta V$$

where the equivalent damper, B_m, is used to replace $P_o(1/b + 1/V_m)$.

Substituting equation 6 for P into equation 10 yields

$$F \doteq P_o + C_f\Delta f_\alpha - B_m\Delta V - K_m\Delta L \tag{11}$$

B_m is directly proportional to P_o, and K_m is also a function of P_o (see fig. 38).

In terms of an analogous physical system, the linearized equation for the muscles' contractile component corresponds to a force source, $P_o + C_f\Delta f_\alpha$, coupled to a parallel spring/viscous-damper combination. The damper element has a damping coefficient which is linearly related to the operating point tension (which is a function of f_o and L_o). This behavior is typical of both individual muscle fibers and of whole muscle, and is a key feature of our succeeding discussion.

Skeletal muscles can only contract actively, so movements involving high-grade skill, such as tracking, generally require coordinated groups of muscles. The simplest of these, the agonist/antagonist pair, is shown in figure 37. For

rotation to occur, one muscle must contract while the other extends. If the opposing muscles each have a steady-state tension, P_o, in the static situation caused by some steady-state or average firing rate, f_o, rotation can be accomplished by increasing the firing rate for the contracting muscle by the increment Δf while simultaneously decreasing the firing rate in the antagonist by about the same increment. The actual muscle system involved in almost any complex limb motion is seldom, if ever, as simple as that described above. However, the same principles hold for each agonist/antagonist pair involved, and a grand summation can be made of all the pairs contributing to the actual limb motion of interest. On this basis the linearized mathematical model developed above for single muscles can be generalized into that appropriate for a specific tracking situation with all the composite muscle groups involved considered in the summation. Equation 11 still holds, but now P_o, C_f, B_m, and K_m are to be interpreted as characteristics of the muscle system. Figure 40 shows the resulting limb/manipulator system schematic for a simple spring-mass

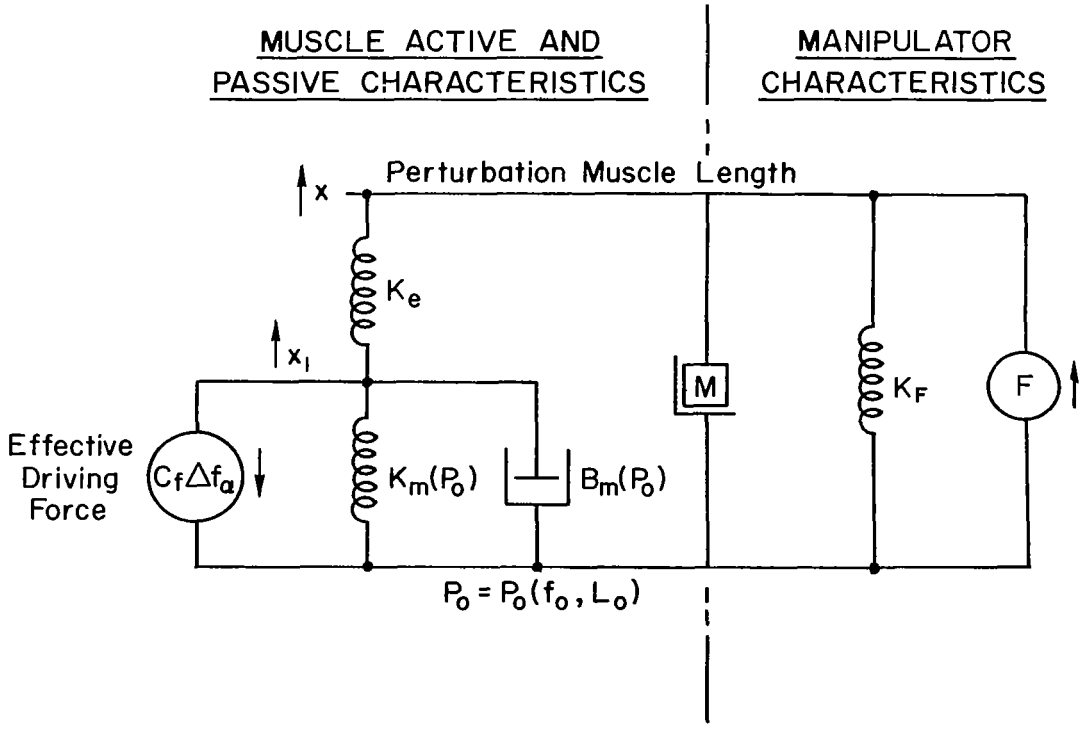

Figure 40. Schematic of Limb/Manipulator Model

manipulator. The muscle characteristics consist of the series connection of the series elastic component, K_e, with the contractile component characteristics given by the force source plus spring and damper (see equation 11). Since the limb and manipulator inertias are in parallel, the two are lumped together in the single effective inertia, M. A load spring, K_F, is also present. Finally, provision is made for a force, F, applied to the manipulator.

The equations of motion for the limb/manipulator dynamics can be found by setting the total force at x and at x_1 equal to zero. In terms of Laplace transforms these can be written as

$$\begin{aligned} F_x &= 0 = -(x-x_1)K_e - (Ms^2 + K_F)x + F \\ F_{x_1} &= 0 = -(x_1 - x)K_e - (B_m s + K_m)x_1 - C_f \Delta f_\alpha \end{aligned} \tag{12}$$

or in matrix form

$$\begin{bmatrix} (Ms^2 + K_F + K_e) & -K_e \\ -K_e & (B_m s + K_m + K_e) \end{bmatrix} \begin{bmatrix} x \\ x_1 \end{bmatrix} = \begin{bmatrix} F \\ C_f \Delta f_\alpha \end{bmatrix} \tag{13}$$

The characteristic equation for this system is

$$\Delta = MB_m \left[s^3 + \frac{K_m + K_e}{B_m} s^2 + \frac{K_F + K_e}{M} s + \frac{K_F(K_m + K_e) + K_m K_e}{MB_m} \right] \tag{14}$$

Separated into terms which isolate, first, the series elastic component and, second, the load spring, this becomes,

$$\Delta = MB_m \left[s^3 + \frac{K_m}{B_m} s^2 + \frac{K_F}{M} s + \frac{K_F K_m}{MB_m} \right] + MK_e \left[s^2 + \frac{B_m}{M} s + \frac{(K_F + K_m)}{M} \right] \tag{15}$$

$$= MB_m \left[s^3 + \frac{K_m + K_e}{B_m} s^2 + \frac{K_e}{M} s + \frac{K_m K_e}{MB_m} \right] + B_m K_F \left[s + \frac{(K_m + K_e)}{B_m} \right] \tag{16}$$

The output response, x, and that at the inboard side of the series elastic component, x_1, are given by:

$$x = \frac{K_e C_f}{\Delta} \Delta f_\alpha + \frac{B_m\left(s + \frac{K_m + K_e}{B_m}\right)}{\Delta} F \qquad (17)$$

and

$$x_1 = \frac{C_f M\left(s^2 + \frac{K_F + K_e}{M}\right)}{\Delta} \Delta f_\alpha + \frac{K_e}{\Delta} F \qquad (18)$$

We are interested in the limb/manipulator subsystem for three manipulator types: spring-restrained, low-inertia; isometric; and no-spring, large-inertia.

Spring-restrained low-inertia manipulator. — Data in reference 83 indicate that the muscle model's series elastic component, K_e, is much larger than K_m. When this is taken into account, and when the manipulator considered is such that the series elastic element overwhelms the load spring and inertia over the frequency range of interest, then the responses are those for $K_e \rightarrow \infty$ (see eq. 15). Equations 17 and 18 then become

$$x = x_1 = \frac{C_f \Delta f_\alpha + F}{M\left[s^2 + \frac{B_m}{M} s + \frac{K_f + K_m}{M}\right]} \qquad (19)$$

For precision movements in tracking, there is always some average tension acting, and in difficult tasks this is sufficient to make the damping ratio considerably greater than unity. For this case the appropriate form for the $x/\Delta f_\alpha$ transfer function is,

$$\frac{x}{\Delta f_\alpha} \doteq \frac{\frac{C_f}{(K_m + K_F)}}{\left(T_{M_1} s + 1\right)\left(T_{M_2} s + 1\right)} \qquad (20)$$

where

$$\frac{1}{T_{M_1}} \doteq \frac{K_F + K_m}{B_m}$$

$$\frac{1}{T_{M_2}} \doteq \frac{B_m}{M}$$

If we presume that $K_F \gg K_m$, such as would occur with a stiff spring restraining the manipulator, then the undamped natural frequency, $\sqrt{(K_m + K_F)/M}$, will be approximately constant, and a change in steady-state tension, P_o, will primarily affect the damping. The dynamics of this equivalent system are illustrated for two cases of steady-state tension by the jω-Bode diagram of figure 41. From this figure it is apparent that the effect of changing the tension of the muscle group is to decrease the low-frequency pole and increase the high-frequency pole. As will be seen later, these changes, due to an increase in steady-state tension, have most important consequences on the neuromuscular system dynamics.

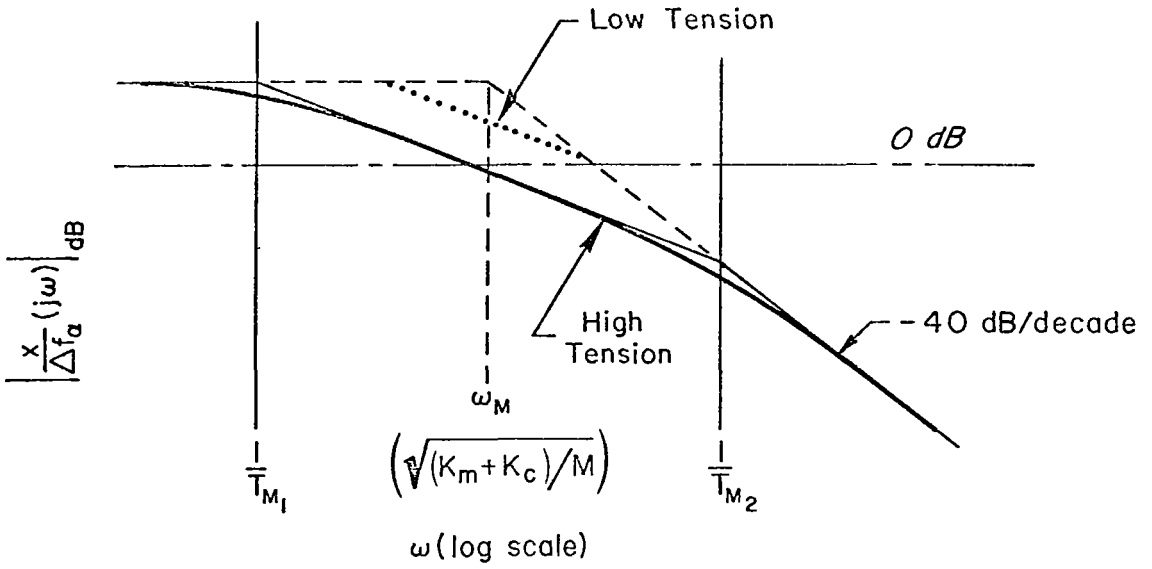

Figure 41. jω-Bode Diagram for Limb/Manipulator Dynamics

Isometric manipulator. —An isometric manipulator implies that K_F is extremely large and x very small. The output signal here will be a force, F_s, equal to $K_F x$. In equation 17, multiplying both sides by K_F and taking the limit as $K_F \to \infty$ yields for the $F_s/\Delta f_\alpha$ transfer function

$$\frac{F_s}{\Delta f_\alpha} = C_f\left(\frac{K_e}{K_m + K_e}\right)\left(\frac{1}{T_h s + 1}\right) \qquad (21)$$

where

$$\frac{1}{T_h} = \frac{K_e + K_m}{B_m}$$

Frequency response data (ref. 87) for a functionally isolated (i.e., feedback path cut) cat skeletal muscle using an isometric load is given in figure 42. The forcing function was a sinusoidal variation in pulse rate (5–30 pps). The magnitude of the frequency response for the muscle is closely fitted by a simple lag as expected from equation 21.

Both references 77 and 89 took measurements of the transient rise of isometric torque for human subjects employing maximum effort. A 70 ms time constant was found for both wrist supination-pronation (ref. 77) and for adduction-abduction (90 deg elbow angle, upper arm kept parallel to body, wrist movement left to right), reference 89. Note that the muscles firing rate changes were not small relative to an operating point. However the final portion of the transient responses (as the new equilibrium was reached) look reliable enough for us to assume that 14 rad/sec is near the lower limit for $1/T_h$ due to maximum values of B_m.

No-spring large-inertia. — For this manipulator the denominator of the $x/\Delta f_\alpha$ will be a cubic. Using equation 16 with $K_F = 0$ yields

$$\Delta = MB_m\left(s^3 + \frac{K_m + K_e}{B_m}\, s^2 + \frac{K_e}{M}\, s + \frac{K_eK_m}{MB_m}\right) \tag{22}$$

This will have either three real roots or one real and two complex roots. For the latter case there are two approximate factorizations of equation 22 which depend on a wide separation of the roots. The first case is

$$\Delta \doteq MB_m\left(s + \frac{K_m + K_e}{B_m}\right)\left[s^2 + \frac{B_m}{M}\left(\frac{K_e}{K_m + K_e}\right)^2 s + \frac{K_m}{M}\left(\frac{K_e}{K_m + K_e}\right)\right] \tag{23}$$

provided that

$$\frac{K_m + K_e}{B_m} \gg \frac{B_m}{M}\left(\frac{K_e}{K_m + K_e}\right)^2$$

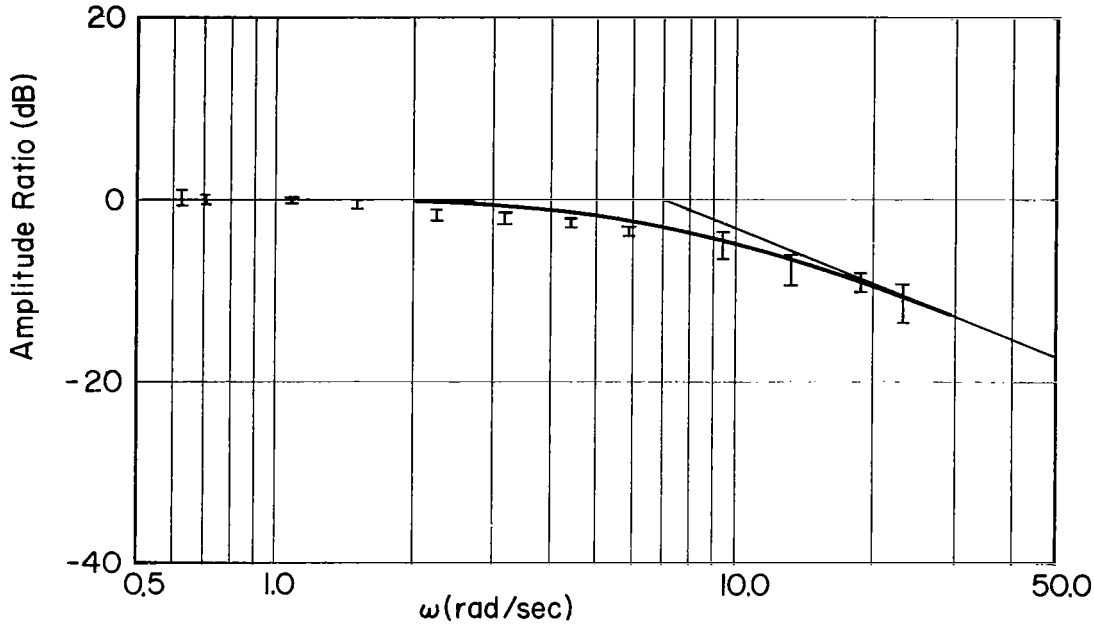

Figure 42. Frequency Response for Isolated Cat Muscle (Isometric Load)

This will hold for large inertia. The real root is seen to be that for the isometric case, $1/T_h$. It will be relatively high frequency whereas the frequency of the quadratic pair will depend on the inertia.

The second case is

$$\Delta \doteq MB_m\left(s + \frac{K_m}{B_m}\right)\left(s^2 + \frac{K_e}{B_m}\, s + \frac{K_e}{M}\right) \tag{24}$$

provided that

$$\frac{K_e}{M} \gg \frac{K_m K_e}{B_m^2} \quad \text{or} \quad \frac{B_m}{M} \gg \frac{K_m}{B_m}$$

These inequalities will hold for large B_m and small K_m and M. Typically this results in a low frequency real root plus a high frequency quadratic.

The first case describes the probable root configuration for large inertia. Data in reference 88 considered a variety of manipulator restraints with a 28:1 range of inertias (the smallest was larger than that provided <u>in situ</u> by the unloaded foot). These showed that as the inertia was increased a high frequency droop appeared in both the magnitude and phase. However even for the largest inertia the data below 4 rad/sec was essentially unchanged. These trends are compatible with equation 23. Specifically, the isometric time constant which is independent of inertia, dominates the unchanged low frequency portion, while the inertia causes the high frequency droop which decreases in frequency as inertia is increased.

We can now build a general case for the approximate factors of the third-order characteristic equation. The data for the special cases discussed above indicate that the isometric root, $1/T_h$, is a factor. Using this, the approximate factors to equation 14 become

$$\Delta \doteq MB_m\left(s + \frac{K_m + K_e}{B_m}\right)\left[s^2 + \frac{B_m}{M}\left(\frac{K_e}{K_m + K_e}\right)^2 s + \frac{1}{M}\left(K_F + \frac{K_m K_e}{K_m + K_e}\right)\right] \tag{25}$$

which applies as long as

$$\frac{K_m + K_e}{B_m} \gg \frac{B_m}{M}\left(\frac{K_e}{K_m + K_e}\right)^2$$

Muscle Spindle Model

A muscle spindle model compatible with the data given on pages 35–42 is shown in figure 43. The output of the spindle is the primary ending firing rate. The inputs are the "dynamic" and "static" fiber firing rates as well as an internal muscle length. The latter arises from the placement of the spindle as spanning a portion of the muscle (fig. 16), i.e., some tendon and muscle elastance intervenes between total muscle length, x, and the spindle feedback length (which we will assume to be x_1) (fig. 40).

In figure 43a, the region of the nuclear bag from which the primary ending originates is represented by a relatively stiff spring. Here the primary ending firing rate is assumed to be proportional to nuclear bag deformation (ref. 38). Thus I_a firing rate is proportional to spring deflection. The intrafusal muscle fiber portions are shown with dynamic, γ_d, and static, γ_s, fiber inputs. Each of these fiber elements are muscles, so each one can be represented as a muscle model similar to that shown in figure 40. This is the basis of the equivalent model shown in figure 43b which also takes advantage of the symmetry about the midpoint of the nuclear bag capsule spring.

The details of the portion of the intrafusal muscle fiber innervated by the dynamic fibers, γ_d, are assumed to be typical of muscle as modeled previously (eq. 11) except for the series elastic component. These comprise a force generator, $P_d = P_{d_o} + C_{f_d}\Delta f_d$, plus an equivalent spring, K_n, and damper, B_n, both of which depend on the operating point conditions, f_{d_o} and fiber length, which determine P_{d_o}. We have omitted the series elastic component since it will not affect the dynamics of the nuclear bag deformation response except as a scale factor.

The portion of the intrafusal muscle fiber innervated by the static fibers has a similar model (force generator plus spring, K_h). However, it lacks a viscosity element, since available data for a step increase in static fiber stimulation (refs. 32 and 67) indicate that it is either not present or is

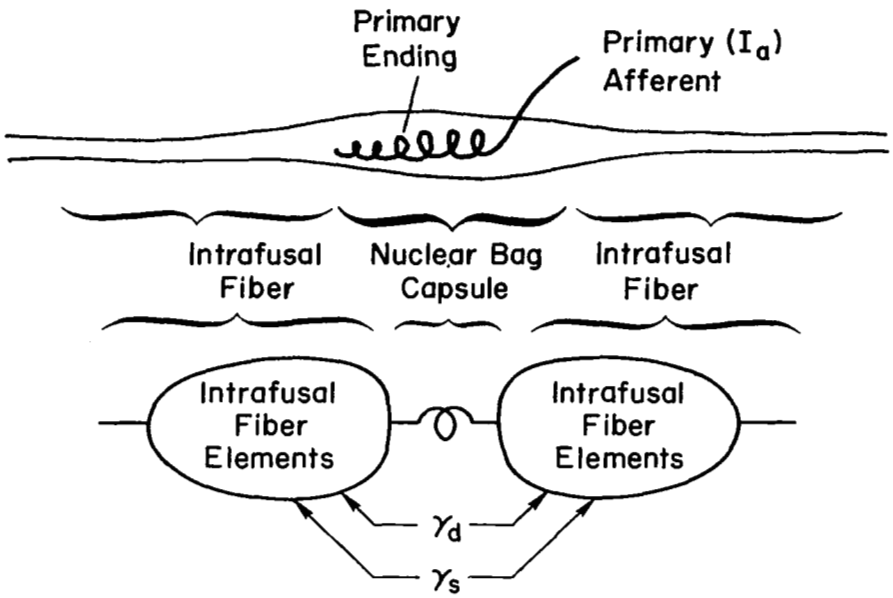

(a) Equivalent Lumped Parameter Mechanical Network

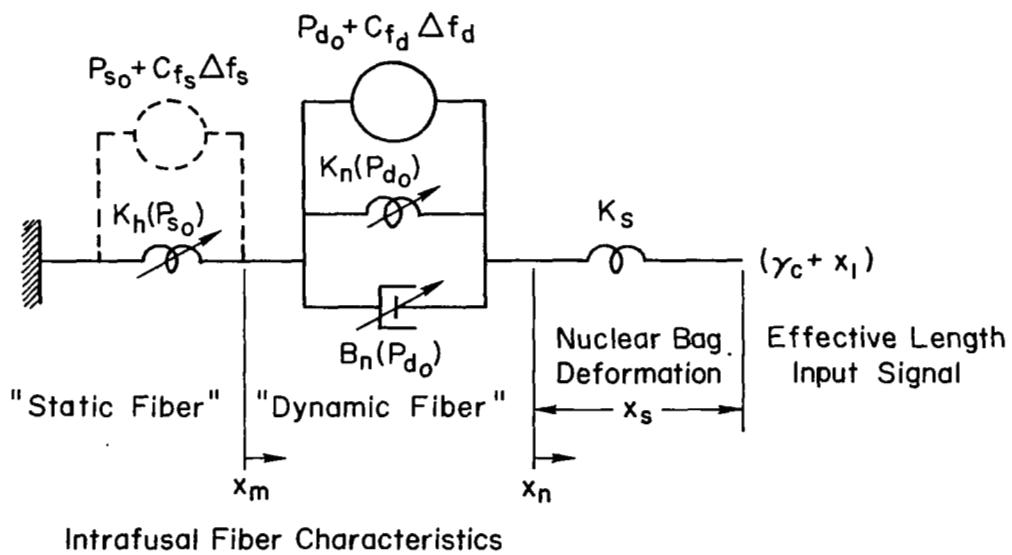

(b) Simplified Mechanical Network

Figure 43. Schematic of Muscle Spindle Model

very small. Note that the effect of the static fiber force generator, $P_s = P_{s_o} + C_{f_s}\Delta f_s$, on nuclear bag deformation can alternatively be described by an equivalent length input, γ_c. This can be seen by applying a step increase in Δf_s (with muscle shortening, x_1, kept constant) which produces a step reduction in x_m. This immediately increases x_s, since the damper, B_n, cannot change length instantaneously. Subsequently, the damper smoothly extends, allowing the length change to distribute throughout all three springs as a new equilibrium is reached. Inspection of figure 43b reveals that this response pattern is the same as that produced by a step length change in x_1. Consequently, the static fiber input will henceforth be replaced by an equivalent length input, γ_c (the static fiber force generator is shown in dashed lines for this same reason).

The equations of motion can be written by summing the forces at each node to zero. On rearranging, these become

$$\begin{bmatrix} (K_s + K_n + B_n s) & -(K_n + B_n s) \\ -(K_n + B_n s) & +(K_h + K_n + B_n s) \end{bmatrix} \begin{bmatrix} x_n \\ x_m \end{bmatrix} = \begin{bmatrix} K_s(\gamma_c + x_1) - P_d \\ P_d \end{bmatrix} \quad (26)$$

where $P_d = P_{d_o} + C_{f_d}\Delta f_d$, the force due to dynamic fiber stimulation

Solving for the nuclear bag deformation, $x_s = (\gamma_c + x_1) - x_n$, which is proportional to the primary ending firing rate, yields

$$x_s = \frac{K_r(s + 1/T_K)(\gamma_c + x_1) + P_d/B_n}{(s + 1/aT_K)} \quad (27)$$

where

$$\frac{1}{T_K} = \frac{K_n}{B_n}$$

$$\frac{1}{aT_K} = \frac{K_r + K_n}{B_n}$$

$$\frac{1}{K_r} = \frac{1}{K_h} + \frac{1}{K_s}$$

[redacted]y ending has a lead/lag response to muscle length and/or static [redacted]. The response to dynamic fiber input is a simple lag. Note that the lead break frequency is dependent on the operating point dynamic fiber stimulation frequency, whereas the lag break frequency depends on both the dynamic and static fiber inputs. There is some indication (fig. 21) that the lead break frequency is relatively constant for different dynamic fiber stimulation rates.

References 63 and 80 contain data that we shall use as an example to illustrate the spindle dynamics as well as the closed-loop spindle/muscle reflex response. Reference 80 studied the properties of muscle spindles via sinusoidal length inputs to the decerebrate cat's soleus muscle with the reflex loop intact. Recordings were made of tension and motor nerve action potentials sensed from a surface electrode on the belly of the muscle. Reference 63 also used sinusoidal inputs, but for the tibialis anterior muscle of both spinal and decerebrate cats. Recordings were made of the motor nerve action potentials with the reflex loop intact as well as severed. For reference 63 none of these motions were small compared to the operating point. This is evidenced by the motor/nerve firing rate responding only during the lengthening portion of the input. Thus we should be cautious when inferring small signal equivalent circuit parameters from such data. The situation in reference 80 was potentially better in that decerebrate preparations show an extensor rigidity due to a steady-state gamma input. However, the only phase data presented was taken from low-gamma situations such that again there was only an intermittent response. Nevertheless the data shown in figure 44 is interesting and illustrates nicely some features of the limb-musculature loop dynamics.

The data indicated by the circles and dots (ref. 63) was taken from a spinal cat, i.e., spinal transection above the level of the reflex pathway. The open circles data were taken from the cut muscle nerve (severing the reflex pathway), whereas the motor action potential data (closed circles) were recorded before cutting the nerve. The open-loop data, which reflects the muscle spindle alone, indicates a lead at about 6 rad/sec. The closed-loop data also exhibits the lead but has a high frequency lag. The closed-loop data from reference 80 has the same general shape, except that is exceeds 90 deg in some regions, possibly indicating more than a simple lead. The single data point calculated

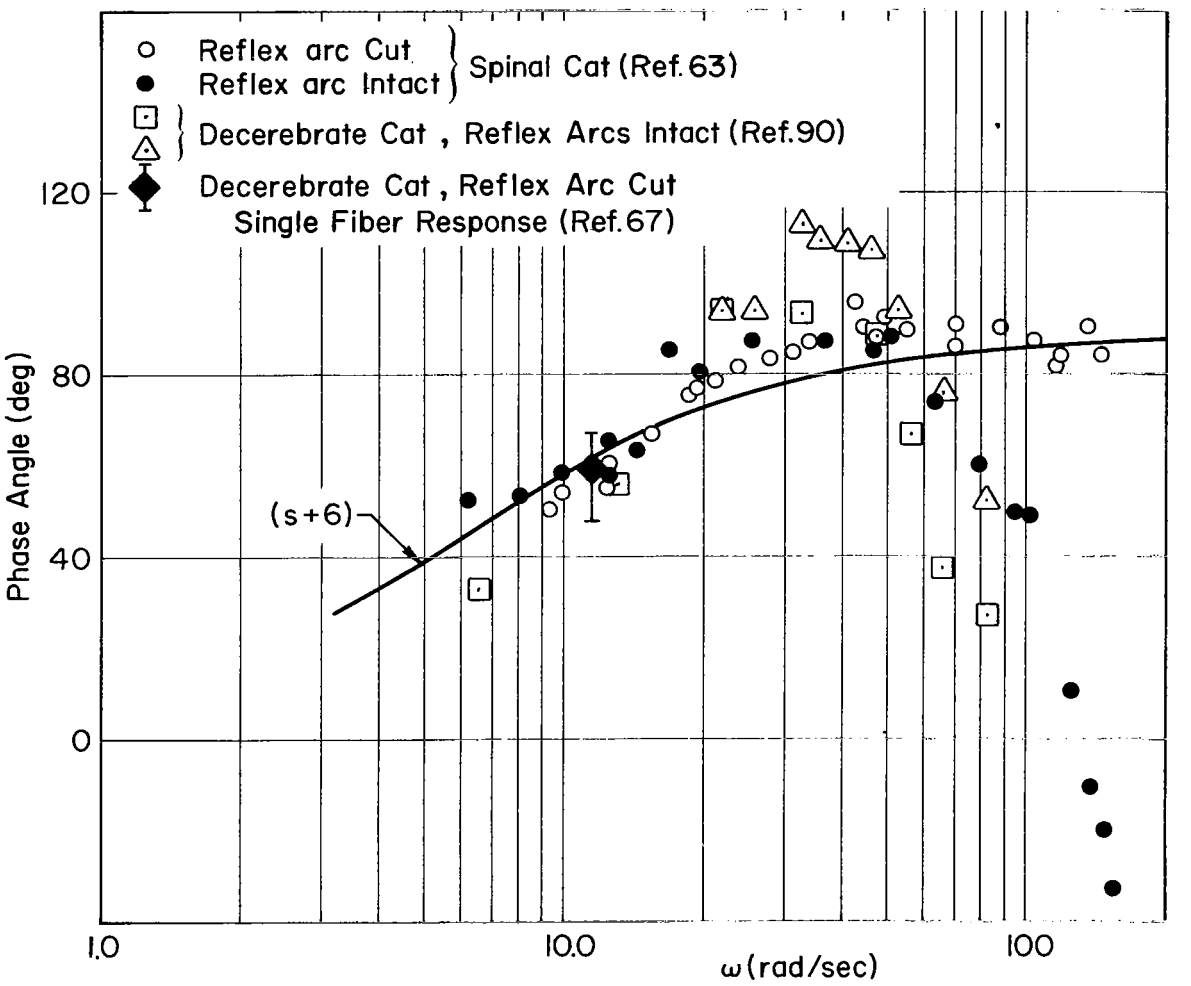

Figure 44. Phase Angle of Reflex Motor Action Potential Response to Sinusoidal Position Input

from figure 21 (ref. 67) is included in figure 44 to show the phase lead of a single I_a afferent (its firing rate displayed a nonintermittent response).

A model to describe these data is shown in figure 45. The dashed line portion indicates that the spindle senses an internal muscle length, x_1, (rather than the total muscle length) and drives the muscle via the reflex pathway. Otherwise the muscle length sensed by the muscle spindle (shown dashed) would be directly driven by the forcing function, thus preventing a closed-loop response between input and the EMG (electromyograph). (Note that the EMG, related to $C_f\Delta f_\alpha$, is activated by the reflex response from the muscle spindle.) We've assumed negligible inertia effects.

The equation of motion for the internal muscle point, x_1, is found by setting the net force at x_1 to zero

$$-C_f\Delta f_\alpha - (K_m + B_m s)x_1 + (x - x_1)K_e = 0 \qquad (28)$$

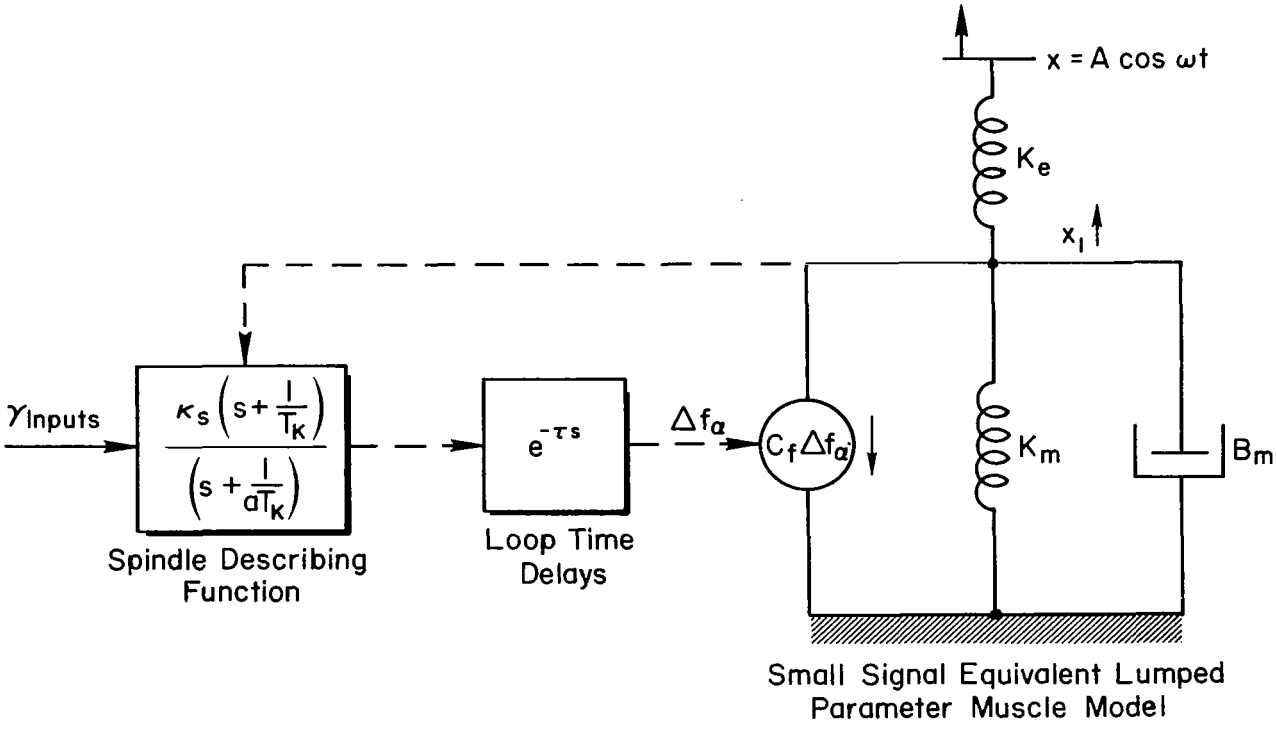

Figure 45. Muscle/Spindle Model for Reflex Response to Sinusoidal Position Input

Noting that the reflex loop gives

$$\Delta f_\alpha = \frac{K_s(s + 1/T_K)e^{-\tau s}}{s + 1/aT_K} x_1 \tag{29}$$

and eliminating x_1 between equations 28 and 29 gives

$$\frac{\Delta f_\alpha}{x} = \frac{K_e K_s(s + 1/T_K)e^{-\tau s}}{\underbrace{(K_e + K_m + B_m s)(s + 1/aT_K)}_{D(s)} + \underbrace{C_f K_s(s + 1/T_K)e^{-\tau s}}_{N(s)}} \tag{30}$$

where N(s) and D(s) are the numerator and denominator of the loop gain transfer function. Note that for large loop gain, $C_f K_s$, one of the denominator roots is driven into the zero at $s = -1/T_K$. Thus this closed-loop pole would cancel the numerator lead term of equation 30; a situation that cannot explain any of the data in figure 44. For low loop gain, $D(s) \gg N(s)$ and $\Delta f_\alpha/x$ exhibits a lead plus two lags and a time delay which is compatible with the basic features of the data in figure 44 for an intact reflex loop, i.e.,

$$\frac{\Delta f_\alpha}{x} \doteq \left(s + \frac{1}{T_K}\right)e^{-\left[\tau + aT_K + B_m/(K_e + K_m)\right]s} \tag{31}$$

When the reflex loop is cut, all inervation to the muscle is lost, which reduces the size of K_m and B_m (eq. 10), thus reducing the phase lag contribution of the denominator term $(K_s + K_m + B_m s)$. Further, since the phase looks like a pure lead, then the phase lag due to $aT_K + \tau$ must be small. However, one set of parameters will not explain all of the figure 44 data. This is partly due to inferring the phase shift from experiments in which the signal excursions of nonlinear systems are not small relative to an operating point.

The phase leads of more than 90 deg are interesting. Naturally the above model cannot explain these phase leads — it's interesting to speculate on possible explanations. It has been conjectured, based on muscle transient responses (ref. 70), that the series elastic component, modeled by the spring,

K_e, may also be paralleled by a damper, B_e. In equation 30, replacing K_e by $(K_e + B_e s)$ yields another numerator lead term (and some modification of a lag term). This could easily account for the additional lead in the data of figure 44.

CLOSED-LOOP NEUROMUSCULAR SYSTEM DYNAMICS

In this section we combine the component models (muscle actuation and spindle feedback and actuation subsystems) developed in the preceding section into a neuromuscular system model. This will be used to describe the trends in the overall input/output human operator data discussed on pp. 63-75. Our closed-loop neuromuscular system model features spindle feedback of an internal muscle length rather than limb position directly. In the first subsection following we develop a system block diagram combining the components already discussed. This is followed by a discussion of the effects of operating point tension on the low and high frequency phase of the closed-loop neuromuscular system for spring-restrained low-inertia manipulators. The trends are compatible with the covariation of low and high frequency phase observed for the whole human. Further the effects of an inertia increase on the high frequency phase is described. In the third subsection the response of the model to a force disturbance input is examined, and the predicted trends are correlated with the observed data. The fit to these data illustrates a key feature of the model — that the spindles feed back an internal muscle length rather than limb position directly. In the final subsection the model is correlated with tremor data. This interpretation provides good evidence for a closed-loop explanation of tremor. In addition it provides further corroboration of the spindle feedback properties just discussed.

Neuromuscular System Block Diagram for Small Perturbations

A combination block and schematic diagram of the muscle/spindle system for small perturbations about an operating point is shown in figure 46. This combines the spindle characteristic with the limb/manipulator characteristics previously shown in figure 40. The internal inputs to the system are command and bias aspects of the static and dynamic gamma muscle spindle fibers and the alpha motor neuron commands; the external input is a force, F, applied to the manipulator. A key feature is the spindle feedback of x_1 (an internal muscle length) rather than x the limb length.

It is to be distinctly understood that the schematic represents perturbation operations about steady-state operating points. Consequently, all the signals

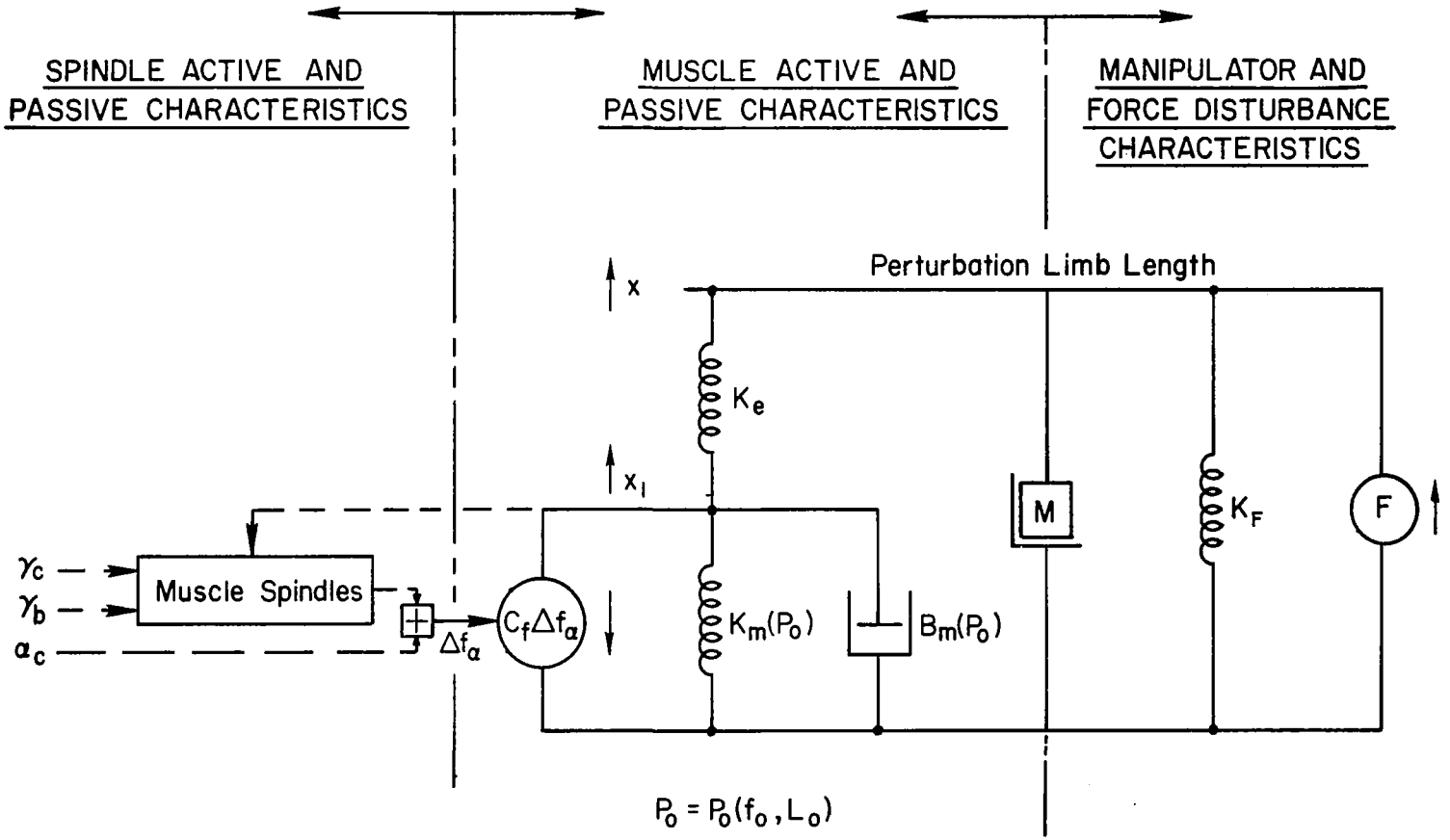

Figure 46. Combination Block and Schematic Diagram for the Muscle/Manipulator/Muscle Spindle System

indicated can be either positive or negative, and the agonist/antagonist relationships are subsumed in the composite schematic.

The single-loop feedback system which corresponds to the neuromuscular system just described is shown in figure 47. Again, this is a perturbation diagram; a block diagram of an agonist/antagonist operation with absolute level signals can be constructed by simply duplicating the diagram, then connecting the two back to back with the limb position, x, being the sum of the two outputs.

The spindle ensemble provides four functions in one entity: (a) the feedback of a limb position; (b) some lead/lag series equalization; (c) the source of one command to the system; and (d) a means for adjustment of the bias or spindle equalization. Those steady-state static, γ_s, and dynamic γ_d signals which effect the spindle adjustments are lumped here as a general gamma bias signal, γ_b. The spindle output differential firing rate is summed with an alpha motor neuron command, with the result, after conduction and synaptic delays, being an incremental alpha motor neuron firing rate, Δf_α. This in turn perturbs the muscles and manipulator, giving rise to limb rotation, which is sensed by the spindle ensemble. The γ motor neuron command, γ_c, is shown with a time delay, τ_γ, before it becomes the γ input to the closed loop. This delay is the relative time difference between α and γ transmission from a common high center (e.g., a visual input).

As discussed in the preceding section, the effective damping of the limb/manipulator dynamics transfer function is set by the operating point muscle tension, P_o, which is due to the steady-state alpha motor neuron firing rate, f_o. This is indicated in figure 47 by a <u>total</u> gamma bias, γ_o, shown entering the G_M block. The notation, γ_o, is based on the assumption that the alpha motor neuron command is not involved in random input tracking. The bias can derive from either of the steady-state values γ_{b_o} or γ_{c_o}, or both, from which the γ_b and γ_c motor neuron signals shown here represent perturbations.

The equations of motion for the elements involved in the closed-loop system are:

$$x_1 = \frac{MC_f\left(s^2 + \frac{K_F + K_e}{M}\right)}{\Delta} \Delta f_\alpha + \frac{K_c}{\Delta} F$$

$$= C_f G_M \Delta f_\alpha + \frac{K_e}{\Delta} F \qquad (32)$$

where $G_M = \frac{N_M}{\Delta}$ and $N_M = Ms^2 + K_F + K_e$

$$x = \frac{K_e}{M\left(s^2 + \frac{K_F + K_e}{M}\right)} x_1 + \frac{F}{M\left(s^2 + \frac{K_F + K_e}{M}\right)} \qquad (33)$$

$$\Delta f_\alpha = \left[\alpha_c + G_s(\gamma - x_1)\right] e^{-\tau_\alpha s} \qquad (34)$$

where Δ in its most complete form is given by equation 14. Combining equations 32 and 34, the closed-loop response for x_1 becomes

$$x_1 = \frac{C_f G_M G_s e^{-\tau_\alpha s}}{1 + C_f G_M G_s e^{-\tau_\alpha s}} \gamma + \frac{C_f G_M e^{-\tau_\alpha s}}{1 + C_f G_M G_s e^{-\tau_\alpha s}} \alpha_c + \frac{K_e/\Delta}{1 + C_f G_M G_s e^{-\tau_\alpha s}} F$$

$$= \frac{1}{\Delta'}\left[C_f N_M N_s e^{-\tau_\alpha s} \gamma + C_f N_M D_s e^{-\tau_\alpha s} \alpha_c + K_e D_s F\right] \qquad (35)$$

where $G_s = N_s/D_s$, $G_M = N_M/\Delta$ and the closed-loop characteristic function, Δ', is

$$\Delta' = \Delta D_s + C_f N_M N_s e^{-\tau_\alpha s} \qquad (36)$$

The limb output x is found by inserting the closed-loop expression for x_1 into equation 33.

The several cases to be discussed in the sequel differ primarily in the details of the muscle and manipulator dynamics block.

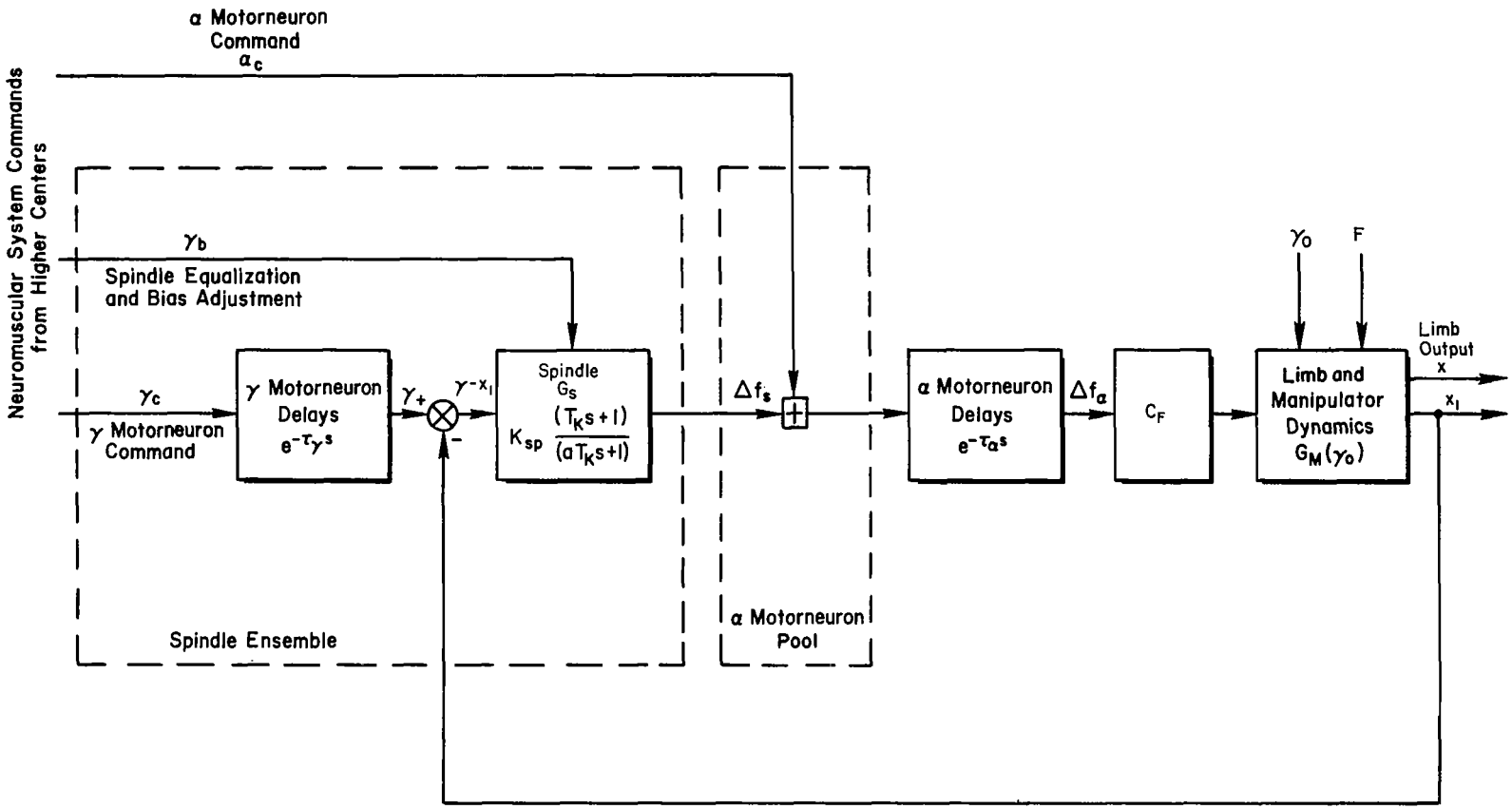

Figure 47. Neuromuscular System Model Block Diagram

Spring-Restrained Low-Inertia Manipulator, Random Input Tracking

As discussed on page 83, the muscle model's series elastic component, K_e, is quite large relative to K_m and B_m. We shall assume that it is also much larger than K_F or M. Thus with $K_e \rightarrow \infty$ then equation 35 for the closed-loop limb response to γ_c becomes (in the absence of any force disturbance or α_c input),

$$x = x_1 = \frac{C_f G_s e^{-\tau_\alpha s} \gamma}{(Ms^2 + B_m s + K_m + K_F) + C_f G_s e^{-\tau_\alpha s}} \qquad (37)$$

In figure 41 we considered the effects of operating point tension changes on the limb/manipulator open-loop roots. Here we shall examine the consequences of operating point tension changes on the closed-loop roots.

A representation of the open- and closed-loop dynamics of the neuromuscular system is indicated in figure 48 via a block diagram, root locus and Bode plot. The open-loop poles and zeros are starting and end points on a conventional root locus; these correspond to breakpoints of the asymptotic Bode plots for the open-loop amplitude ratio $|x/(\gamma - x)|$, i.e., the low frequency muscle/manipulator root, $1/T_{M_1}$, the spindle lead, $1/T_K$, the high frequency muscle root, $1/T_{M_2}$, and the spindle lag, $1/aT_K$. (Note that the small pure time delay within the loop, τ_α, is neglected since its effects are minor at the frequencies of interest here.) For a particular tension level these plots show that as gain is increased, the low frequency muscle/manipulator root approaches the lead zero of the spindle, while the high frequency muscle root and the spindle lag approach one another, rendezvous, and break into a second-order pair. For a particular loop gain, e.g., that shown by the zero-dB line, the closed-loop asymptotic plot of $|x/\gamma|$ is indicated by the dashed asymptotes. The real-axis closed-loop poles are, of course, given by the intersection of the zero-dB line and the Siggy diagrams (refs. 94 and 95), while the closed-loop zero is the same as the open-loop, i.e., $1/T_K$. On the approximate closed-loop phase curve, the low frequency phase lag is due to the low frequency closed-loop lag/lead,

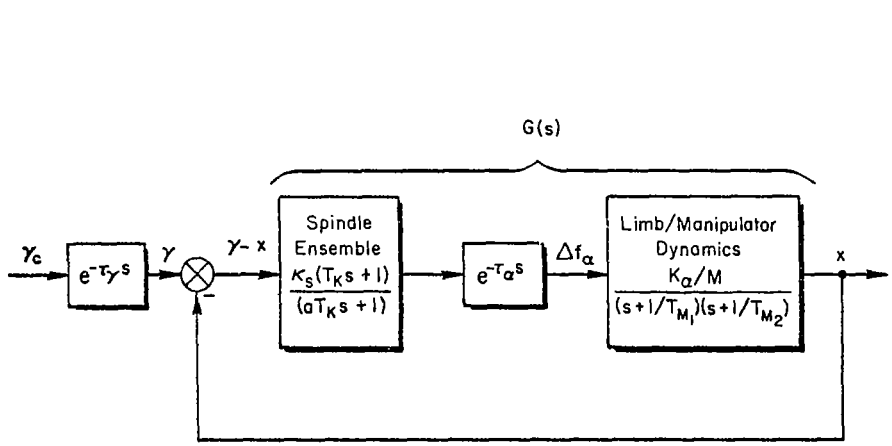

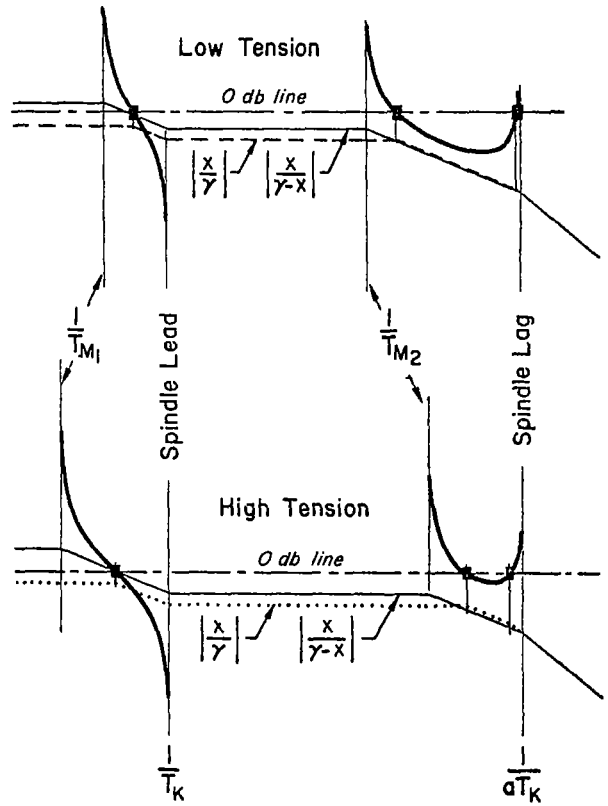

a) Amplitude Ratios

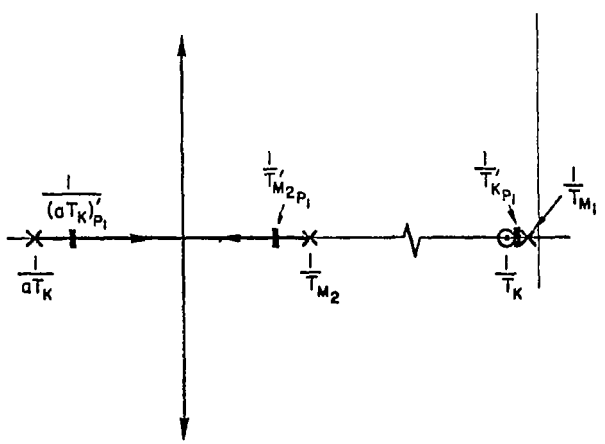

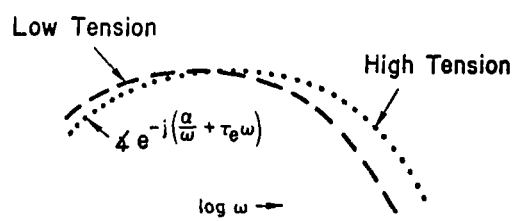

b) Approximate Phases

Figure 48. Root Loci of Neuromuscular Subsystem Dynamics with Two Levels of Tension

whereas the high frequency phase lag is a lower frequency view of the two high frequency closed-loop lags. The phases reflect, of course, the α and τ_e approximations described on pages 64 and 65.

Consider, now, the effect of an operating point tension increase on the neuromuscular system dynamics. Presume that the upper plot is typical of a low tension condition. Now, change the steady-state tension; then the open-loop amplitude ratio will change to that in the bottom plot labeled "high tension." On these, the low frequency muscle root is decreased while the high frequency root is increased, as in figure 48. For simplicity, assume for now that the spindle lead and lag are unmodified by the steady-state tension change. Then, even with the mid-frequency gain unchanged, the closed-loop dynamics are modified significantly. The closed-loop low frequency lag/lead is more widely spaced than for the low tension case, giving rise to a larger low frequency phase lag, as seen from mid-frequencies; and the high frequency lag is substantially reduced. The net effect of the tension increase is to shift the phase umbrella to the right, a result which is consistent with the data in figures 29 and 30. These effects are even more pronounced if the spindle gain is increased by the gamma bias sufficiently to increase the mid-frequency gain. This result is also consistent with the data in figures 32, 33, and 34, which describe high frequency phase effects as a function of tension. Thus we have demonstrated that this extremely simple neuromuscular system model described in our block diagram is qualitatively compatible with the α-τ_e covariation data and the τ_e-tension data summarized on pages 64-66.

The general trend of increased manipulator inertia causing an increased effective time delay is also supported by this system. This is easy to see by imagining the joint shift of $1/T_{M_1}$ and $1/T_{M_2}$ on figure 48 from a reference condition. The joint shift corresponds to a net change in manipulator inertia, with an increase causing a joint shift to the left. The result in the closed-loop system is an increased effective time delay, τ_e.

Large-Inertia, No-Spring Manipulator, Force Distribution Input

In this section the force disturbance data (figs. 32 and 33) shall be explained. This is especially important to illustrate a key feature of the spindle feedback. For this situation equation 35 applies with α_c and $\gamma_c = 0$.

Also, for the data in figure 32, $K_F = 0$. The subject's task was merely to set muscle tone and let the transient run its course. For this situation the limb position response to a force disturbance input becomes on inserting equation 35 into equation 33 and using the identity $\Delta + K_e^2 = N_M(B_m s + K_m + K_e)$

$$\frac{x}{F} = \frac{(B_m s + K_m + K_e) + C_f G_s e^{-\tau_\alpha s}}{\Delta + C_f G_s (Ms^2 + K_e) e^{-\tau_\alpha s}} \tag{38}$$

where G_s is as shown in figure 47, i.e.,

$$G_s = \kappa_s \frac{(s + 1/T_K)}{(s + 1/aT_K)} \tag{39}$$

and the appropriate limb/manipulator dynamic characteristic function is

$$\Delta \doteq MB_m \left(s + \frac{K_m + K_e}{B_m}\right)\left[s^2 + \frac{B_m}{M}\left(\frac{K_e}{K_e + K_m}\right)^2 + \frac{K_m}{M}\left(\frac{K_e}{K_e + K_m}\right)\right] \tag{40}$$

Both the numerator and denominator of the closed-loop function x/F are functions of the gain parameter $C_f\kappa_s$. The joint movement of the numerator and denominator singularities as a function of this loop gain ($C_f\kappa_s$) can be demonstrated by treating both the numerator and the denominator as loop closures. Then both closed-loop poles and closed-loop zeros will move as loop gain is changed. Root locus sketches of the denominator and numerator closures are given in figure 49a and figure 49b, respectively. These two closures have common real-axis poles and time delay terms. Only the denominator will have quadratic roots (at high frequency). The closed-loop low frequency real root will be approximately the same in both closures. Thus the closed-loop system describing function x/F is dominated by a second-order mode which has an undamped natural frequency which is a function of the loop gain (operating point tension dependent) as well as the external mechanical element (inertia). This describes the reference 77 results in figure 33. However the degree of pole/zero cancellation will be affected by the proximity of the quadratic terms. Some of the different responses are shown in figure 32. In

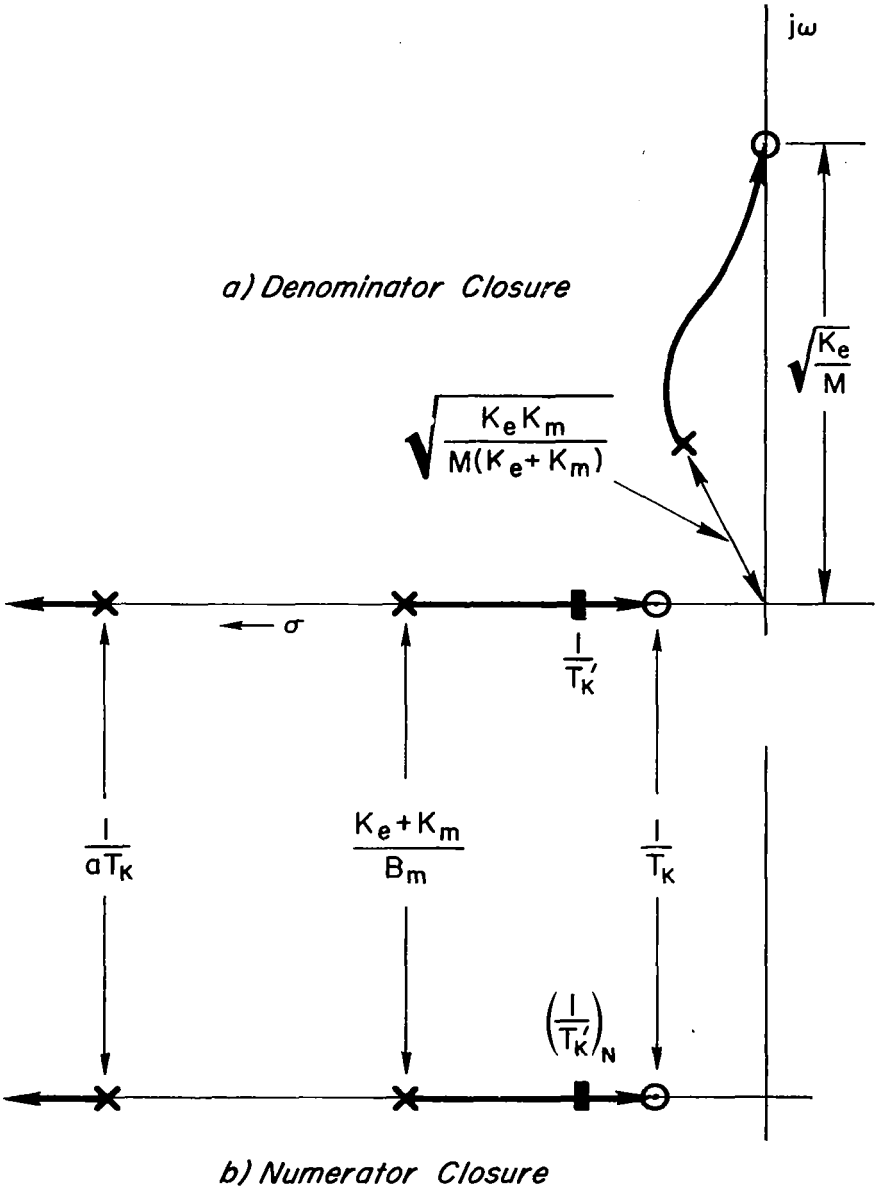

Figure 49. Root Locus Sketch for Denominator and Numerator Roots for Force Disturbance Input

figure 32b the response seems to contain some of the first-order pole, whereas in figure 32a the response is nearly a pure second-order transient.

Now examine the consequences of assuming that the spindles feedback x instead of x_1 (fig. 46). Carrying this through the equations reveals that the numerator of equation 38 will not contain $C_f G_s$; hence the pole-zero near cancellation will not take place. Thus the transient response will be third order. The real root will be more evident at the higher tensions since this increases loop gain and drives the $1/T_K'$ root to lower frequency away from the numerator zero. This trend is just the opposite of that in figure 32b which becomes more like a second-order system at higher tensions.

Tremor

A number of theories have been advanced to account for tremor oscillations, among them they arise from: (1) periodically fluctuating activity in supra-spinal centers; (2) spinal neuronal rhythmicity; (3) resonance of the moving parts of the limbs; (4) oscillations arising from the stretch-reflex loop itself.

At present, the evidence very much favors the last hypothesis, since (1) in tabetic patients* with loss of dorsal root fibers the tremor frequency (8–10 Hz) peak is absent; (2) there does not seem to be any correlation of EEG activity (alpha rhythm) with limb tremor; (3) tremor seems to disappear with section of the dorsal roots; (4) there is no evidence of inherent rhythmicity of spinal alpha or gamma motor neurons in the absence of sensory input. Also, tremor occurs primarily under conditions where fine control of position is involved, and that much less tremor is produced under rest conditions or when a gross, rapid ("ballistic") type of movement is executed. This also tends to support the stretch-reflex (closed-loop) explanation.

The "tremor peak" in the frequency spectrum is said by some (e.g., ref. 64) to be indifferent to changes in the load, but the data of references 80, 81, and 102 (figs. 35 and 36) clearly contradict this, and in addition indicate that the

*Patients suffering from advanced stages of syphilis who show extreme loss of large sensory afferents, specifically spindle I_a fibers (loss of the stretch reflex) and joint receptors (loss of proprioceptive cues).

peak frequency is dependent on the mean tension generated, spring rate, and inertia. An excellent example of tremor while tracking (involving fine control of position) is provided by some unpublished data taken during experiments reported in reference 91. This was a multiloop task in which the pilot's feet were controlling rudder pedals and his hand was controlling a spring-restrained side stick. One of the subjects used a high tension technique, i.e., tensed both legs against the pedals and performed the rudder task with differential force changes. Simultaneously, his hand tracking displayed an intermittent tremor of 8 Hz, which was largest at the extreme stick excursions (which requires the largest tensions).

The data cited above indicate that any neuromuscular system model must be compatible with ambient noise excitation of an almost neutrally stable mode near 7 – 11 Hz which varies with spring rate and tension. Figure 49a depicts a likely tremor source, i.e., the closed-loop mode determined by the locus branch proceeding to the zero at $\omega = \sqrt{K_e/M}$. Increases in inertia will decrease the frequency of this mode, whereas increases in tension, by increasing loop gain, will drive the roots closer to the zeros on the $j\omega$-axis. Both of these trends are compatible with the figure 36 data.

The above explanation also applies to the figure 35 data which used a spring restraint but now the zeros are located at $\omega = \sqrt{(K_F + K_e)/M}$ (see eqs. 32 and 36 for N_M). Now increases in K_F lead to higher tremor frequencies, whereas tension increases (by increasing loop gain) drive the mode into the zeros. The flattening of the curves in figure 35 indicates that the root is already near a limit. Attempting to put the above explanation on a quantitative basis by estimating the inertia involved in the figure 35 data (see page 73 for the limb motion), using reasonable values of K_e and then calculating the effect of K_F yields predicted ω values of between 7 and 14 Hz. These are "infinite gain" tremor frequencies, as compared to the actual tremor frequency range from 7 to 11 Hz given in figure 35. The difference between the infinite gain tremor frequency and the actual is explained by the sketch in figure 50 which shows the loop dynamics pertinent to figure 35. Note that the effect of the time delay, τ_α, is to make the instability frequency less than that of zero. The spread between the zero and the instability frequency is likely to be greater for the stiffer spring rates since this raises the zero and the pole to higher frequency where

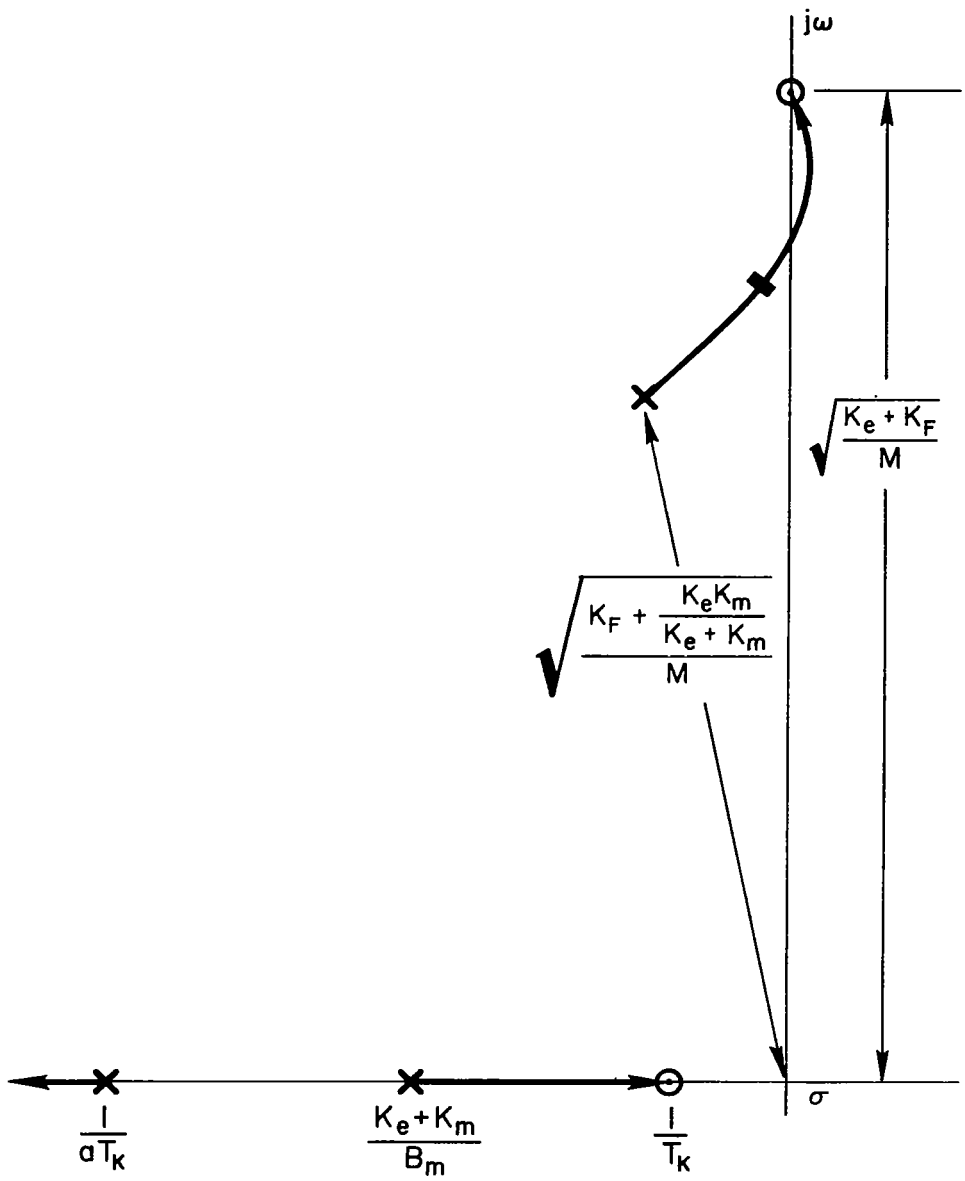

Figure 50. Root Locus Sketch for Characteristic Equation

the loop time delay (eq. 36) has more effect. At higher frequencies the time delay causes the root locus departure from the pole to occur at a lower angle, i.e., it tends to proceed more directly to the $j\omega$-axis. Thus increases in spring rate yield an instability frequency that is less than the frequency of the zero, and this difference increases at the higher frequencies.

A time delay on the order of 25 ms is compatible with nerve conduction time from periphery to spinal cord to periphery (refs. 92 and 93). Such a value would contribute 90 deg phase shift at 10 Hz leaving 90 deg to be contributed by the other loop dynamics to produce the 180 deg instability frequency. The loop gain function $C_f G_M G_S$ can be compatible with phase shifts of 90 deg near 10 Hz.* Thus the tremor data is compatible with ambient noise excitation of a closed-loop neuromuscular system mode.

*For the special case of an isometric manipulator ($K_F \rightarrow \infty$), the quadratic poles and zeros tend to infinity, leaving only the two real poles and a zero. If the frequency of these singularities is smaller than 10 Hz, then they would contribute approximately 90 deg phase lag at 10 Hz.

CONCLUSIONS

The data and analysis presented in this report indicate that simple quasi-linear models can describe the small perturbation behavior of the neuromuscular system components (muscles and muscle spindles). Further, the closed-loop behavior of ensembles of these components is compatible with input/output data for the whole human in tracking situations.

The more specific conclusions are:

Component ensembles. — Our quasi-linear models provide a useful description of an enormous amount of component physiological data. They describe in detail the dynamics of an extremely important subsystem revealing an adaptive actuator of extraordinary flexibility.

- The muscle's transfer characteristics are described by a third-order system whose roots are an adaptive function of the operating point tension (which depends on muscle length and average motor nerve firing rate).

- The muscle spindle ensemble provides four functions in one entity: (a) feedback of an internal muscle length, (b) lead/lag series equalization, (c) the source of one command input to the neuromuscular system, and (d) a bias signal which determines the average motor nerve firing rate to the muscle actuation system.

System behavior. — The system behavior of the neuromuscular system model is consistent with data for a variety of manipulator and forcing functions.

- For a spring-restrained low-inertia manipulator the third-order muscle system is closely approximated by a second-order system. An increase in the bias signal to the muscle causes adaptive changes in the low and high frequency phase of the closed-loop neuromuscular system that are consistent with observed phase changes of the pilot's overall describing function.

- Changes in the transient response to a torque impulse input as a function of muscle tension (large inertia, no-spring manipulator) support the models muscle spindle feedback of an internal muscle length. The effect of this feedback is to produce a closed-loop numerator zero which approximately cancels a denominator root since both are influenced by operating point tension. The resulting dominant second system response closely describes the torque disturbance data.

- Variations in muscle tremor frequency for various spring, inertia, and average muscle tension values support a closed-loop neuromuscular system model. The trends and limits of the tremor data provide further evidence of spindle feedback of an internal muscle length. The series elastic element coupled with limb/manipulator inertias produces zeros which constrain the closed-loop characteristic equation roots and provide an upper limit for tremor frequency.

REFERENCES

1. Devanandan, M. S.; Eccles, R. M.; and Westerman, R. A.: Single Motor Units of Mammalian Muscle. J. Physiol., vol. 178, 1965, pp. 359–367.

2. Basmajian, V. J.: Muscles Alive. Second ed., Williams and Wilkins, Baltimore, 1967.

3. Romanes, G. J.: The Motor Pools of the Spinal Cord. Prog. in Brain Res., vol. 11, 1964, pp. 93–116.

4. Eccles, J. C.; and Schade, J. P., eds.: Organization of the Spinal Cord. Prog. in Brain Res., vol. 11, Elsevier, Amsterdam, 1964.

5. Glees, P.: Experimental Neurology. Clarendon Press, Oxford, 1961.

6. Kernell, D.: The Repetitive Discharge of Motoneurons. Nobel Symposium I: Muscular Afferents and Motor Control. R. Granit, ed., John Wiley and Sons, New York, 1966, pp. 351–362.

7. Granit, R., ed.: Nobel Symposium I: Muscular Afferents and Motor Control. John Wiley and Sons, New York, 1966.

8. Merton, P. A.: Voluntary Strength and Fatigue. J. Physiol., vol 123, 1954, pp. 553–564.

9. Buller, A. J.: Mammalian Fast and Slow Skeletal Muscle. Scien. Basis of Med., Annual Rev., Univ. London, Athlone Press, 1965.

10. Bach-y-Rita, P.; and Ito, F.: In Vivo Studies of Fast and Slow Muscle Fibers in Cat Extraocular Muscles. J. Gen. Physiol., vol. 49, 1966, pp. 1177–1198.

11. Eccles, J. C.; Eccles, R. M.; and Lundberg, A.: The Action Potentials of the Alpha Motoneurons Supplying Fast and Slow Muscles. J. Physiol., vol. 142, 1958, pp. 275–291.

12. Bigland, B.; and Lippold, O. C. J.: Motor Unit Activity in the Voluntary Contraction of Human Muscle. J. Physiol., vol. 125, 1954, pp. 322–335.

13. Bracchi, F.; Decandia, M.; and Gualtierotti, T.: Frequency Stabilization in the Motor Centers of Spinal Cord and Candal Brain Stem. Amer. J. Physiol., vol. 210, 1966, pp. 1170–1177.

14. Henneman, E.; Somjen, G.; and Carpenter, D. O.: Functional Significance of Cell Size in Spinal Motoneurons. J. Neurophysiol., vol. 28, 1965, pp. 560–580.

15. Henneman, E,; Somjen, G.; and Carpenter, D. O.: Excitability and Inhibitibility of Motoneurons of Different Sizes. J. Neurophysiol., vol. 28, 1965, pp. 599–620.

16. Sexton, A. W.; and Gerslen, J. W.: Isometric Tension Differences in Fibers of Red and White Muscles. Science, vol. 157, 1967, p. 199.

17. McPhedran, A. M.; Wuerker, R. B.; and Henneman, E.: Properties of Motor Units in a Homogeneous Red Muscle (Soleus) of the Cat. J. Neurophysiol., vol. 28, 1965, pp. 71—84.

18. Wuerker, R. B.,: McPhedran, A. M.; and Henneman, E.: Properties of Motor Units in a Heterogeneous Pale Muscle (the gastrocnemius) of the Cat. J. Neurophysiol., vol. 28, 1965, pp. 85—99.

19. Eldred, E.; Granit, R.; and Merton, P. A.: Supraspinal Control of the Muscle Spindles and its Significance. J. Physiol., vol. 122, 1953, pp. 498—523.

20. Gordon, A. M.; Huxley, A. F.; and Julian, F. J.: The Length-Tension Diagram of Single Vertebrate Striated Muscle Fibers. J. Physiol., vol. 171, 1964, pp. 28—30P.

21. Kuno, M.: Excitability Following Antidromic Activation in Spinal Motoneurones Supplying Red Muscles. J. Physiol., vol. 149, 1959, pp. 374—393.

22. Ridge, R. M. A. P.: The Differentiation of Conduction Velocities of Slow Twitch Muscle Motor Innervations in Kittens and Cats. Quar. J. Exp. Physiol., vol. 52, 1967, pp. 293—304.

23. Robinson, D. A.: Mechanics of Human Saccadic Eye Movement. J. Physiol., vol. 174, 1964, pp. 245—264.

24. Wells, J. B.: Comparison of Mechanical Properties Between Slow and Fast Mammalian Muscles. J. Physiol., vol. 178, 1965, pp. 252—269.

25. Wilkie, D. R.: The Relation Between Force and Velocity in Human Muscle. J. Physiol., vol. 110, 1950, pp. 249—280.

26. Bigland, B.; and Lippold, O. C. J.: The Relation Between Force, Velocity, and Integrated Electrical Activity in Human Muscles. J. Physiol., vol. 123, 1954, pp. 214—224.

27. Barker, D., ed.: Muscle Receptors. Hong Kong Univ. Press, 1962.

28. Lippold, O. C. J.; Nicholls, J. G.; and Redfearn, J. W. T.: Electrical and Mechanical Factors in the Adaptation of a Mammalian Muscle Spindle. J. Physiol., vol. 153, 1960, pp. 209—217.

29. Lundberg, A.; and Winsbury, G.: Selective Adequate Activation of Large Afferents from Muscle Spindles and Golgi Tendon Organs. Acta Physiol. Scand., vol. 49, 1960, pp. 155—164.

30. Whitteridge, D.: The Effect of Stimulation of Intrafusal Muscle Fibers on Sensitivity to Stretch of Extraocular Muscle Spindles. Quar. J. Exp. Physiol., vol. 44, 1959, pp. 385–393.

31. Harvey, R. J.; and Matthews, P. B. C.: The Response of De-efferented Muscle Spindle Endings in the Cat's Soleus to Slow Extension of the Muscle. J. Physiol., vol. 157, 1961, pp. 370–392.

32. Crowe, A.; Matthews, P. B. C.: The Effect of Stimulation of Static and Dynamic Fusimotor Fibres on the Response to Stretching of the Primary Endings of Muscle Spindles. J. Physiol., vol. 174, 1964, pp. 109–131.

33. Matthews, P. B. C.: Muscle Spindles and Their Motor Control. Physiol. Rev., vol. 44, 1964, pp. 219–288.

34. Jansen, J. K. S.; and Rudjord, T.: On the Silent Period and Golgi Tendon Organs of the Soleus Muscle of the Cat. Acta Physiol. Scand., vol. 62, 1964, pp. 364–379.

35. Houk, J.; and Henneman, E.: Responses of Golgi Tendon Organs to Active Contractions of the Soleus Muscle of the Cat. J. Neurophysiol., vol. 30, 1967, pp. 466–481.

36. Rexed, B.: A Cytoarchilectonic Atlas of the Spinal Cord in the Cat. J. Comp. Neurol., vol. 100, 1954, pp. 297–379.

37. Rexed, B.: Some Aspects of the Cytoarchilectonics and Synaptology of the Spinal Cord. Progress in Brain Res., vol. 11, J. C. Eccles and J. P. Schade, eds., Elsevier, Amsterdam, 1964, pp. 58–90.

38. Wall, P. D.: Presynaptic Control of Impulses at the First Central Synapse in the Culaneous Pathway. Progress in Brain Research, vol. 12, J. C. Eccles and J. P. Schade, eds., Elsevier, Amsterdam, 1964, pp. 92–115.

39. Matthews, P. B. C.: The Dependence of Tension Upon Extension in the Stretch Reflex of the Soleus Muscle of the Decerebrate Cat. J. Physiol., vol. 147, 1959, pp. 521–546.

40. Granit, R.: Neuromuscular Interaction in Postural Tone of the Cat's Isometric Soleus Muscle. J. Physiol., vol. 143, 1958, pp. 387–402.

41. Gill, P. K.: The Effects of End-tidal CO_2 on the Discharge of Individual Phrenic Motoneurones. J. Physiol., vol. 168, 1963, pp. 239–257.

42. Sears, T. A.: Efferent Discharge in Alpha and Fusimotor Fibres of Intercostal Nerves of the Cat. J. Physiol., vol. 174, 1964, pp. 295–315.

43. Sears, T. A.: Investigations on Respiratory Motoneurones of the Thoracic Spinal Cord. Prog. in Brain Res., vol. 12, 1964, pp. 259–273.

44. Sears, T. A.: Pathways of Supraspinal Origin Regulating the Activity of Respiratory Motoneurones. Nobel Symposium I: Muscular Afferents and Motor Control, R. Granit, ed., John Wiley and Sons, New York, 1966, pp. 187–196.

45. von Euler, C.: Proprioceptive Control in Respiration. Nobel Symposium I: Muscular Afferents and Motor Control, R. Granit, ed., John Wiley and Sons, New York, 1966, pp. 197–207.

46. Eklund, G.; von Euler, C.; and Rutkowski, S.: Intercostal γ-Motor Activity. Acta Physiol. Scand., vol. 57, 1963, pp. 481–482.

47. Eklund, G.; von Euler, C.; and Rutkowski, S.: Spontaneous and Reflex Activity of Intercostal Gamma Motoneurones. J. Physiol., vol. 171, 1964, pp. 139–163.

48. Critchlow, V.; and von Euler, C.: Intercostal Muscle Spindle Activity and its γ Motor Control. J. Physiol., vol. 168, 1963.

49. Corda, M.; Eklund, G.; and von Euler, C.: External Intercostal and Phrenic α Motor Responses to Changes in Respiratory Load. Acta Physiol. Scand., vol. 63, 1965, pp. 391–400.

50. Campbell, E. J. M.; Dickinson, C. J.; and Howell, J. B. L.: The Immediate Effects of Added Loads on the Inspiratory Musculature of the Rabbit. J. Physiol., vol. 172, 1964, 321–331.

51. Corda, M.; von Euler, C.; and Lennerstrand, G.: Reflex and Cerebellar Influences on α and on 'Rhythmic' and 'Tonic' γ Activity in the Intercostal Muscle. J. Physiol., vol. 184, 1966, pp. 898–923.

52. Hunt, C. C.; and Perl, E. R.: Spinal Reflex Mechanisms Concerned with Skeletal Muscle. Physiol. Rev., vol. 40, 1960, pp. 538–579.

53. Eccles, J. C.; and Schade, J. P., eds.: Physiology of Spinal Neurons. Progress in Brain Research, vol. 12, Elsevier, Amsterdam, 1964.

54. Eccles, J. C.: Functional Organization of the Spinal Cord. Anesthesiology, vol. 28, 1967, pp. 31–44.

55. Eccles, R. M.; and Lundberg, A.: Integrative Pattern of Ia Synaptic Actions on Motoneurones of Hip and Knee Muscles. J. Physiol., vol. 144, 1958, pp. 271–298.

56. Eccles, J. C.; Eccles, Rosamond M.; Iggo, A.; and Ito M.: Distribution of Recurrent Inhibition Among Motoneurones. J. Physiol., vol. 159, 1961, pp. 479–499.

57. Wilson, V. J.; and Burgess, P. R.: Disinhibition in the Cat Spinal Cord. J. Neurophysiol., vol. 25, 1962, pp. 392–404.

58. Kidd, G. L.: An Analysis of β-Axon Excitation of the Muscle Spindle in the Cat. Control and Innervation of Skeletal Muscle, B. L. Andrew, ed., Univ. St. Andrews, 1966, pp. 83–94.

59. Andrew, B. L., ed.: Control and Innervation of Skeletal Muscle. Univ. St. Andrews, 1966.

60. Roberts, T. D. M.: Rhythmic Excitation of a Stretch Reflex, Revealing (a) Hysteresis and (b) a Difference Between the Responses to Pulling and to Stretching. Quar. J. Exp. Physiol., vol. 48, 1963, pp. 328–345.

61. Jansen, J. K. S.; and Rack, P. M. H.: The Reflex Response to Sinusoidal Stretching of Soleus in the Decerebrate Cat. J. Physiol., vol. 183, 1966, pp. 15–36.

62. Rack, P. M. H.: The Reflex Response to Sinusoidal Movement. Control and Innervation of Skeletal Muscle, B. L. Andrew, ed., Univ. St. Andrews, 1966, pp. 112–117.

63. Lippold, O. C. J.; Redfearn, J. W. T.; and Vuco, J.: The Effect of Sinusoidal Stretching Upon the Activity of Stretch Receptors in Voluntary Muscle and Their Reflex Responses. J. Physiol., vol. 144, 1958, pp. 373–386.

64. Lippold, O. C. J.; Redfearn, J. W. T.; and Vuco, J.: The Rhythmical Activity of Groups of Motor Units in the Voluntary Contraction of Muscle. J. Physiol., vol. 137, 1957, pp. 473–487.

65. Roberts, T. D. M.: The Nature of the Controlled Variable in the Muscle Servo. Control and Innervation of Skeletal Muscle, B. L. Andrew, ed., Univ. St. Andrews, 1966, pp. 160–168.

66. Anderson, B.; and Lennerstrand, G.: Dynamic Analysis of Muscle Spindles. Nobel Symposium I: Muscular Afferents and Motor Control, R. Granit, ed., John Wiley and Sons, New York, 1966, pp. 107–113.

67. Crowe, A.; and Matthews, P. B. C.: Further Studies of Static and Dynamic Fusimotor Fibres. J. Physiol., vol. 174, 1964, pp. 132–151.

68. Szentágothai, J.: Propriospinal Pathways and Their Synapses. Organization of the Spinal Cord. Progress in Brain Research, vol. 11, J. C. Eccles and J. P. Schade, eds., Elsevier, Amsterdam, 1964, pp. 155–174.

69. Kuypers, H. G. J. M.: The Descending Pathways to the Spinal Cord, Their Anatomy and Function. Organization of the Spinal Cord. Progress in Brain Research, vol. 11, J. C. Eccles and J. P. Schade, eds., Elsevier, Amsterdam, 1964, pp. 178–200.

70. Katz, Bernhard: The Relation Between Force and Speed in Muscular Contraction. J. Physiol., vol. 96, 1939, pp. 45–64.

71. Basmajian, V. J.: Control and Training of Individual Motor Units. Science, vol. 141, 1963, pp. 440–441.

72. McRuer, Duane; Graham, Dunstan; Krendel, Ezra; and Reisener, William, Jr.: Human Pilot Dynamics in Compensatory Systems: Theory, Models, and Experiments with Controlled Element and Forcing Function Variations. AFFDL-TR-65-15, July 1965.

73. McRuer, Duane: Remarks on Some Neuromuscular Subsystem Dynamics. IEEE Trans. on Human Factors in Electronics, vol. HFE, no. 3, Sept. 1966, pp. 129–130.

74. Jex, H. R.; McDonnell, J. D.; and Phatak, A. V.: A "Critical" Tracking Task for Man-Machine Research Related to the Operator's Effective Delay Time. Part I: Theory and Experiments with a First-Order Divergent Controlled Element. NASA CR-616, Nov. 1966.

75. Young, Laurence R.; and Stark, Lawrence: Biological Control Systems—A Critical Review and Evaluation, Developments in Manual Control. NASA CR-190, Mar. 1965.

76. Okabe, Y.; Rhodes, H. E.; Stark, L.; and Willis, P. A.: Transient Responses of Human Motor Coordination System. MIT Res. Lab. Elec. Quar. Prog. Rept. No. 66, July 1962, pp. 389–395.

77. Houk, James Charles, Jr.: A Mathematical Model of the Stretch Reflex in Human Muscle Systems. Master of Science Thesis, MIT, 1963.

78. Sun, H. H.; Eisentein, B. A.; and Bomze, H.: Dynamic Model for Hand Motor Coordination System. Eng. in Med. and Biology, Proc. 19th Annual Conference, 1966.

79. Holliday, A. M.; and Redfearn, J. W. T.: An Analysis of the Frequencies of Finger Tremor in Healthy Subjects. J. of Physiol., vol. 134, 1956, pp. 600–611.

80. Robson, J. G.: The Effect of Loading on the Frequency of Muscle Tremor. J. of Physiol., 1959, pp. 29P.

81. Gydikov, A.: Sampling with Adjustable Frequency in the Hand Movement Control System. IEEE Trans. on Human Factors in Electronics, vol. HFE-8, no. 2, June 1967, pp. 135–140.

82. Magdaleno, R.; and McRuer, D. T.: Effects of Manipulator Restraints on Human Operator Performance, AFFDL-TR-66-72, Dec. 1966.

83. Wilkie, D. R.: The Mechanical Properties of Muscle. Brit. Med. Bull., vol. 12, no. 3, 1956, pp. 177–182.

84. Granit, Ragnar: Neuromuscular Interaction in Postural Tone of the Cat's Isometric Soleus Muscle. J. Physiol., vol. 143, 1958, pp. 387–402.

85. Close, J. R.; Nickel, E. D.; and Todd, F. N.: Motor-Unit Action-Potential Counts, Their Significance in Isometric and Isotonic Contractions. J. Bone and Joint Surgery, vol. 42-A, no. 7, Oct. 1960.

86. Rack, P. M. H.: The Behaviour of a Mammalian Muscle During Sinusoidal Stretching. J. Physiol., vol. 183, 1966, pp. 1–14.

87. Partridge, Lloyd D.: Modifications of Neural Output Signals by Muscles: A Frequency Response Study. J. Appl. Physiol., vol. 20, no. 1, 1965, pp. 150–156.

88. Partridge, Lloyd D.: Signal-Handling Characteristics of Load-Moving Skeletal Muscle. Amer. J. Physiol., vol. 210, no. 5, May 1966, pp. 1178–1191.

89. Eppler, Walter G.: Analytical Design of Manned Control Systems. Palo Alto Res. Lab., Lockheed Rept. 6-62-66-1, May 1966.

90. Jansen, J. K. S.; and Rack, P. M. H.: The Reflex Response to Sinusoidal Stretching of Soleus in the Decerebrate Cat. J. Physiol., vol. 183, 1966, pp. 15–36.

91. Stapleford, R. L.; McRuer, D. T.; and Magdaleno, R.: Pilot Describing Function Measurements in a Multiloop Task. NASA CR-542, Aug. 1966.

92. Margaria, R.; Gualtierotti, T.; and Spinelli, D.: Effect of Stress on Lower Neuron Activity. Exp. Med. Surg., vol. 16, no. 2-3, June-Sept. 1958.

93. Dewhurst, D. J.: Neuromuscular Control System. IEEE Trans. on Bio-Med. Eng., vol. BME-14, no. 3, July 1967, pp. 167–170.

94. Krendel, Ezra S.; and McRuer, Duane T.: A Servomechanisms Approach to Skill Development. J. Franklin Institute, vol. 269, no. 1, Jan. 1960.

95. McRuer, Duane T.: Unified Analysis of Linear Feedback Systems. ASD-TR 61-118, July 1961.

96. Stapleford, Robert L.; Johnston, Donald E.; Teper, Gary L.; and Weir, David H.: Development of Satisfactory Lateral-Directional Handling Qualities in the Landing Approach. NASA CR-239, July 1965.

97. McRuer, D. T.; Hofmann, L. G.; Jex, H. R.; et al: New Approaches to Human-Pilot/Vehicle Dynamic Analysis. Systems Technology, Inc., Tech. Rept. 164-2, June 1967 AFFDL-TR-67-150, Feb. 1968.

98. Diete-Spiff, K.: Tension Development by Single Isolated Muscle Spindles of the Cat. J. Physiol., vol. 193, 1967, pp. 31–43.

99. Close, R.: Properties of Motor Units in Fast and Slow Skeletal Muscles in the Rat. J. Physiol., vol. 193, 1967, pp. 45–55.

100. Burke, R. E.: Motor Unit Types of Cat Triceps Surae Muscle. J. Physiol., vol. 193, 1967, pp. 141–160.

101. Alnaes, E.: Static and Dynamic Properties of Golgi Tendon Organs in the Anterior Tibial and Soleus Muscles of the Cat. Acta Physiol. Scand., vol. 70, 1967, pp. 176–187.

102. Sutton, G. G.; and Sykes, K.: The Variation of Hand Tremor with Force in Healthy Subjects. J. Physiol., vol. 191, 1967, pp. 699–711.

103. Houk, J.; and Simon, W.: Responses of Golgi Tendon Organs to Forces Applied to Muscle Tendon. J. Neurophysiol., vol. 30, 1967, pp. 1466–1481.

104. Houk, J.: A Viscoelastic Interaction which Produces One Component of Adaptation in Responses of Golgi Tendon Organs. J. Neurophysiol., vol. 30, 1967, pp. 1482–1493.

105. Stark, Lawrence: Neurological Feedback Control Systems. Advances in Bioengineering and Instrumentation. Ch. 4, Fred Alt, ed., Plenum Press (New York), 1966, pp 289–385.